

NUREG/CR-3678

EA-10038

43

CIC-14 REPORT COLLECTION  
**REPRODUCTION  
COPY**

Los Alamos National Laboratory is operated by the University of California for the United States Department of Energy under contract W-7405-ENG-36.

*Estimation Methods for Process Holdup  
of Special Nuclear Materials*

LOS ALAMOS NATIONAL LABORATORY  
3 9338 00310 2703

**Los Alamos** Los Alamos National Laboratory  
Los Alamos, New Mexico 87545

An Affirmative Action/Equal Opportunity Employer

Composition by Sharon L. Hurdle, Group Q-4,  
and Pamela H. Mayne, Group IS-6

**NOTICE**

This report was prepared as an account of work sponsored by an agency of the United States Government. Neither the United States Government nor any agency thereof, or any of their employees, makes any warranty, expressed or implied, or assumes any legal liability or responsibility for any third party's use, or the results of such use, of any information, apparatus, product or process disclosed in this report, or represents that its use by such third party would not infringe privately owned rights.

NUREG/CR-3678

LA-10038

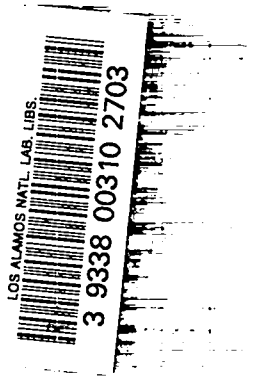
RS

## Estimation Methods for Process Holdup of Special Nuclear Materials

K. K. S. Pillay  
R. R. Picard  
R. S. Marshall

Manuscript submitted: February 1984

Date published: June 1984



Prepared for  
Safeguards Research Branch  
Division of Facility Operations  
Office of Nuclear Regulatory Research  
US Nuclear Regulatory Commission  
Washington, DC 20555

NRC FIN No. A7226

**Los Alamos** Los Alamos National Laboratory  
Los Alamos, New Mexico 87545

## Executive Summary

This is the final report on a research program sponsored by the Safeguards Research Branch of the Nuclear Regulatory Commission (NRC) to explore the possibilities of developing statistical estimation models for residual holdup of highly enriched uranium (HEU) at processing facilities. This study was initiated as part of an effort to refocus the resources of materials control and accounting for timely detection of special nuclear material (SNM) loss. Throughout this investigation, periodic reports of the status of the study were submitted to the NRC, and this report is a compilation of all the work done during the project. A formal report on this project, titled "Uranium Holdup Modeling," was issued in 1983. It is a generic report on holdup estimation that highlights the value of predictive models for estimating quantities of materials and their variances.

The task of gathering holdup information and the development of holdup estimators for specific processes underwent several stages of examination. Historical data available from HEU-processing facilities, which were gathered as part of periodic inventory development, were considered first as a readily available source of long-term holdup data. The poor quality of these data made this source of information of limited value to statistical model development. The next step in gathering good-quality holdup data was through carefully designed measurements of SNM holdup at two of the materials-processing facilities of the Los Alamos National Laboratory. Selected measurements conducted over a period of 1 yr showed that certain equipment, such as air filters and calciners, lend themselves to good-quality holdup measurements and have potentials for estimation-model development. Attempts to develop these holdup data without interference with plant schedules imposed limitations on the quality of some of the data gathered during this phase of the investigation. However, these measurements did provide valuable data on holdup of uranium and plutonium on exhaust air filters under several operating conditions. The holdup estimation models developed from these data formed a sound basis for developing estimation models and demonstrated the need for good-quality data gathered under reasonably stable conditions. The value of these models was further confirmed when controlled experiments were performed using radioactive tracers and high-quality data collection.

The next step in the direction of improving the quality of holdup data was the design and performance of a series of controlled experiments to simulate several unit processes common to HEU process facilities. Two of these experiments were conducted outside of Los Alamos under the supervision and control of Los Alamos personnel. One of the controlled experiments on uranium dust generation was performed at the San Diego facilities of GA Technologies, Inc., and the other experiment on uranium inventory development, in liquid-liquid extraction pulse columns, was conducted at the Allied-General Nuclear Services plant at Barnwell, South Carolina. All the other controlled experiments were conducted at Los Alamos and were designed to measure uranium holdup as a function of throughput during feed dissolution processes, ammonium diuranate precipitation and calcination, and the circulation of uranyl solutions through pipes and pipefittings. The total throughput of uranium in these experimental facilities ranged from 50 kg to ~50 tonnes.

The quality of measured holdup data during these controlled experiments (except for the pulse-column experiments) was improved by at least an order of magnitude by using carefully selected radioactive tracers. These tracers, at concentration levels of ~1ppb, were homogeneously incorporated into the process materials. The tracers with their high specific activity and unique gamma-emission characteristics provided the additional advantage for improving the quality of the holdup data. Considerable attention was paid during these experiments to fabricate instrument calibration standards that were compatible with the equipment measured and the distribution of holdup within the equipment. This also contributed to improving the quality of holdup data from nonintrusive, nondestructive assays (NDAs) using gamma-ray spectrometry.

Development of statistical models for HEU holdup used a variety of techniques including multiple regression, Kalman filtering, and response surface methodology. Uranium holdup in glove boxes, ductwork, air filters, calciners, precipitators, filter funnels, rotary drum filters, feed dissolvers, pulse

columns, and pipes and pipefittings of uranium circulation systems were measured. The models, in most cases, demonstrated the value of statistical models developed from good-quality measurements for estimating both present and future residual holdup as a function of material throughput. The findings of this investigation revealed that several factors such as the layout of pipes, corrosion of construction materials, concentrations of solutions, and so forth impact holdup of materials in processing facilities, and in many instances the holdup of SNM is not simply a function of the material throughput. In addition, this investigation has been able to identify both the advantages and limitations of holdup data and estimation models developed from a variety of data-gathering approaches. One of the unique advantages of the use of statistical models is that data necessary for updating the models can be gathered during planned plant shutdown conditions without major disruption of production schedules.

Section I is an introduction to this study and its evolution including a brief survey of present knowledge on materials holdup. Section II highlights some of the successful attempts to measure and use holdup data from operating process facilities and the advantages and limitations of these measurements for developing predictive models.

Sections III-VI describe the controlled experiments and the details of model development specific to each type of equipment used during these experiments. Various designs of experiments, adaptations of instruments, calibration standards fabrications, and the use of mathematical techniques for developing functional relationships between holdup and throughput are discussed. Cleanout measurements were incorporated routinely into these controlled experiments to evaluate NDA measurements. Various approaches to improve the quality of holdup data are mentioned throughout these sections.

Section VII summarizes the findings of this investigation and highlights the value of controlled experiments and modeling for the development of holdup estimators. The potential applications of the holdup estimation techniques to fuel cycle facilities and the conclusions derived from various observations are also included.

The major findings of this investigation are the following:

1. Measurement of the residual holdup of SNM at large processing facilities is a difficult problem and will remain so because of the inherent limitations of plant layout and NDA techniques.
2. It is often difficult to assign a high priority for holdup estimation, which also contributes to the inherent problems of holdup measurement.
3. Statistical estimation models can assist plant operators in meeting regulatory requirements of holdup estimation as part of periodic inventory development.
4. The development of useful prediction models of holdup hinges on the quality of data and the stability of process operations.
5. There are several approaches to improving the quality of measurements using better instrumentation and better calibration standards and through the application of carefully chosen secondary measurement techniques. If there are no improvements in the quality of measurements, it is unrealistic to expect statistical models to provide estimates of high quality.
6. Holdup estimation models require periodic updating to remain useful as facilities and process variables change.
7. Significant improvements to holdup measurements and data development for holdup estimations can be accomplished if this problem is addressed during the design stages of a plant to incorporate the features necessary to accomplish the measurement goals.

Appendix A treats in detail the potentials and limitations of the use of tracers to improve the quality of holdup measurements. This discussion is supplemented by some of the results of preliminary investigations to determine whether the tracers chosen truly represent the SNM during all phases of the unit process. Appendix B provides introductory information on two of the mathematical techniques—regression analysis and Kalman filtering—used repeatedly during this study for the development of statistical estimation models. Appendix C is a compilation of the results of controlled experiments. These are presented in a concise fashion to conserve space and to provide enough details for those who wish to examine the approaches described for the development of good-quality data for holdup modeling.

## CONTENTS

ABSTRACT . . . . .	1
I. INTRODUCTION . . . . .	1
A. Survey of Present Knowledge . . . . .	2
B. Background to This Investigation . . . . .	3
C. This Report . . . . .	3
II. HOLDUP MEASUREMENTS AT PROCESSING FACILITIES . . . . .	3
A. Measurement Techniques . . . . .	4
B. Holdup Measurement Results . . . . .	5
1. Plutonium Facility Filter Holdup . . . . .	5
2. Uranium Scrap Recovery Facility Air Filter Holdup . . . . .	5
3. Uranium Holdup in Batch Calciners . . . . .	5
4. Precipitator and Rotating Drum Filter Holdup . . . . .	5
5. Uranium Holdup in Air Ducts . . . . .	5
C. Modeling . . . . .	8
III. EXPERIMENTAL STUDY OF URANIUM HOLDUP IN A DUST-GENERATING FACILITY . . . . .	13
A. Facility Description . . . . .	14
B. Experimental Procedures . . . . .	16
1. Tracer Application . . . . .	16
2. Measurements . . . . .	17
C. Dust Generation and Holdup Measurements . . . . .	17
D. Experimental Results and Discussion . . . . .	19
E. Modeling . . . . .	22
1. The Filter . . . . .	22
2. Elbows . . . . .	23
3. The Glove Box Floor . . . . .	24
4. The Vertical and Horizontal Ducts . . . . .	27
5. Modeling the Glove Box System . . . . .	33
6. Comparison of Experiments . . . . .	34
IV. EXPERIMENTAL STUDY OF URANIUM HOLDUP IN A LIQUID-LIQUID EXTRACTION PULSE COLUMN . . . . .	35
A. Experimental Study . . . . .	36
B. Equipment and Facilities . . . . .	36
C. Experimental Procedures . . . . .	36
D. Uranium Concentration Profiles of Pulse Columns . . . . .	38
E. Pulse-Column Inventory Estimation . . . . .	38
1. Model Development . . . . .	41
2. Profile Approximation by Regression Methods . . . . .	42
3. Estimation Based on Theoretical Considerations . . . . .	45

V. EXPERIMENTAL STUDY OF URANIUM HOLDUP DURING AMMONIUM DIURANATE (ADU) PRECIPITATION AND CALCINATION . . . . .	51
A. Experimental Study . . . . .	51
B. Facility Description . . . . .	53
C. Holdup Measurements . . . . .	53
D. Experimental Results . . . . .	56
E. Materials Balance and Cleanout Measurements . . . . .	58
F. Residual Holdup Estimation . . . . .	60
1. Calciner Trays . . . . .	60
2. Feed Dissolver . . . . .	61
3. Filter Funnels . . . . .	62
4. Calciner . . . . .	63
5. Precipitator . . . . .	65
VI. EXPERIMENTAL STUDY OF URANIUM IN SOLUTION LOOPS . . . . .	67
A. Facility Description . . . . .	67
B. Experimental Procedures . . . . .	69
C. Holdup Measurements . . . . .	70
D. Experimental Results . . . . .	70
E. Modeling . . . . .	72
VII. DISCUSSION AND CONCLUSIONS . . . . .	80
A. Value of Controlled Measurements . . . . .	81
B. Motivation for Modeling . . . . .	82
C. Applications to Fuel Cycle Facilities . . . . .	83
D. Conclusions . . . . .	84
ACKNOWLEDGMENTS . . . . .	85
REFERENCES. . . . .	85
APPENDIX A: USE OF TRACERS IN MATERIALS HOLDUP STUDY . . . . .	89
I. INTRODUCTION. . . . .	89
II. EXPERIMENTAL STUDIES USING TRACERS . . . . .	89
A. Qualities of a Tracer . . . . .	90
B. Tracers Used in HEU Holdup Measurements . . . . .	91
C. Limitations of Experimental Facilities . . . . .	92
D. Tracer Levels and Measurement Methods . . . . .	92
III. RESULTS AND DISCUSSION. . . . .	94
A. Homogenization of Tracers in Uranium Matrices. . . . .	94
B. NDAs and Cleanout Measurements for Holdup Determination. . . . .	94
REFERENCES. . . . .	96
APPENDIX B: PRINCIPLES OF REGRESSION AND KALMAN FILTERING . . . . .	97
I. REGRESSION . . . . .	97
II. KALMAN FILTER . . . . .	98
REFERENCES. . . . .	99
APPENDIX C: DETAILED DATA FROM CONTROLLED EXPERIMENTAL STUDIES . . . . .	100

## TABLES

I. Holdup of Plutonium on a Glove Box Air Filter . . . . .	6
II. Holdup of Uranium on Exhaust Air Filters at TA-21 . . . . .	7
III. Grams of Uranium Holdup for Calciners Weighted by Material Profiles . . . . .	7
IV. Locations of Measurement Points . . . . .	15
V. Experimental Conditions . . . . .	18
VI. Comparison of Model-Based Estimates with Weight-Loss Values . . . . .	21
VII. A Comparison of Holdup Estimates by Different Methods . . . . .	21
VIII. Summary of Modeling Results for Low-Airflow Experiment with $U_3O_8$ . . . . .	34
IX. Pulse-Column Operating Conditions . . . . .	38
X. Summary of Modeling Results . . . . .	46
XI. Estimated Concentration Profiles . . . . .	50
XII. Experimental Parameters of ADU Precipitation and Calcination Experiments . . . . .	56
XIII. Comparison of NDA Measurements of Holdup with Cleanout Measurements . . . . .	59
XIV. Holdup Estimates and Cleanout Values for the ADU Experiment . . . . .	66
XV. Component Description and Experimental Parameters of Circulation Loop . . . . .	69
XVI. Cleanout Measurements—Uranium Solution Loop Experiments . . . . .	71
XVII. Values of Measurement Variability ( $\sigma_m^2$ ) and Process Variability ( $\sigma_p^2$ ) Used in Filtering the Solution Loop Data . . . . .	72
A-I. Specific Activities of $^{235}U$ and Tracer Isotopes . . . . .	91
A-II. Tracers and Their Compatible Forms . . . . .	91
A-III. Per Cent Tracer Found at Various Stages of ADU Precipitation and Calcination . . . . .	95
A-IV. Comparison of NDA Measurements of Holdup with Cleanout Measurements . . . . .	95
C-I. Summary of Modeling Results for Medium-Airflow Experiment with $U_3O_8$ . . . . .	101
C-II. Summary of Modeling Results for High-Airflow Experiment with $U_3O_8$ . . . . .	101
C-III. Constants of Integration . . . . .	102
C-IV. Table of Measured Holdup Per Unit Area . . . . .	102
C-V. Table of Measured Holdup Per Unit Area . . . . .	102
C-VI. Table of Measured Values . . . . .	103
C-VII. Table of Measured Holdup Per Unit Length of Ductwork . . . . .	103
C-VIII. Table of Holdup Measurements . . . . .	104
C-IX. Summary of Modeling Results for Experiment with Coarse $U_3O_8$ . . . . .	104
C-X. Table of Holdup Measurements . . . . .	105
C-XI. Summary of Modeling Results for Low-Airflow Experiment with Ash . . . . .	105
C-XII. Table of Holdup Measurements . . . . .	106
C-XIII. Summary of Modeling Results for Medium-Airflow Experiment with Ash . . . . .	106
C-XIV. Table of Holdup Measurements . . . . .	107
C-XV. Summary of Modeling Results for High-Airflow Experiment with Ash . . . . .	107
C-XVI. Concentration Profile Data . . . . .	109
C-XVII. Concentration Profile Data . . . . .	109



TABLES (cont)

C-XVIII.	Holdup of Uranium in the Precipitation Column . . . . .	111
C-XIX.	Holdup of Uranium in the Filter Funnels . . . . .	111
C-XX.	Holdup of Uranium in Calciner . . . . .	112
C-XXI.	Holdup of Uranium in Calciner Trays . . . . .	112
C-XXII.	Holdup of Uranium in the Dissolver Vessel . . . . .	113
C-XXIII.	Data from Solution Loop Experiments: CPVC Loop, Low Flow Rate . . . . .	115
C-XXIV.	Data from Solution Loop Experiments: CPVC Loop, High Flow Rate . . . . .	115
C-XXV.	Data from Solution Loop Experiments: Stainless Steel Loop, Low Flow Rate . . . . .	116
C-XXVI.	Data from Solution Loop Experiments: Stainless Steel Loop, High Flow Rate . . . . .	116
C-XXVII.	Holdup Estimates for Each Measurement Location at the Conclusion of the Experiment . . . . .	117

## FIGURES

Fig. 1. Total holdup of uranium in four duct systems at GA Technologies, Inc. . . . .	8
Fig. 2. Measurement history of the holdup of plutonium on an air filter at TA-55. . . . .	9
Fig. 3. Measurement history of the holdup of uranium on air filter DB-1. . . . .	10
Fig. 4. Measurement history of the holdup of uranium on air filter DB-30. . . . .	10
Fig. 5. Measurement history of the holdup of uranium on air filter DB-24. . . . .	11
Fig. 6. An isometric view of the experimental facility. . . . .	15
Fig. 7. A schematic of the dust-generation apparatus. . . . .	16
Fig. 8. Change in holdup as a function of throughput of fine $U_3O_8$ powder at the exhaust air filter (measurement location 14). . . . .	20
Fig. 9. Change in holdup as a function of throughput of fine $U_3O_8$ powder at the first elbow of the ductwork (measurement location 8). . . . .	20
Fig. 10. Holdup of uranium on the filter from the dust-generation experiment at low airflow. . . . .	23
Fig. 11. Holdup measurement history (for the low-air-flow experiment with $U_3O_8$ ) at measurement location 8. . . . .	24
Fig. 12. Three detectors suspended over a glove box floor. . . . .	25
Fig. 13. A single detector over $(x_1, y_1)$ . . . . .	26
Fig. 14. Measurements on the glove box floor. . . . .	27
Fig. 15. Spherical coordinates in three-dimensional space. . . . .	28
Fig. 16. Side view of detector and vertical cylinder. . . . .	29
Fig. 17. Overhead view of detector and vertical cylinder. . . . .	30
Fig. 18. Measurements on the vertical cylinder. . . . .	32
Fig. 19. Holdup measurement history (for low-airflow measurements with $U_3O_8$ ) at locations 11-13. . . . .	33
Fig. 20. A schematic representation of the pulse columns used. . . . .	37
Fig. 21. Uranium concentration profile of the extraction/scrub column. . . . .	39
Fig. 22. Uranium concentration profile of the stripping column. . . . .	40
Fig. 23. A hypothetical concentration profile of uranium concentrations. . . . .	41
Fig. 24. Estimated profile—piecewise linear approximation. . . . .	42
Fig. 25. Estimated profile—regression methods. . . . .	43
Fig. 26. Estimated profile—Burkhart model. . . . .	46
Fig. 27. Estimated profile—regression methods. . . . .	47
Fig. 28. Estimated profile—Burkhart model. . . . .	48
Fig. 29. Estimated profile—regression methods. . . . .	48
Fig. 30. Estimated profile—Burkhart model. . . . .	49
Fig. 31. Estimated profile—regression methods. . . . .	49
Fig. 32. Estimated profile—Burkhart model. . . . .	50
Fig. 33. An isometric view of the precipitator during solution transfer. . . . .	52
Fig. 34. An isometric view of the precipitator during ammonia addition. . . . .	52
Fig. 35. Detector assembly and its pedestal. . . . .	54
Fig. 36. Detector positioning in front of the precipitator for measurements A and B. . . . .	55

## FIGURES (cont)

Fig. 37. Different profiles of ADU holdup along the precipitator column. . . . .	58
Fig. 38. A comparison of inventory differences with NDA-measured total holdup. . . . .	59
Fig. 39. Linear regression fit to calciner data. . . . .	60
Fig. 40. Application of Kalman filter to the feed dissolver data. . . . .	61
Fig. 41. Application of Kalman filter to filter funnels data. . . . .	62
Fig. 42. Change-point model for the calciner data. . . . .	42
Fig. 43. Measurement history of holdup in the precipitator. . . . .	65
Fig. 44. A smooth curve superimposed on early portions of the precipitator data. . . . .	66
Fig. 45. Application of Kalman filter to steady-state portion of precipitator data. . . . .	67
Fig. 46. An isometric view of the stainless steel loop for uranyl nitrate solution. . . . .	68
Fig. 47. An isometric view of the CPVC loop for uranyl fluoride solution. . . . .	68
Fig. 48. Shielded NaI(Tl) detector mounted on a long arm with a designed capability to reproduce measurement locations on the solution loop. . . . .	70
Fig. 49. Measurement history and filtered values for pumps at low flow rates. . . . .	74
Fig. 50. Measurement history and filtered values for pumps at high flow rates. . . . .	74
Fig. 51. Measurement history and filtered values for stainless steel unions. . . . .	75
Fig. 52. Measurement history and filtered values for CPVC unions. . . . .	75
Fig. 53. Measurement history and filtered values for stainless steel valves. . . . .	76
Fig. 54. Measurement history and filtered values for CPVC valves. . . . .	76
Fig. 55. Measurement history and filtered values for stainless steel pipes. . . . .	77
Fig. 56. Measurement history and filtered values for CPVC pipes. . . . .	77
Fig. 57. Measurement history and filtered values for stainless steel elbows. . . . .	78
Fig. 58. Measurement history and filtered values for CPVC elbows. . . . .	78
Fig. 59. Measurement history and filtered values for stainless steel tees. . . . .	79
Fig. 60. Measurement history and filtered values for CPVC tees. . . . .	79
Fig. A-1. A combination of the gamma-spectra of $^{232}\text{Th}$ and its daughters, $^{235}\text{U}$ , and the tracer nuclide $^{95}\text{Zr-Nb}$ . . . . .	93
Fig. A-2. A combination of the gamma-spectra of natural and/or low-enriched uranium, $^{235}\text{U}$ , and tracer nuclide $^{46}\text{Sc}$ . . . . .	93

# ESTIMATION METHODS FOR PROCESS HOLDUP OF SPECIAL NUCLEAR MATERIALS

by

K. K. S. Pillay, R. R. Picard, and R. S. Marshall

## ABSTRACT

The US Nuclear Regulatory Commission sponsored a research study at the Los Alamos National Laboratory to explore the possibilities of developing statistical estimation methods for materials holdup at highly enriched uranium (HEU)-processing facilities. Attempts at using historical holdup data from processing facilities and selected holdup measurements at two operating facilities confirmed the need for high-quality data and reasonable control over process parameters in developing statistical models for holdup estimations. A major effort was therefore directed at conducting large-scale experiments to demonstrate the value of statistical estimation models from experimentally measured data of good quality. Using data from these experiments, we developed statistical models to estimate residual inventories of uranium in large process equipment and facilities. Some of the important findings of this investigation are the following:

- Prediction models for the residual holdup of special nuclear material (SNM) can be developed from good-quality historical data on holdup.
- Holdup data from several of the equipment used at HEU-processing facilities, such as air filters, ductwork, calciners, dissolvers, pumps, pipes, and pipe fittings, readily lend themselves to statistical modeling of holdup.
- Holdup profiles of process equipment such as glove boxes, precipitators, and rotary drum filters can change with time; therefore, good estimation of residual inventories in these types of equipment requires several measurements at the time of inventory.
- Although measurement of residual holdup of SNM in large facilities is a challenging task, reasonable estimates of the hidden inventories of holdup to meet the regulatory requirements can be accomplished through a combination of good measurements and the use of statistical models.

---

## I. INTRODUCTION

One of the basic elements of a system for nuclear material safeguards is materials accountability, which includes measurement, accounting, and procedures designed to provide an accurate knowledge of the quantities and disposition of materials. Section 70.51 of Title 10 of the Code of Federal Regulations requires, in part, that certain licensees of special nuclear materials (SNM) conduct at specified intervals physical inventories of SNM in their possession under the license. The accumulation of SNM in process equipment as hidden inventories in the form of residual holdup following shutdown, draindown, and

cleanout generally has adverse effects on the quality of physical inventories and materials control programs. Residual holdup is characterized by the materials that are difficult to locate, sample, identify, analyze, and quantify. Regulatory Guide 5.37, "In-Situ Assay of Enriched Uranium Holdup," defines the residual holdup of enriched uranium as the inventory component remaining in and about process equipment and handling areas after those collection areas have been prepared for inventory. This *in situ* assay guide describes methods to ensure that a measured value of residual holdup is included in each materials balance. Similarly, Regulatory Guide 5.23 provides guidance for the assay of residual plutonium in processing facilities. These two regulatory guides, issued in 1974, are being revised to reflect present knowledge on holdup estimation and new requirements of materials accountability.

Materials generally accumulate in cracks, pores, and zones of poor circulation within and around process equipment. Some processes lead to the accumulation of sizable and sometimes continually increasing amounts of SNM in difficult-to-recover form. The walls of the process vessels, plumbing, ductwork, glove boxes, and filters often become coated with SNM during materials processing. In addition, SNM may chemically interact with the components of the process equipment, causing another form of residual holdup. The absolute amount of SNM in residual holdup must be small for efficient processing and hazards control. However, in practice, the total amount of SNM holdup is significant in the context of the plant inventory difference. This points to the need for better design of processing facilities and improved methods of holdup estimation.

#### A. Survey of Present Knowledge

The identification of the process holdup of fissionable materials is important not only to materials accountability but also to process safety. Current regulatory practices to prevent the diversion of SNM are based on the calculation of inventory differences and their standard deviations. Reliable measurements and estimates of inventories are essential to this regulatory process. The role of hidden inventories, or residual holdup, as a problem area in nuclear material safeguards was recognized very early in attempts to establish effective safeguards systems in the US.<sup>1</sup>

For holdup measurements, *in situ* assay techniques are preferable to process-disruptive and time-consuming cleanout measurements. The general principles of these nondestructive radiation measurement techniques are well understood, and their applications to safeguards measurements are described in detail in several publications generally available to the nuclear material safeguards community.<sup>2,3</sup> Assay procedures acceptable to regulatory staff are detailed in regulatory guides for the measurement of uranium and plutonium.<sup>4,5</sup> Accuracies in holdup measurements are generally poor<sup>6,7</sup> because of complexities of the residual deposition pattern and the geometries of the facilities. There have been suggestions to avoid obvious bias in standards and facility-specific calibration procedures.<sup>8-11</sup>

Holdup can be measured by neutron and/or gamma-ray measurements.<sup>12,13</sup> Generally, gamma-ray techniques are used because of the ready availability of the instrumentation and the ease of measurement. When attenuation of gamma radiation and geometry become dominant factors, passive neutron measurements are attempted.<sup>14</sup> Also, a noninvasive method<sup>15</sup> employing a <sup>60</sup>Co gamma-ray transmission technique has been employed in the determination of uranium in a centrifuge plant dump trap.

The recognition of the difficulties associated with the estimation of process holdup is reflected in proposals to use secondary methods of measurement.<sup>12,16-19</sup> Design considerations for facilities to minimize holdup have been published in a regulatory guide<sup>20</sup> to meet safety requirements and to ease holdup estimation problems. In the past, there have been attempts to develop estimates of the contents of process vessels with the help of elaborate computer programs using previous inventory measurements, operating data, and on-line process measurements.<sup>21-23</sup> These efforts, still in early stages of development, are intended to be specific to unit operations.

## **B. Background to This Investigation**

As a result of the stringent requirements for the timely detection of the losses of SNM and in recognition of difficulties of measuring process holdup, the US Nuclear Regulatory Commission (NRC) initiated a research program at Los Alamos National Laboratory to evaluate the use of statistical models to estimate the holdup of highly enriched uranium (HEU) at processing facilities. Originally, models were to be developed using historical process measurement data. Holdup problems of HEU in processing facilities and scrap recovery operations were reviewed with several facility operators, and an attempt was made to use available holdup data for developing estimation models. The limited availability of useful data and their large uncertainties made this a futile effort. The next step was to initiate a series of measurements at a few locations in three processing facilities without interfering with normal plant operation and to use these data for estimation models. Although this effort had limited success, the problems associated with holdup measurements and the quality of data required for estimation models became more evident. It was recognized that the development of statistical estimation models had to be preceded by good measurements, preferably with controlled process parameters. As a result, the program objective was redirected toward designing and performing several large-scale experiments to establish reliable relationships between materials throughput and residual holdup. This report highlights these experimental studies of holdup measurement and estimation model development with a brief review of the holdup measurements conducted at processing facilities and a discussion of the potential values and limitations of such measurements for the prediction of residual inventories of SNM at processing facilities.

## **C. This Report**

This final project report includes summaries of various topical and status reports submitted to NRC during this investigation, details of the controlled experiments to gather data, and the use of these data for developing holdup estimators. Section II summarizes the efforts to gather holdup data from processing facilities and the potential value of these nondisruptive measurements for developing estimation models. Sections III-VI summarize the controlled experiments to gather highly reliable data on holdup and the use of these data for developing prediction models of holdup. Section VII is a detailed discussion of all the results and the significance of the major findings of this study. A justification of the use of tracers to measure holdup of uranium during some of the experimental studies, with adequate details on the general principles of tracer applications, are presented in Appendix A. Appendix B provides some introductory information regarding the various statistical techniques employed in developing holdup estimators from experimental data. Detailed results of controlled experiments on holdup studies are presented in Appendix C with summaries and illustrations in the individual sections on experimental studies. Some of the results gathered during our search for holdup data from process facilities are not included because of the proprietary nature of the information.

The findings of this investigation further confirm the difficulties associated with estimating residual SNM in processing facilities. However, the task of estimating holdup inventories can be made easier through the development of process- and plant-specific estimation models. This approach to holdup estimation is less disruptive to plant operations, and the measurements required to develop reasonable estimates of the hidden inventories can be carried out with minimal disruptions in production schedules.

## **II. HOLDUP MEASUREMENTS AT PROCESSING FACILITIES**

This section summarizes the important accomplishments of the attempts to measure and model the holdup of SNM in selected equipment at three processing facilities. In recognition of the limitations of historical data on holdup available from HEU-processing facilities, an attempt was made to perform

nondestructive assay (NDA) measurements on selected equipment to gather data and to determine the feasibility of developing estimation models of holdup from these carefully designed measurements. These measurements were conducted at TA-55 (the Plutonium Processing Facility at Los Alamos) and TA-21 (the HEU Scrap Recovery Facility at Los Alamos). In addition, some of the historical data on uranium holdup in ducts at the high-temperature gas-cooled reactor (HTGR) Fuel Fabrication Facility of GA Technologies, Inc., at San Diego, California, were of value. Although the measurements were made on air filters, air ducts, conversion calciners, and some precipitation and filtration equipment, the measurements on air filters were particularly useful for developing dynamic estimation models. The data obtained from other equipment showed stable or erratic holdup or had serious limitations because of high background levels in the areas of measurement and the apparent lack of stability in the holdup during the measurement. The holdup measurements were conducted for continuous periods ranging from 6 months to 1 yr. It is significant that measurements were made during normal process operations and that there was no additional control over the operation of these facilities for the purposes of holdup measurements. Measurements were made at the convenience of the facility operators with minimal interference with their production schedules.

#### A. Measurement Techniques

The holdup measurements of plutonium on a high-efficiency particulate air (HEPA) filter at TA-55 were performed using a shielded and collimated NaI(Tl) detector installed on top of the glove box about 18 cm from the filter. A multichannel analyzer system was used to scan the gamma spectrum, and the 320- to 470-keV region was integrated to determine the holdup on this filter. Standards used in calibrating this detector system were fabricated to resemble the filter being measured by preparing standards on HEPA filters with known amounts of PuO<sub>2</sub> dispersed on the filter medium. Transmission and attenuation corrections were determined using a thin source of PuO<sub>2</sub>.

All the holdup measurements conducted at TA-21 were performed using a two-channel stabilized assay meter (SAM-2, manufactured by Eberline Corp.) and a <sup>241</sup>Am-doped NaI(Tl) detector shielded and collimated with lead. The filters were measured in-place in steel housings on top of the glove boxes. Thin foil sources of <sup>235</sup>U were used for detector calibration and attenuation corrections.

Most of the holdup measurements of uranium in conversion calciners at TA-21 were done using gamma-assay techniques with a SAM-2 unit. Holdup of uranium in eight batch calciners—four of them in use for 8 yr and the other four in use for 28 yr—were measured for ~15 months. Several sets of measurements, using both thermoluminescent dosimeters (TLDs) and a NaI(Tl) detector, were made when the furnaces were cooled down between process batches. The shielded NaI(Tl) detector with a wide viewing angle was reproducibly placed in front of the entrance to the calciners, which were located in glove boxes, to make periodic measurements of holdup. For thermoluminescent dosimetry, pairs of TLDs were placed at three locations inside the calciner. The measurements were made using CaF<sub>2</sub> (Mn) bulb TLDs and a Model 2810 TLD reader, manufactured by Victoreen Instruments. The TLDs were placed in the calciners at room temperature for 2-4 days and were read within 24 h after exposure to limit the loss of stored energy to <1%. Because of the nonuniform distribution of holdup within the calciners, the TLD data were much more readily normalized than the NaI(Tl)-detector-measured data. The distribution profiles of the uranium holdup inside the calciners were determined using a very small, highly collimated NaI(Tl) interior survey probe.

The holdup measurement data gathered from the HTGR Fuel Fabrication Facility of GA Technologies, Inc., covered 18 months, although not all facilities were in continuous use during this period. These were bimonthly inventory records (historical data). Holdup measurements on the facility exhaust duct system were examined as part of this effort. The NDA measurements of holdup in the duct system used SAM-2 gamma-assay instrumentation.

## B. Holdup Measurement Results

1. **Plutonium Facility Filter Holdup.** The holdup measurement data from the air filter at TA-55 are probably the best on air filter holdup obtained during these measurements. This is due to the location of this filter away from high-background areas; the fixed, shielded position of the detector; and the use of better calibration standards and instrumentation for routine measurements. This is further demonstrated by the confirmatory measurements on the filters at the end of the experiment. The air filter removed was measured using a neutron coincidence counter to determine the plutonium content. The coincidence counter measurement was within 8% of the in-place NDA estimates of the holdup of plutonium. Table I lists the holdup measurement values and process throughput data corresponding to ~13 months.

2. **Uranium Scrap Recovery Facility Air Filter Holdup.** Exhaust air filters from three glove boxes (DB-1, DB-24, and DB-30) at TA-21 were periodically measured to determine uranium holdup and its variation with throughput (Table II). These data indicate that the first three measurements for filter DB-24 were erratic. This was due to the very high background values in that location and the very small amount of uranium on the filter. The data from the other two filters appear to be reasonably well behaved. An estimate of the standard error applicable to all the holdup values in Table II is 0.2 g of  $^{235}\text{U}$ .

3. **Uranium Holdup in Batch Calciners.** The holdup measurements on the calciners were done at the convenience of the facility operators to minimize process disruptions. Also, the routine procedures at the facility were not altered significantly for these measurements. These procedures included periodic cleanout of the calciner with a brush or vacuum cleaner to remove obvious spills and residuals. These activities made it very difficult to gather holdup data that could be correlated with throughput of uranium in the calciners.

Table III summarizes a significant part of the calciner holdup data. However, these data cannot be used for accurate prediction of future holdup because of large variations in the use pattern and cleanout regimen of the calciners during these measurements.

4. **Precipitator and Rotating Drum Filter Holdup.** A precipitation and filtration system at TA-21 was measured for uranium holdup during routine use. The equipment consisted of two stainless steel tanks (one of which was a precipitation vessel with a mechanical stirrer) and a rotary drum filter. The filter medium was a strip of polypropylene fabric placed around the drum. Uranium from the scrap recovery solution is precipitated as uranium peroxide ( $\text{UO}_4 \cdot x\text{H}_2\text{O}$ ) at a pH of ~2.0 using hydrogen peroxide as a precipitant and  $\text{NH}_4\text{OH}$  as a buffer. The slurry is sucked onto the filter strip to separate the precipitated uranium. When the moist cake deposit reaches a thickness of ~3 mm, it is scraped into a collection boat using a doctor blade. Under normal conditions, an 8-kg batch can be precipitated and filtered within 6 h. However, if precipitation does not proceed smoothly, the process is terminated, the filter drum is hand-scraped, the drum is pickled in 10-M  $\text{HNO}_3$ , and the process is continued the next day. Because of differing end-of-shift conditions, the precipitation tanks and the rotary drum filter can have very different end-of-shift uranium holdups. Six measurements made during a 6-month period indicate that the end-of-shift holdup can vary from ~10 g for normal runs to ~150 g for the problematic precipitations, those in which the filters were hand-scraped rather than pickled.

5. **Uranium Holdup in Air Ducts.** Extensive measurements at GA Technologies, Inc., from November 1979 through May 1981 on five duct systems showed no discernible change in the holdup. It should be added that not all the duct systems were in continuous use during the period because of the production schedule for various operations at this facility. The ducts were measured between the glove boxes serviced and the first filter. Figure 1 shows the average holdup in four of the five duct systems that were in use for at least 6 months during these measurements.



TABLE I. Holdup of Plutonium on a Glove Box Air Filter

Throughput (kg)	Holdup (g)	Throughput (kg)	Holdup (g)
3.3	0.6	148.1	53.5
12.7	4.0	151.8	54.7
17.4	3.9	151.8	54.9
17.4	3.8	151.8	56.0
18.9	3.9	155.4	57.6
23.7	5.3	159.2	59.6
25.3	5.4	165.0	61.2
26.2	6.6	166.9	62.3
30.9	6.6	166.9	63.2
30.9	6.7	170.3	64.1
32.6	6.9	170.3	64.1
38.3	8.1	174.3	65.8
38.3	8.0	176.1	65.8
59.5	14.7	176.1	67.5
64.3	16.7	176.1	68.0
71.4	18.0	185.4	68.0
73.3	17.0	194.0	69.9
77.0	19.2	198.3	70.4
85.4	24.1	198.3	71.7
113.3	35.1	202.7	73.9
113.3	35.0	206.2	73.9
113.3	35.2	211.5	76.0
116.9	35.9	211.5	76.2
117.8	37.3	211.5	76.5
122.1	39.0	215.1	76.5
125.5	42.3	215.1	76.25
127.0	42.4	235.3	87.27
127.0	42.7	238.9	88.7
129.2	42.9	242.8	89.5
132.8	43.0	244.6	91.0
132.8	44.0	244.6	91.3
136.6	45.1	255.5	91.3
142.3	48.7	280.6	98.9
142.3	49.9	287.2	100.8
144.1	52.3		

TABLE II. Holdup of Uranium on Exhaust Air Filters at TA-21

Date of Measurement	DB-1		DB-24		DB-30	
	t <sup>a</sup>	h <sup>a</sup>	t <sup>a</sup>	h <sup>a</sup>	t <sup>a</sup>	h <sup>a</sup>
8/11/81	0.1	1.3	0.0	1.7	0.0	1.6
		0.9		2.0		0.6
9/02/81	3.5	2.9	0.6	2.2	4.7	0.5
						0.5
9/22/81	7.0	3.0	1.2	3.1	5.6	2.1,2.5
						2.5
11/05/81	15.0	3.5	2.5	1.1,1.6	9.3	3.7
				1.2,0.8		3.8
11/25/81	18.0	3.7	3.1	0.7	10.0	4.0
				1.1		4.0
12/23/81	22.0	3.5	3.8	1.4	12.0	5.1
				2.4		4.6
2/24/82	32.0	4.9	5.6	1.3	18.0	5.3
				1.4		5.7
4/01/82	39.0	5.4	filter replaced		23.0	6.3
						5.9
6/15/82	50.0	5.8	---	--	filter replaced	

<sup>a</sup>Here t denotes process throughput in kilograms of uranium, and h denotes holdup in grams of uranium.

TABLE III. Grams of Uranium Holdup for Calciners Weighted by Material Profiles

Calciner	Probe	Aug.27,	Sept.23,	Oct.22,	Oct.26,	Nov.5,	Nov.10,	Dec.22,	Mar.15,	April 30,
		1981	1981	1981	1981	1981	1981	1981	1982	1982
35	NaI	11	12	13	13	13	12	11	11	11
	TLD	14			16		14	20	20	19
34	NaI	33	37	37	40	39	36	36	38	32
	TLD	46			47		47	47	51	56
33	NaI	41	47	44	46	45	39	42	41	34
	TLD	61			47		43	49	51	59
32	NaI	30	35	35	35	37	31	33	35	28
	TLD	33			30		28	41	39	43
5	NaI	87	119	132	123	116	117	115	115	105
	TLD	139			92		78	118	108	114
4	NaI	108	157	154	146	141	124	98	103	82
	TLD	123			93		99	82	82	83
3	NaI	113	166	152	136	132	132	126	138	121
	TLD	126			103		96	118	118	118
2	NaI	130	175	165	156	145	155	--	156	141
	TLD	162			149		131	204	167	160

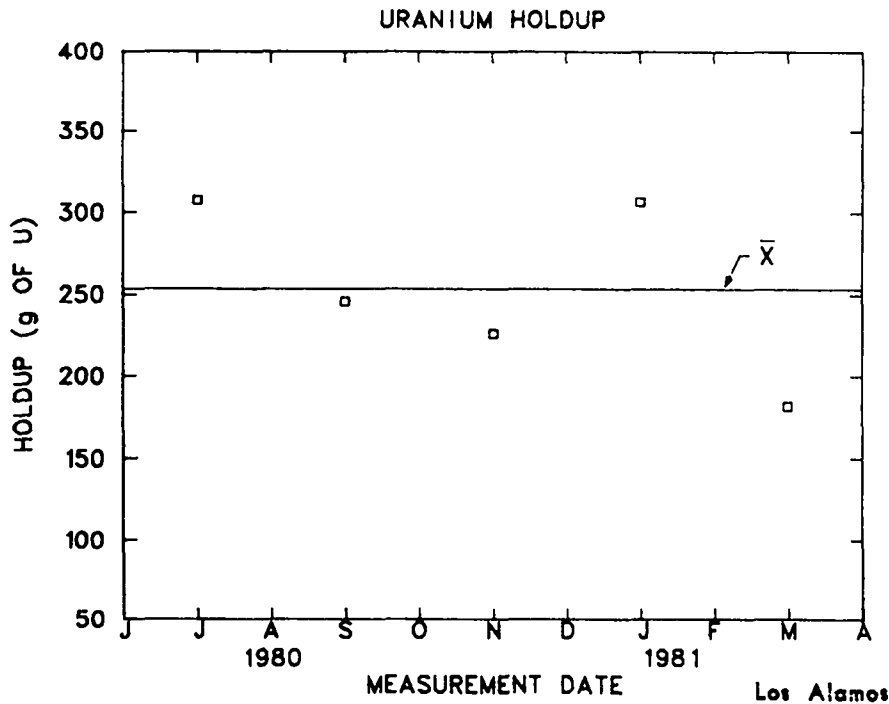


Fig. 1. Total holdup of uranium in four duct systems at GA Technologies, Inc.

### C. Modeling

An air filter at TA-55 was monitored periodically for 13 months. The results are listed in Table I and plotted in Fig. 2. A clear relationship between measured holdup and throughput exists and can be exploited for predictive purposes. That is, given the measurement history of the filter up to a particular time, holdup estimates for future times can be derived.

For these data, a smooth curve is derived that estimates the functional relationship between holdup and throughput under the existing operating conditions. The curve, superimposed on Fig. 2, is

$$\hat{h}(t) = 0.2845t + 0.0003974t^2, \quad (1)$$

where  $\hat{h}(t)$  is the estimated filter holdup (in grams of plutonium) when the process throughput is  $t$  kilograms. The coefficients 0.2845 and 0.0003974 are produced by a least squares fit to all but the final three points. The presence of a quadratic term in Eq. (1) reflects a nonlinearity in the accumulation of material; that is, holdup on the filter does not simply increase proportionally to throughput. Data from the filters used in the dust-generation experiments (Sec. III) exhibit similar nonlinear behavior.

Despite the good overall fit of the model [Eq. (1)] to the data, careful inspection of Fig. 2 indicates a few minor "discontinuities." For example, at  $\sim 235$  kg of throughput, over 200 archive samples of 50 g of  $\text{PuO}_2$  each were opened and poured into a single container, thereby generating a slightly increased amount of dust. The final three measurements, coming after 250 kg of throughput, represent blending and packaging operations, which are relatively dustfree compared with blending and screening. The minor inadequacies of the fitted model for this filter are primarily the consequence of operational changes. Because it is impossible to maintain exactly the same process conditions over time, some judgment may be required to determine whether a model developed in one context applies in another. In the case at hand, it seems clear that the holdup generated during blending/screening is markedly different from that during blending/packaging.

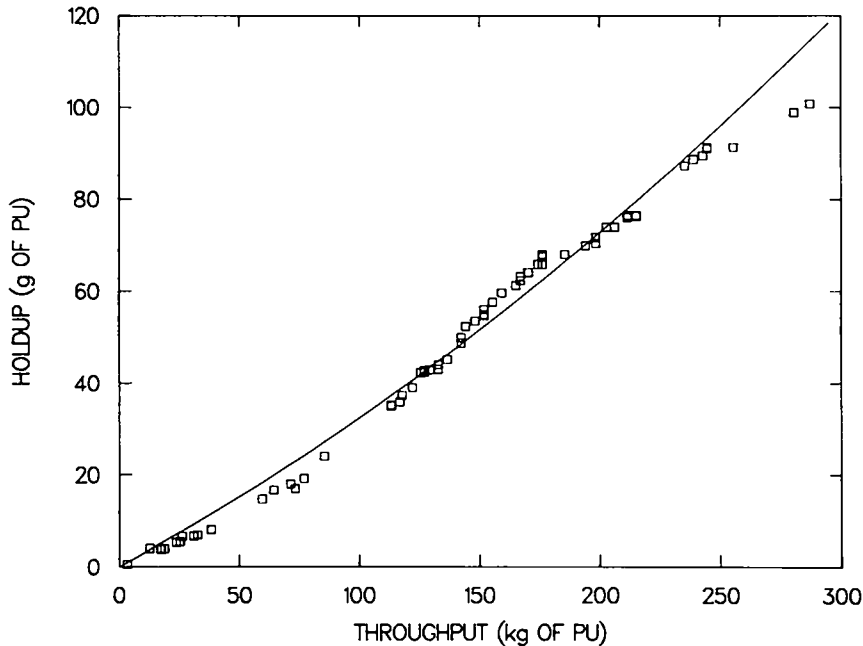


Fig. 2. Measurement history of the holdup of plutonium on an air filter at TA-55.

Central to good predictability are the stable (consistent) operation of the glove box and the high quality of measurement data. These prerequisites may not be achieved for all operations at all facilities, and modeling efforts would suffer as a result. For example, if a holdup model is to be developed solely on the basis of throughput, it is important to hold constant all other factors that affect the accumulation of holdup (such as the level of airflow and the type of material handled for the TA-55 filter). If such relevant factors are varied over time and are unmeasured, they cannot be accounted for in a model. For the filter at TA-55, the process operation remained relatively stable and facilitated useful modeling.

Also contributing to successful modeling here is the high quality of data. Large measurement errors can easily obscure the nature of material deposition and make difficult the extraction of a model. These difficulties can be compounded if data are obtained infrequently. As the accurate accountability of holdup has not often been a high priority at processing facilities in the past and as it is nontrivial to overcome some of the measurement problems, historical data are often of limited value.

The measurement histories for three filters at TA-21 are plotted in Figs. 3-5. As described previously, uranium holdup on these filters behaved somewhat differently from the holdup on filters at TA-55. Consider the filter labeled DB-1. Following two unusual measured values at zero throughput, the accumulation on this filter was approximately linear during the observation. In contrast to the filter at TA-55, the initial measurements here were expected to be nonzero because of residual material in the housing into which the clean filter was inserted; however, no definitive explanation exists of the (apparent) large increase in holdup over the first 3.5 kg of throughput. It is possible that the first two measurements were poor, but there is no firm evidence of this.

The rest of the data are well fit by the model

$$\hat{h}(t) = 2.496 + 0.068t . \tag{2}$$

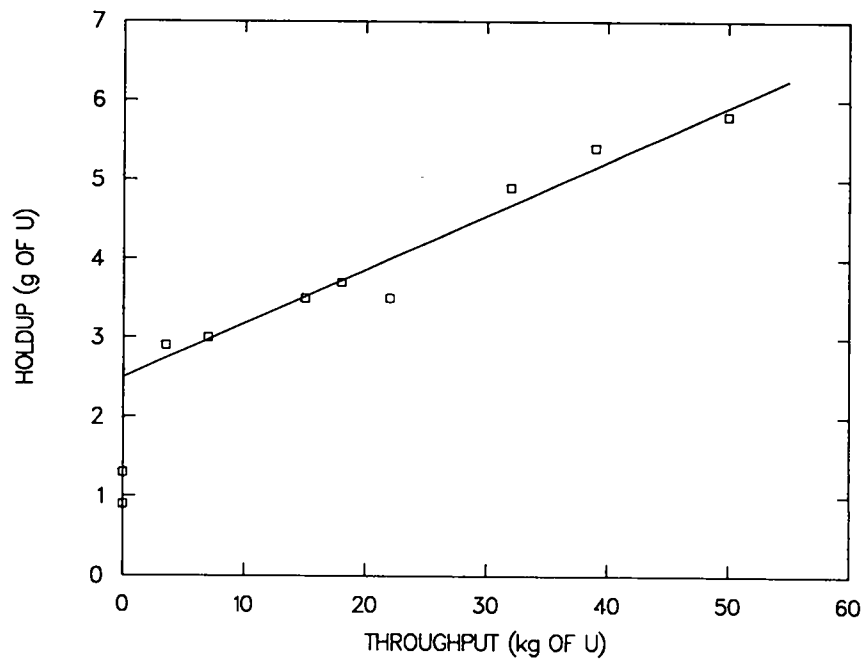


Fig. 3. Measurement history of the holdup of uranium on air filter DB-1.

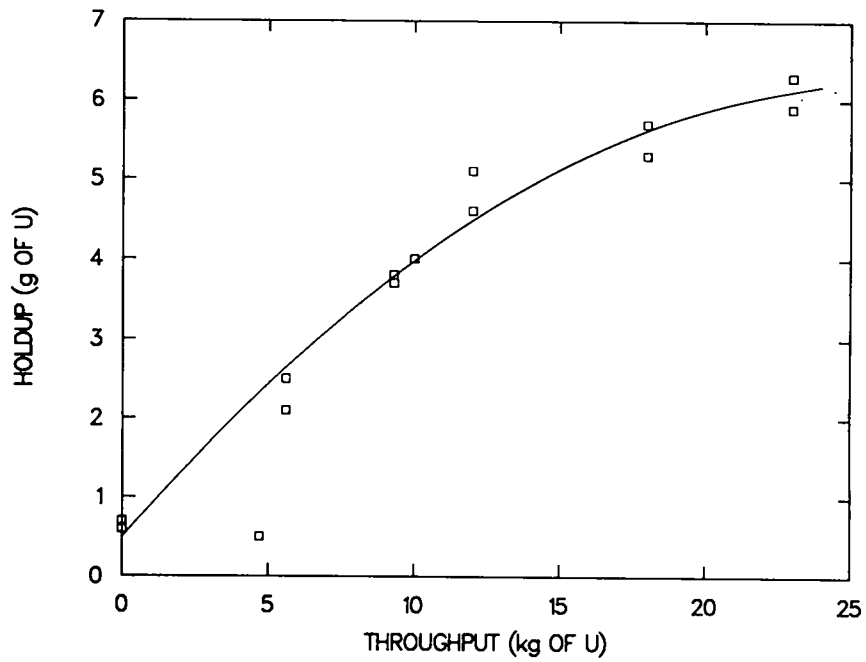


Fig. 4. Measurement history of the holdup of uranium on air filter DB-30.

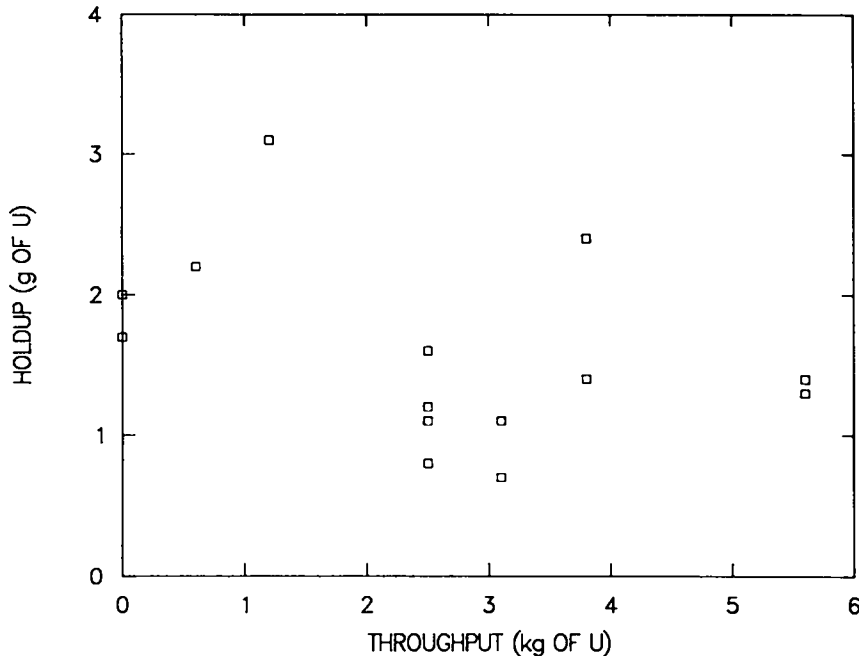


Fig. 5. Measurement history of the holdup of uranium on air filter DB-24.

There is no detectable curvature here in contrast to the previous plutonium blending/screening example and to the filters used in the dust-generation experiments (see Sec. III). Use of Eq. (2) for predictive purposes is straightforward. The future throughput value  $t_0$  of interest is substituted into Eq. (2) and  $\hat{h}(t_0)$  is calculated. The standard deviation of  $\hat{h}(t_0)$  is acquired following standard regression theory and can be used for accountability purposes.

When models such as Eq. (2) are used to "extrapolate" outside the range of the measurement data, there are two important considerations to keep in mind. First, it is implicitly assumed that the nature of the process operation will remain reasonably constant. As seen for the TA-55 filter, the model constructed based on the blending/screening data did poorly in explaining the blending/packaging results. The second consideration involves the nature of the standard deviation of  $\hat{h}(t_0)$ , which increases as a function of  $t_0$ . In other words, prediction of holdup a day in advance is likely to be more accurate than prediction of holdup a month in advance. Although it is certainly possible to substitute into Eq. (2) values of  $t$  well beyond the range of the existing data, the resulting estimates would have very large standard deviations. Thus, extrapolated values should be interpreted with caution. Maintaining good accountability requires that measurements be obtained periodically and used to update the fitted model. The frequency of data collection thus depends on the desired accuracy of estimation.

The procedure for updating the model is a simple one. When a new measurement  $m(t_0)$  is obtained at throughput  $t_0$ , it is compared with its prediction  $\hat{h}(t_0)$  based only on earlier data. The difference  $m(t_0) - \hat{h}(t_0)$  should fall within a prescribed range—for example, plus or minus three standard deviations of the difference. Indeed, control charts of such quantities are useful in evaluating model performance. If  $m(t_0) - \hat{h}(t_0)$  is sufficiently small, then  $m(t_0)$  is added to the previous data and parameters of the model re-estimated based on all available information. If the difference  $m(t_0) - \hat{h}(t_0)$  is outside its prescribed limits, this is an indication that the model may have broken down or, perhaps, that the new measurement  $m(t_0)$  is an outlier; in either case, further investigation is suggested.

The updating procedure works quite well for short-term prediction and testing. For example, given a model based on present and past data, predicted values  $\hat{h}(t)$  and their associated standard deviations can be computed for values of  $t$  in the near future. The predictions can then be combined with other information to assess potential loss in the short term. When the next inventory takes place and another holdup measurement is made, the model is updated as described, and short-term predictions can then be made using the updated model.

Consider now the DB-30 filter (Fig. 4). It appears that this filter is approaching a plugged state by the end of the observation period. The material being processed here is nominally 2.6 wt%  $^{235}\text{U}$ , so 6 g of  $^{235}\text{U}$  represents a total deposition on the filter of well over 200 g. By contrast, the incinerator ash on the DB-30 filter is roughly 15 wt%  $^{235}\text{U}$ , and 6 g of  $^{235}\text{U}$  are equivalent to a 40-g accumulation. When an air filter becomes completely plugged, airflow through it ceases and essentially no material is transported onto it. This phenomenon is reflected in the measurement history (Fig. 4). At such a point, it is necessary to replace the filter.

Over the range of the data, the second-order model

$$\hat{h}(t) = 0.496 + 0.427t - 0.008t^2 \quad (3)$$

captures the increasing deposition. The intercept term, 0.496, in Eq. (3) reflects the presence of residual material in the housing at the time of filter installation. If there were no initial material, a model "forced through the origin" would be appropriate. The concave shape of the fitted curve is the consequence of the plugging and is unique among the filters analyzed during this investigation. Such shapes can also be described by more complex models such as isotonic regressions<sup>24</sup> that impose monotonicity constraints on  $h(t)$ . Certain types of mixture models might also be of use. In any case, it seems clear that the amount of holdup on the filter is rapidly approaching a limit.

Finally, consider the measurement history of the DB-24 filter (Fig. 5). These data are quite erratic, not exhibiting sufficient temporal continuity<sup>25</sup> for modeling. Very high background levels (or poor signal-to-noise ratio) made the nondestructive measurement of the relatively small quantities of material difficult. Lacking information from external sources, such as from analyses of other filters "known" to behave in the same fashion as this one, there is little on which to place confidence in a model when the signal-to-noise ratio is very low.

The measurement of the conversion calciners at TA-21 provided much useful information, and the controlled experiment (Sec. V) on calciner holdup benefited as a result. However, the data derived were not amenable to modeling for reasons described below. Basically, the particular constraints imposed by processing operations prohibited construction of a model capturing all the relevant factors known to affect the holdup.

An initial difficulty arose in attempting to obtain a single NDA measurement of each calciner, that of overcoming the effects of nonuniform deposition. To some extent, this difficulty exists with respect to nondestructive measurement of many other objects. The nonuniform deposition was caused primarily by the nature of the construction, use, and maintenance of the equipment and was the largest single source of error for these measurements.

There are alternative approaches to overcome the effects of nonuniform deposition. One is to begin by carefully characterizing the nonuniformity, which can be done by obtaining measurements from individual locations. For example, TLDs could be inserted at various places within the calciner to provide for such a characterization. A future single-measurement count rate can then be converted to quantities of material after properly accounting for the holdup profile. Of course, such a measurement procedure implicitly assumes relatively little change in the deposition pattern over time, but few alternatives exist when external constraints allow for only a single measurement. If several measured values are obtained from distinct locations, a more exact profile model can be constructed and more accurate single-measurement corrections can be made. The analysis of the pulse-column data (Sec. IV) is a good example of profile estimation.

A final note of interest regarding the calciner measurements involves the cleaning of the calciner. For most processing operations, a "typical" state of cleanliness exists. In this case, the calciners were brushed out after each calcination. Starting October 1981, they were vacuumed after each calcination, and the material collected was sent to recovery. Obviously, such activities greatly influence the residual holdup—observed changes in measured values over time may reflect more on the levels of the cleanout efforts than on anything else. For example, the scintillation detector data indicated that the calciners tended to become cleaner as the vacuuming continued. The factor "cleanout efficiency" is quite difficult to quantify for incorporation into a model, and when such important factors are allowed to vary considerably over time, there is little hope for successful modeling. Such was the case for the calciners.

Data obtained from fuel fabrication facility ducts at GA Technologies, Inc., where holdup had accumulated for many years, offered the possibility of studying the process under near-steady-state conditions. It was hoped that changes in holdup over the brief period of observation (brief relative to duct lifetime) would be minor and that the effects of other factors—such as duct geometry—could be evaluated. For example, the amount of holdup per unit area of interior surface at an elbow might be a predictable multiple of the amount per unit area for the preceding straight segment.

Unfortunately, it was not possible to reach substantive conclusions regarding the effects of such factors. The major problem lay in the quality of measured values. From counting statistics and replicate measurements, it was apparent that a low signal-to-noise ratio largely obscured the observation of small quantities of holdup. Unusually high background levels from thorium daughters at the facility were the primary cause, and it was very impractical to circumvent this difficulty through the use of heavy shielding or through the removal of the ducts to a better environment for measurement.

Estimating geometrical effects from the individual duct systems was quite difficult. Based on results from areas of larger holdup (and thus better signal-to-noise ratio), the anticipated conclusion that elbows serve as accumulation points was clearly substantiated. Making a more definitive statement to quantify this effect would be ill-advised because of the magnitudes of measurement errors and, perhaps, because of "interaction" with other relevant factors; that is, the "elbow effect" may not remain constant over all combinations of other factors such as duct composition, duct diameter, and type of equipment serviced.

Quantification of other effects is similarly precluded. Though steady-state models (Sec. V) might be used to provide estimates of holdup at individual locations, it is quite difficult to make comparative statements regarding various factors affecting holdup.

### III. EXPERIMENTAL STUDY OF URANIUM HOLDUP IN A DUST-GENERATING FACILITY

The problem of fissile materials accounting in fuel material preparation and fabrication facilities is increased by the difficulty of accurately estimating the amount of SNM that is held up as residuals in glove boxes, ducting, ventilation filters, and other processing equipment. The residual holdup associated with dust-generating operations can be a serious safety problem as well as a materials accountability problem. The safety problem can be minimized by facility design considerations and periodic radiation monitoring with appropriate portable instruments followed by cleanout of areas with large material accumulation potentials. However, there are no simple noninvasive procedures for reasonable estimations of residual holdup of SNM in glove boxes, ducts, and ventilation filters. The recognized limitations of historical data on residual holdup in dust-generating facilities have prompted this attempt to perform controlled experiments and to develop holdup data as a function of material throughput.



## A. Facility Description

An experiment was designed to generate uranium holdup data to examine the build-up of uranium dust on glove boxes, exhaust ducts, and exhaust air filter surfaces at the HTGR fuel fabrication facility of GA Technologies, Inc. This facility contains coated-particle and fuel rod-production facilities, scrap recovery lines, low-level combustible incineration equipment, and fuel storage areas. At the time of the holdup experiments, this plant was processing only fertile material (thorium). It was, therefore, possible to dedicate glove boxes and duct/filter systems containing fissile material and the necessary measurement equipment for this task.

The facility is equipped with air ducts of three different designs. Many of these ducts are made from round, spiral-lockseam, galvanized steel. The ductwork varies in material thickness from 1 to 2 mm. Also used extensively throughout the facility are round polyvinyl chloride (PVC) ducts. These ducts have a wall thickness of  $\sim 6.0$  mm with diameters ranging from 10 to 40 cm. In addition, there are spiralwire-reinforced rubber ducts. The spiral-lockseam ducts use automatic air-control (constant volume) valves to control airflow. These controllers are generally preset at 100 cfm ( $2.8 \text{ m}^3/\text{min}$ ) and serve the ducts leading to several glove boxes. Small ducts servicing the glove boxes, where significant quantities of airborne SNM are generated, were equipped with prefilters. The prefilters are located as close to the equipment enclosure as possible (1-3 m). Small ducts are combined into large ducts that route the exhaust air to a final filter bank. In this filter bank, the exhaust air passes through 5-cm-thick medium-efficiency filters, called intermediate filters, and finally through a bank of large HEPA filters.

A glove box and ventilation system, using materials and designs similar to those used at GA Technologies, Inc., for the uranium- and thorium-processing equipment, was set up to generate uranium dust and for *in situ* holdup measurements. Figure 6 shows a schematic diagram of the glove box and duct/filter system, occupying  $\sim 6 \times 5 \times 7$  m.

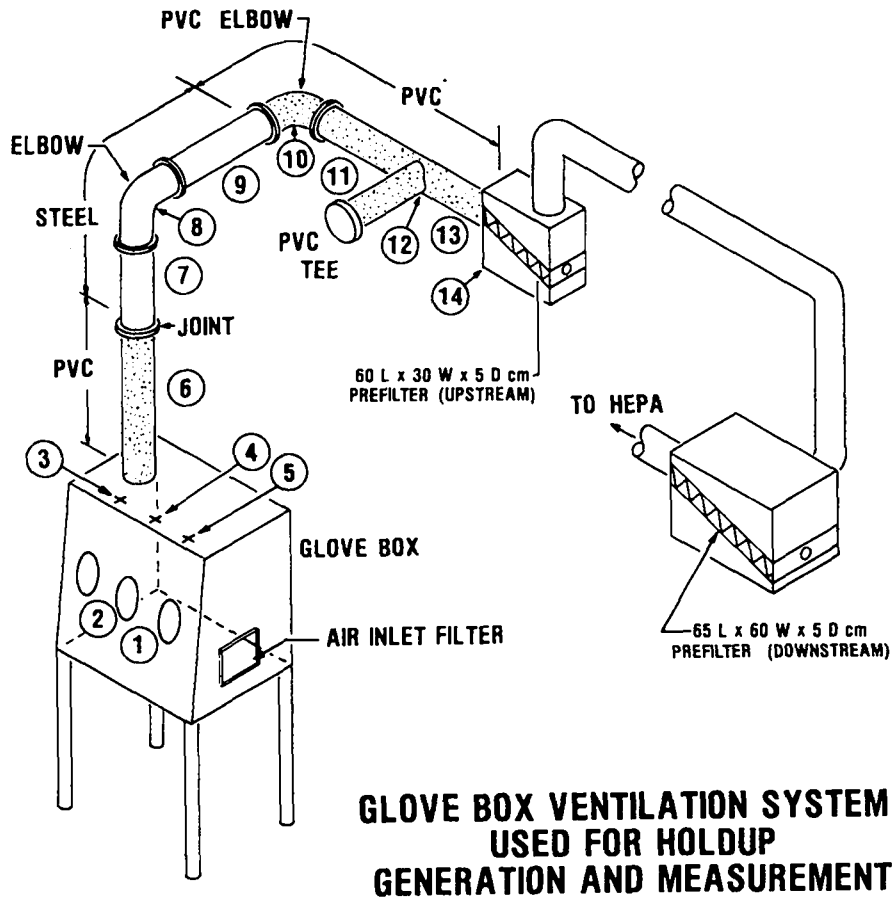
As shown in the illustration, 10-cm-diam ducting made of spiral-lockseam galvanized steel as well as PVC ducting were used in the construction of the exhaust air system. Elbows and tees constructed from both types of materials were also included. To facilitate rapid teardown and reconstruction of this ventilation system, the ducting was not attached to the facility structure permanently but was held together using rubber joints and clamps.

The glove box ( $1.5 \times 0.9 \times 1.2$  m) was located so that the ducting could be connected to existing prefilter boxes and airflow controllers within the facility (Fig. 6) and to provide easy access for measurement equipment. The locations of 14 background measurement points used in the experiments are detailed in Table IV.

The prefilters are located in steel enclosures, equipped with pressure differential gauges to monitor airflow through the filter. The prefilter media was a nonwoven glass-fiber fabric supported on a wire cloth grid, pleated to a 2-in. depth with an "open" rounded pleat edge design, and supported within a water-resistant paperboard frame. They were medium-efficiency filters with an efficiency rating of 92%. To further capture the SNM in the ventilation system, the filtration system used for this experiment was modified to accommodate two prefilters (shown as upstream and downstream filters on Fig. 6) before the intermediate and absolute filters.

All HEPA absolute filters and their associated ventilation mechanisms are located centrally rather than located at or near the equipment itself. The absolute filters, rated as 99.97% efficient, were made of fire-retardant particle board frame with a waterproof glass-mat filter media resistant to organic solvents, acids, alkalis, and fire. The absolute filter was immediately preceded by an "intermediate" filter located in the HEPA cabinet to extend the life of the HEPA filter.

A mechanical dust-generating apparatus, designed and fabricated for this experiment, is shown schematically in Fig. 7. The dust generator consisted of (1) a delivery and receiving bottle with funnel assembly, (2) a vibrator assembly to assist uniform material flow from the delivery to the receiving bottle, (3) a modified bottle cap with adjustable orifice for flow adjustments, and (4) adjustment for drop angle and height.



### GLOVE BOX VENTILATION SYSTEM USED FOR HOLDUP GENERATION AND MEASUREMENT

Fig. 6. An isometric view of the experimental facility.

TABLE IV. Locations of Measurement Points

Measurement Point <sup>a</sup>	Background Measurement Location
1	60 cm behind glove box
2	60 cm behind glove box
3	60 cm to left of glove box
4	60 cm in front of glove box
5	60 cm to right of glove box
6	45 cm to right of assay point
7	45 cm to right of assay point
8	45 cm to right of assay point
9	30 cm below assay point
10	30 cm below assay point
11	30 cm below assay point
12	30 cm below assay point
13	30 cm below assay point
14	60 cm to right of prefilter housing

<sup>a</sup>These numbers refer to points marked in Fig. 6.

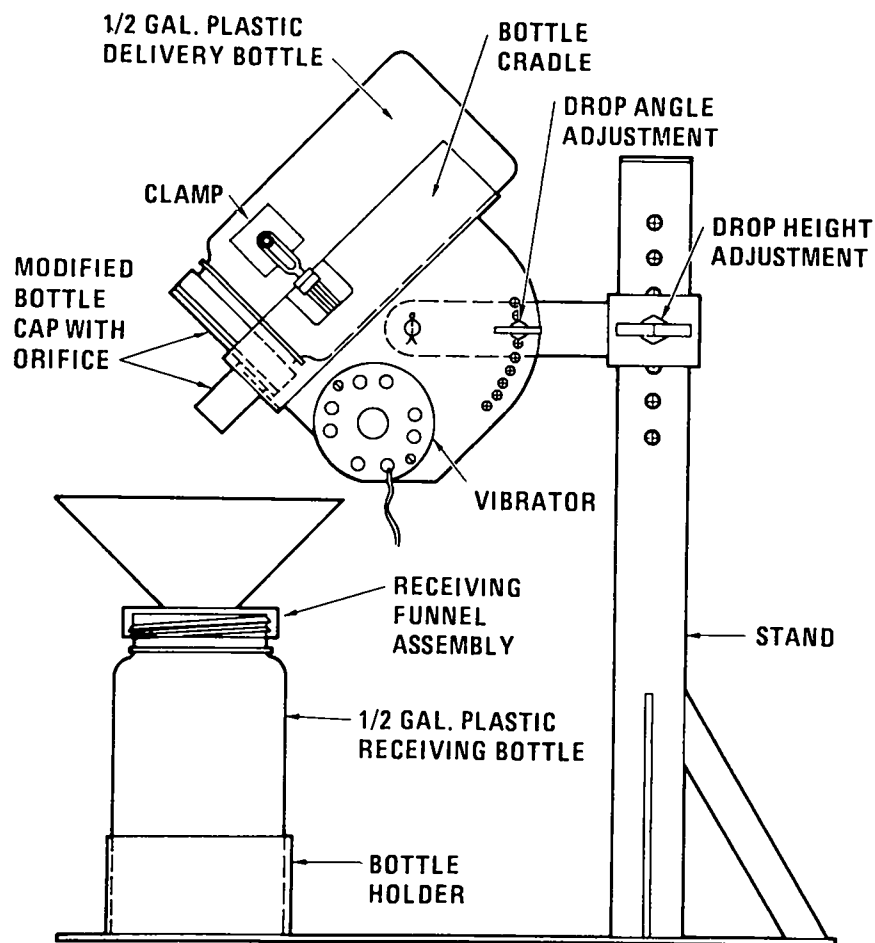


Fig. 7. A schematic of the dust-generation apparatus.

## B. Experimental Procedures

For the *in situ* measurement of holdup in the glove box and ventilation system, commercially available gamma-ray instrumentation [NaI(Tl) detector and single-channel analyzer] was used. The critical aspect of these measurements, however, is the precise measurement of small depositions of uranium (milligram quantities) in the system. The estimation of these depositions by the direct measurement of gamma rays emitted from  $^{235}\text{U}$  has serious limitations caused by the low specific activity of the nuclide and the high background levels of thorium daughter radiations in the process facility.

**1. Tracer Application.** The sensitivity of such holdup measurements can be improved significantly by the judicious incorporation (spiking) of trace levels of radionuclides with high specific activity and desirable gamma spectral characteristics. The principles of the uses of tracers and their unique advantages are discussed in Appendix A.

The tracer material was prepared by irradiating several sealed quartz capsules, each containing  $\sim 200$  mg of  $\text{U}_3\text{O}_8$ . For experiments involving incinerator ash, samples of ash materials were irradiated to prepare the tracer. The irradiations were performed in the neutron flux of a TRIGA Mark-F Research Reactor Facility. The core position had a thermal flux of  $\sim 2 \times 10^{13}$  n/cm $^2$ ·s. Irradiation time varied from  $\sim 30$  to 60 min depending on the sample material and the activity desired in the sample. Thus,  $\sim 10^{16}$

fissions were induced in the 200 mg of 95%-enriched  $U_3O_8$  sample. This amounts to  $<10^{15}$  nuclides of the tracer  $^{95}Zr$ - $^{95}Nb$  with an initial activity of  $\sim 3 \times 10^7$  Bq. Following irradiation, the sample was left in the reactor pool for a cooling period of  $\sim 2$  weeks to optimize the relative gamma flux of the desired fission products before being used for the experiments.

The homogenization or blending procedure following irradiation and cooling was as follows: The irradiated samples were transferred to a large mortar and pestle along with 150-200 g of the bulk material. The materials were ground together to improve blending in the bulk material. Two or four irradiated capsules (400-800 mg of  $U_3O_8$  or incinerator ash) were blended to obtain the desired activity level in the bulk sample. The ground material and the bulk material were transferred to a V-blender and blended for 20-30 min. At least five grab samples were then obtained from the blended material for homogeneity determination. Each sample was counted to determine its activity (net counts per minute per gram of sample) from the desired fission products. The blended material was considered homogeneous if the relative standard deviation on the average activity was  $<5\%$ . Standards were prepared from the blended material for daily calibration of the counting system.

**2. Measurements.** A 5- × 5-cm NaI(Tl) scintillation detector (integral assembly) was used with a Ludlum Model 2218 dual-channel analyzer to measure the *in situ* activity from uranium holdup. A lead shield/collimator was constructed for the detector to provide a 7.5-cm-long collimator and 1.5 cm of shielding around the detector that tapered to 0.75 cm around the photomultiplier tube. A 1024-channel multichannel analyzer (Canberra Series 30) was used in parallel with the single-channel analyzers in the Ludlum dual-channel analyzer to provide a pulse-height spectrum of the fission-product gamma rays and an energy calibration to determine the peaks of interest. The multichannel analyzer was also used to qualitatively determine the spectrum shifts on a day-to-day basis. A 6-m-long shielded coaxial cable carried the signal from the photomultiplier tube to the Ludlum instrument amplifier. The same cable was used to supply the high voltage to the tube.

A separate 7.5- × 7.5-cm NaI(Tl) crystal/single-channel analyzer counting system was used to assay cleanout materials from dust generation. This counter was located in a low-background area of the facility and used a totally enclosed, lead-shielded assay chamber to maximize the signal-to-background ratio and hence improve the sensitivity of the measurements. This system gave a signal-to-background ratio improvement of  $\sim 3$  over the *in situ* measurements, which coupled with the fixed detector configuration, allowed for greater precision and accuracy in the measurements.

All airflow measurements were made in linear feet per minute of air flowing across the air inlet to the glove box. These measurements were made with an Alnor Junior Type 8100 hand-held velometer for airflows below 800 ft/min (245 m/min). For the higher air velocities, an Alnor Series 6000 P velometer, capable of measuring air velocities up to 10000 ft/min (3000 m/min), was used. This velometer used a pitot tube arrangement with a probe, which was inserted perpendicular to the laminar airflow. To accommodate this velometer, a 75-cm-long rectangular duct extension was attached to the air inlet filter, allowing several measurements across the width and length of the tube. Care was taken that these measurements were not obtained at points very close to the glove box face or the duct sides as the airflow patterns along these edges may vary because of "end effects." With the Alnor Junior velometer, six readings were usually recorded at the face of the air inlet filter as a measurement of the airflow into the glove box.

### C. Dust Generation And Holdup Measurements

Uranium dust was generated from three different materials: an incinerator ash containing  $\sim 10\%$  uranium, a finely powdered  $U_3O_8$  with particle size up to 45  $\mu m$ , and a coarse  $U_3O_8$  powder with particle size up to 200  $\mu m$ . Each experiment involved 10 dusting cycles wherein 1 kg of the material was reproducibly poured from the delivery bottle of the mechanical dust generator to the receiving bottle. The

airflow through the glove box was set at one of three settings (high, medium, or low) by adjusting a MITCO control valve located beyond the exhaust filter of the experimental system (Table V).

Seven separate experiments were conducted using various airflow rates and materials combinations as shown in Table V. Briefly, the dust-generation and holdup measurement procedures included the following steps:

1. The delivery and receiving bottles of the mechanical dust-generating apparatus were initially weighed. A known quantity of  $U_3O_8$  (or ash) was placed inside the delivery bottle and mounted on the dust generator.
2. The airflow control valve was adjusted to get the desired flow rate at the inlet of the glove box as measured by a velometer.
3. Dust generation was initiated by opening the spout of the delivery bottle and starting the vibrator attached to the stand (Fig. 7). The dust generator was located in the glove box such that the airflow through the glove box flowed across the falling  $U_3O_8$  (or ash) and carried the dust through the glove box, ducts, and filters.
4. The processes of pouring the delivery bottle contents into the receiving bottle and repouring the material to generate dust were continued until  $\sim 10$  kg of the material was poured from the delivery bottle. The pouring of the contents of the delivery bottle into the receiving bottle constituted one dusting cycle. Each experiment had 10 such cycles.
5. The delivery and receiving bottles were reweighed to determine the weight loss of material during the dusting cycle.
6. The bulk  $U_3O_8$  (or ash) in the bottles was removed from the glove box and placed in a shielded storage area.
7. The *in situ* holdup of uranium was measured at 14 points (Fig. 6 and Table IV) using the shielded portable NaI(Tl) crystal and the Ludlum dual-channel analyzer described in Sec. III.B.2. These measurements were made after either each cycle or a pair of cycles. At the end of the 10th dusting cycle, the airflow was reduced to minimize material movement in the ventilation system, and replicate *in situ* measurements were made.
8. At the end of each experiment, the ventilation system serving the experimental glove box was carefully dismantled and cleaned out using rags. These rags were carefully collected and placed in special containers, and the amount of uranium in these cleanout samples was determined nondestructively using a separate counting system described in Sec. III.B.2.

These steps of dust generation, *in situ* holdup measurements, and cleanout measurements were repeated for the seven experiments.

TABLE V. Experimental Conditions

Materials	Airflow		
	Low (5 cfm) <sup>a</sup>	Medium (45 cfm) <sup>a</sup>	High (100 cfm) <sup>a</sup>
Fine $U_3O_8$	Expt. 1	Expt. 2	Expt. 3
Ash	Expt. 4	Expt. 5	Expt. 6
Coarse $U_3O_8$	---	---	Expt. 7

<sup>a</sup>1 cfm = 28.32 L/min =  $2.832 \times 10^{-2}$  m<sup>3</sup>/min.

## D. Experimental Results and Discussion

Seven experiments were conducted during this investigation of holdup of uranium in a dust-generating operation. The highlights of the results are presented in this section. A more detailed discussion of the modeling of holdup is given in Sec. III.E, and the results of NDA measurements employing the radioactive tracer and gamma-ray spectroscopy are provided in Tables C-I through C-XV.

In general, the effects of varying operating conditions were reasonably predictable. For example, the change in measured holdup of uranium dust on the exhaust air filter as a function of material throughput and airflow level is illustrated in Fig. 8. As expected, holdup increases with throughput as well as with airflow.

Data collected at the first elbow, (measurement location 8 in Fig. 6) provide another example of material deposition as a function of throughput as shown in Fig. 9. The dependence of holdup on operating conditions is not as well defined as for the filter because of the relative magnitude of measurement errors. The elbow and filter represent the two extremes of the kind of holdup data obtained during this experimental study.

The quality of the holdup estimates obtained was generally quite good. Weight-loss values, which are simply the differences between the amount of materials at the start of an experiment and the amount remaining at the end of dusting operations, were obtained for each of the seven experiments. A comparison of gravimetric weight-loss values with their associated model-based estimates (which used only NDA data) gives the best measure of the accuracy of the estimate of overall system holdup. Tables VI and VII summarize this information.

For the uranium dust-generation experiments described above, holdup was estimated with roughly 20% accuracy. Had the objectives of the work been somewhat different, accuracy of ~10% could have been achieved with the same overall level of effort. This would have entailed devoting proportionally more resources toward measurement of the glove box floor and filter, which combined represent >80% of the total system holdup but received only about one-third of the measurement effort. Proportionally more work on instrument calibration also would have improved the final holdup estimate. As it was, much attention was given to examination of materials deposition in the 5-m length of ductwork that connected the glove box and filter even though a relatively small amount of holdup was involved. This attention enabled the development of useful models for the various components of the system, such as vertical and horizontal sections of ductwork about measurement points 6-7 and 11-13. Although differences were observed in the pattern of material deposition along the length of the ductwork, no relationship between holdup and the materials (metal and plastic) used in the construction of this system was identified.

In practice, it is not possible to obtain measurements analogous to the weight-loss values listed in Table VI. Data collection usually involves either *in situ* measurements acquired through use of NDA instrumentation or measurements made following a shutdown and cleanout of process equipment. The latter procedure is more time consuming and process disruptive. Of these two alternatives, better information is typically available following a cleanout since holdup measurements can be obtained in a better environment and, perhaps, using more accurate analytical methods. However, it should be recognized that a cleanout cannot recover 100% of the actual holdup because a small residue invariably remains. In the context of this experimental study, the gravimetric measurements of the loss of uranium from the dust generator is the best estimate of the total holdup within the system. Of this amount, the measured regions retain most of the uranium; a small amount has escaped the prefilter. An examination of Table VII shows that the "gravimetric" values of the holdup derived from the weight loss of uranium in the dust generator are generally higher than in most other processes.

When care is exercised in *in situ* measurements, however, results can be comparable with cleanout. Such was the case in this experimental study (Table VII). Because of the controlled experimental conditions, use of tracers, and frequent collection of data, estimates of holdup based on *in situ* measurements were as good as those based on cleanout. However, there was no systematic attempt made to measure the amounts of uranium that may have passed through the prefilter and escaped from the

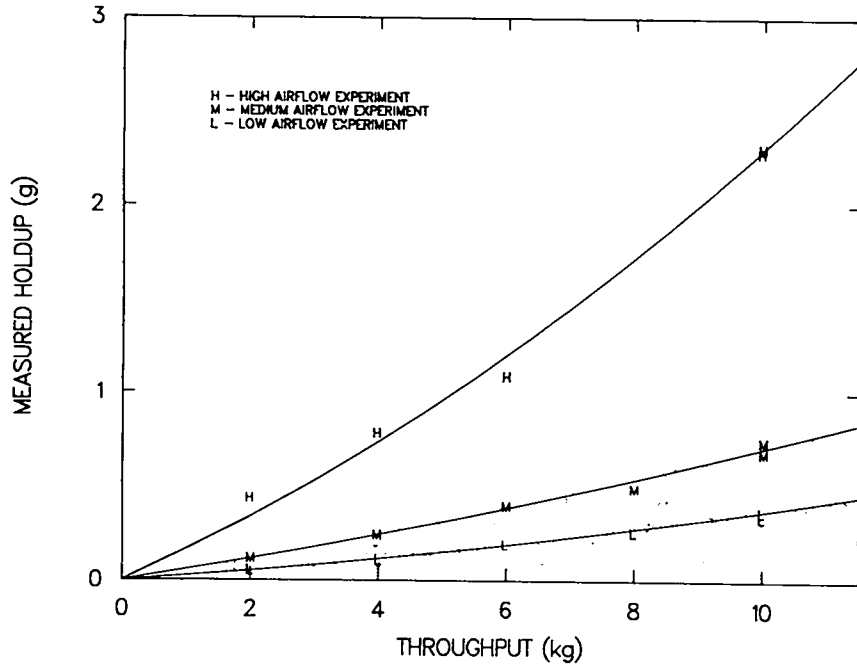


Fig. 8. Change in holdup as a function of throughput of fine  $U_3O_8$  powder at the exhaust air filter (measurement location 14).

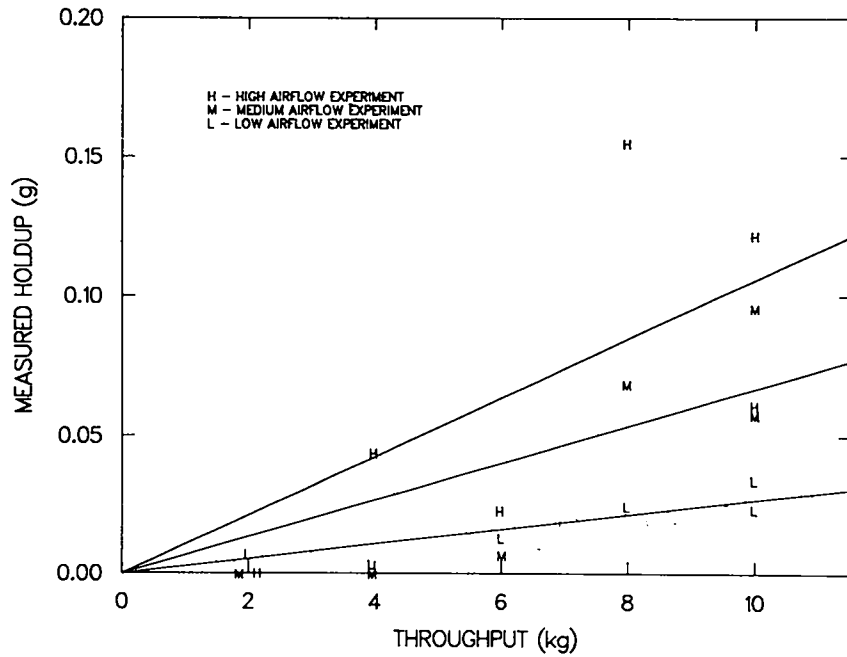


Fig. 9. Change in holdup as a function of throughput of fine  $U_3O_8$  powder at the first elbow of the ductwork (measurement location 8).

TABLE VI. Comparison of Model-Based Estimates with Weight-Loss Values<sup>a</sup>

Material Type	Airflow Level		
	Low (g)	Medium (g)	High (g)
Fine U <sub>3</sub> O <sub>8</sub>	3.56	3.11	6.22
	(4.19)	(3.20)	(6.20)
	15%	3%	1%
Ash	1.66	1.20	2.50
	(1.31)	(1.53)	(3.06)
	27%	22%	18%
Coarse U <sub>3</sub> O <sub>8</sub>	---	---	1.60
	---	---	(2.26)
	---	---	29%

<sup>a</sup>For each set of experimental conditions, the first value is the estimated total system holdup obtained by modeling. The second value (in parentheses) is the measured weight loss of material and represents the "best" figure for the actual amount of material in the system. The final value is the relative error, or difference between estimate and weight loss divided by weight loss. As is often the case with historical data, the relative error here is larger when small amounts of material are involved because the background is higher relative to the source.

TABLE VII. A Comparison of Holdup Estimates by Different Methods

Experiment No.	Material	Aiflow	Estimated Holdup (g)		
			NDA	Cleanout	Gravimetric
1	Fine U <sub>3</sub> O <sub>8</sub>	low	3.56	3.59	4.19
2	Fine U <sub>3</sub> O <sub>8</sub>	medium	3.11	2.70	3.20
3	Fine U <sub>3</sub> O <sub>8</sub>	high	6.22	5.10	6.20
4	Ash	low	1.66	1.06	1.31
5	Ash	medium	1.20	1.25	1.53
6	Ash	high	2.50	2.51	3.06
7	Coarse U <sub>3</sub> O <sub>8</sub>	high	1.60	1.89	2.26



monitored regions of the experimental glove box/ventilation system. It should be reiterated that the spiking of material in the experiments allowed for considerable improvement in the quality of measurement data over what would have been otherwise attained.

The findings of this investigation confirm that estimation of uranium holdup in a dust-generating operation using direct NDA measurement is a nontrivial, time-consuming task. Cleanout measurements to accomplish the same objective, although highly disruptive for a facility operation, may not in all cases provide any greater confidence in the holdup estimates.

It is possible to obtain high-quality estimates of holdup from either modeling of *in situ* measurements or from cleanout measurements if a sufficient effort is invested. The potential value of holdup estimation models should be judged in the context of other options that are available and the costs and process disruptions that accompany such efforts.

## E. Modeling

A generic report<sup>25</sup> presented a nontechnical discussion of the benefits and limitations of the statistical modeling of materials holdup. Here, models for several of the components are introduced and used to develop a single model for estimating holdup in the entire glove box/ventilation system.

1. **The Filter.** The development of a holdup estimation model for an exhaust air filter, based on the physical features of the filter system, the characteristics of the airflow, and/or the materials suspended in the airstream, is extremely difficult. However, careful measurements of the materials retained on an exhaust filter over time and a knowledge of the materials throughput of the system provide a simple, reliable method of developing a holdup estimator. Previous work on the air filter at TA-55 addressed this topic, and a model demonstrated in Sec. II.C to have value for holdup estimation on exhaust filters is

$$h(t) = \alpha t + \beta t^2,$$

where  $t$  denotes the throughput of the process as measured from the time the filter was installed and  $h(t)$  is the accumulated holdup at throughput  $t$ . The unknown parameters  $(\alpha, \beta)$  depend on operating conditions and are usually estimated from the data at hand. Given estimators  $(\hat{\alpha}, \hat{\beta})$  of the parameters, the associated function is

$$\hat{h}(t) = \hat{\alpha} t + \hat{\beta} t^2,$$

which can be used to provide holdup estimates for known throughputs, even for those for which no measurements are made.

Consider the data from the low-airflow run of the  $U_3O_8$  experiment (Fig. 10). The fitted model here is

$$\hat{h}(t) = 0.0232t + 0.0014t^2,$$

where throughput is measured in kilograms and holdup is measured in grams. Obtaining estimated values is straightforward. For example, at the conclusion of the experiment,  $t = 10$  kg and the estimated holdup is  $\hat{h}(10) = 0.372$  g. A similar approach can be pursued for the results of other experiments, though the values of  $(\hat{\alpha}, \hat{\beta})$  will be different for different operating conditions (Fig. 8).

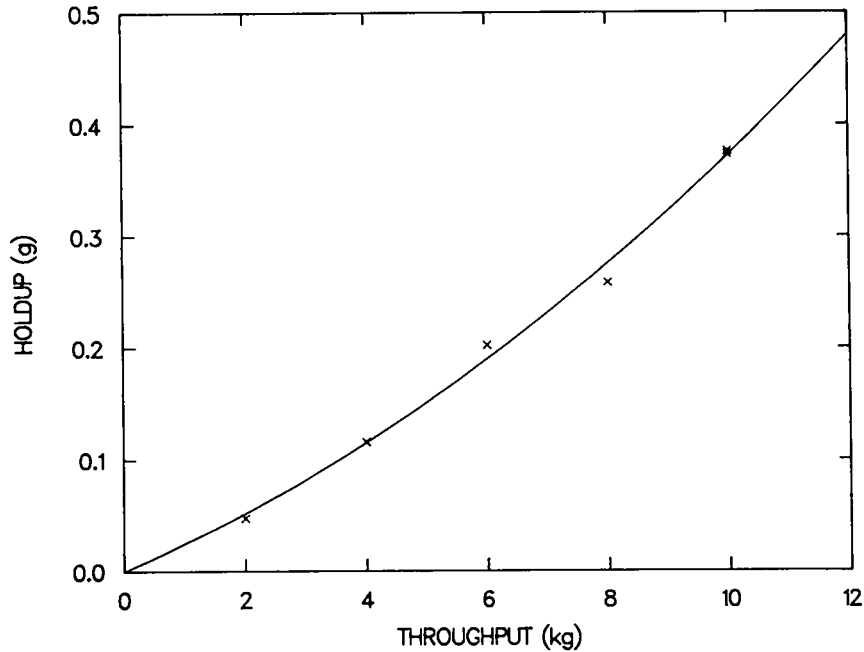


Fig. 10. Holdup of uranium on the filter from the dust-generation experiment at low airflow.

2. Elbows. Consider the elbow at measurement point 8 in Fig. 6. Because of the geometry involved, the amount of holdup (per unit area) near the elbow can be markedly different from that at the top of the vertical segment associated with measurement point 7. This spatial "discontinuity" means it is useful to model the elbow separately.

The measurement history for the elbow at location 8 for the low-airflow experiment with  $U_3O_8$  is plotted in Fig. 11. Note the increase in holdup as a function of throughput. Unlike data from the filter, however, there appears to be no strong evidence of a nonlinear increase. The holdup model for the area about location 8 at throughput  $t$  is then

$$\hat{h}_8(t) = \hat{\alpha}_8 t,$$

where the estimated parameter  $\hat{\alpha}_8$  is obtained from the observed data.

Similar models for the areas corresponding to measurement points 9 and 10 can also be derived; that is,

$$\begin{aligned} \hat{h}_9(t) &= \hat{\alpha}_9 t \text{ and} \\ \hat{h}_{10}(t) &= \hat{\alpha}_{10} t. \end{aligned}$$

In all cases, it is possible that if the measurement histories were based on a longer time period, a model nonlinear in  $t$  might be appropriate. For the cases at hand, though, linear approximations are adequate.

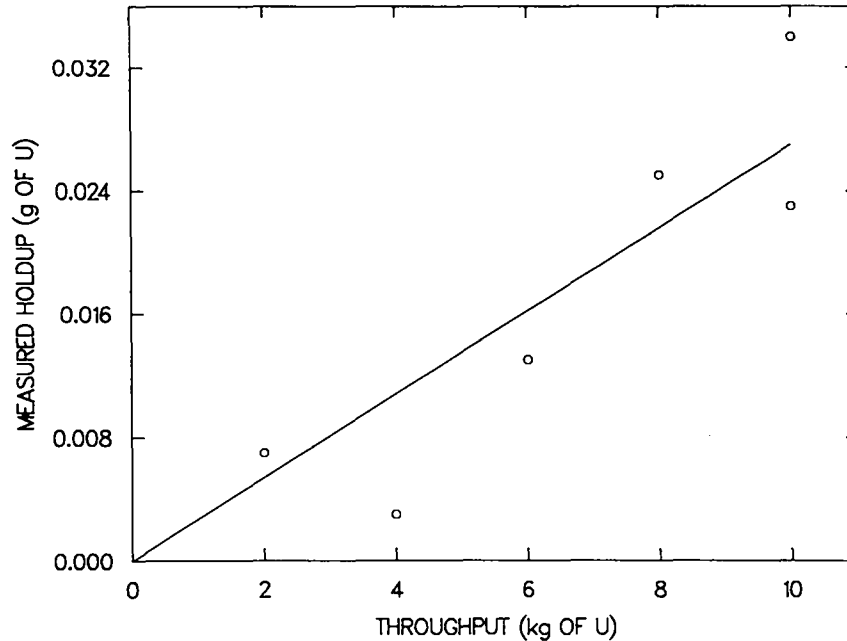


Fig. 11. Holdup measurement history (for the low-air-flow experiment with  $U_3O_8$ ) at measurement location 8.

3. **The Glove Box Floor.** Modeling of the filter and elbows involved capturing the measurement history by a function of one variable,  $\hat{h}(t)$ . In some cases, a function of several variables is involved.

Consider estimating the amount of material that has accumulated on the glove box floor through the use of measurements obtained from detectors suspended at a height  $h$  over the floor. Figure 12 depicts this situation when three measurement locations are employed. At throughput  $t$ , let the function  $d(t,x,y)$  denote the density of material at location  $(x,y)$  on the floor. The total holdup is then

$$h(t) = \int_0^L \int_0^W d(t,x,y) dy dx \quad ,$$

where  $(L,W)$  denotes the (length, width) of the glove box floor. The objective of modeling is to use the data to develop an estimated density function  $\hat{d}(t,x,y)$  and estimate the holdup by

$$\hat{h}(t) = \int_0^L \int_0^W \hat{d}(t,x,y) dy dx \quad . \quad (4)$$

The data used for this application arise from the low-airflow run of the  $U_3O_8$  experiment. The glove box floor is  $132 \times 66$  cm, and measurements are collected from a height of 97 cm above the three locations:

$$(x,y) = (13.97,42.55), (54.61,31.75), \text{ and } (97.79,34.29) .$$

The measured amount of material accumulated on the walls was negligible, and the deposition on the ceiling of the glove box was assumed to be negligible.

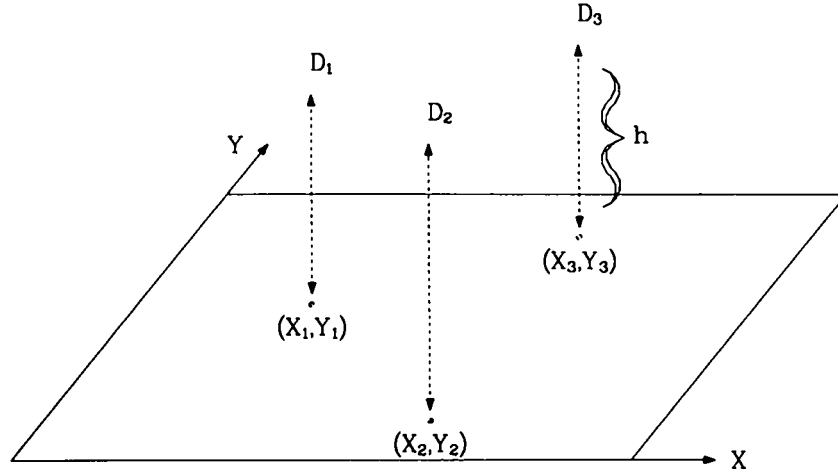


Fig. 12. Three detectors suspended over a glove box floor.

To develop the model, it is useful to consider a single measured value obtained over location  $(x_1, y_1)$  at throughput  $t$  (see Fig. 13). The limiting value of the holdup at the point  $(x, y)$  recorded by the detector is

$$n(t, x, y) = \begin{cases} c_1 \frac{d(t, x, y)}{h^2 + (x - x_1)^2 + (y - y_1)^2} & \text{if } (x - x_1)^2 + (y - y_1)^2 < r^2 \\ 0 & \text{otherwise} \end{cases} ,$$

where  $h^2 + (x - x_1)^2 + (y - y_1)^2$  is the square of the distance between the detector location and  $(x, y)$ ,  $r$  reflects the "range of vision" of the detector, and the normalization constant  $c_1$  corrects for such factors as efficiency of the measuring device. For the example,  $r = 34.3$  cm. The detector above  $(x_1, y_1)$ , which receives signals from many locations, records an integral holdup represented by

$$N(t, x_1, y_1) = \int_0^{66} \int_0^{132} n(t, x, y) dx dy \quad . \quad (5)$$

In practice, the limiting value of holdup  $n(t, x_1, y_1)$  cannot be measured directly, and this adds a minor complication to derivation of the estimated function  $\hat{d}(t, x, y)$ . However, the process of integration in Eq. (5) "smooths"  $n(t, x, y)$  about a region of  $(x_1, y_1)$ . If the density function  $d(t, x, y)$  is approximately linear in  $x$  and  $y$  or if the range of vision of the detector is sufficiently small to ensure that  $d(t, x, y)$  does not change much for  $(x, y)$  in that range of vision, then net count rates can be calibrated as if the material were uniformly spread over that range.

A first step in modeling is to determine, to whatever extent possible, the form of the density function  $d(t, x, y)$ . The model used for the GA Technologies, Inc., data is

$$d(t, x, y) = \alpha t + \beta t x + \gamma t y \quad , \quad (6)$$

where  $t$  denotes throughput and  $(\alpha, \beta, \gamma)$  are unknown parameters. The postulated model follows from standard response-surface methodology<sup>26</sup> and is easily interpreted. At a given location  $(x, y)$  on the floor, the density increases proportionally to throughput. At a given throughput  $t$ , the density varies linearly as a function of  $x$  and  $y$ . Uniform deposition is included as a special case ( $\beta = \gamma = 0$ ). Of course, other forms of density functions besides Eq. (6) could be considered if warranted by the data.

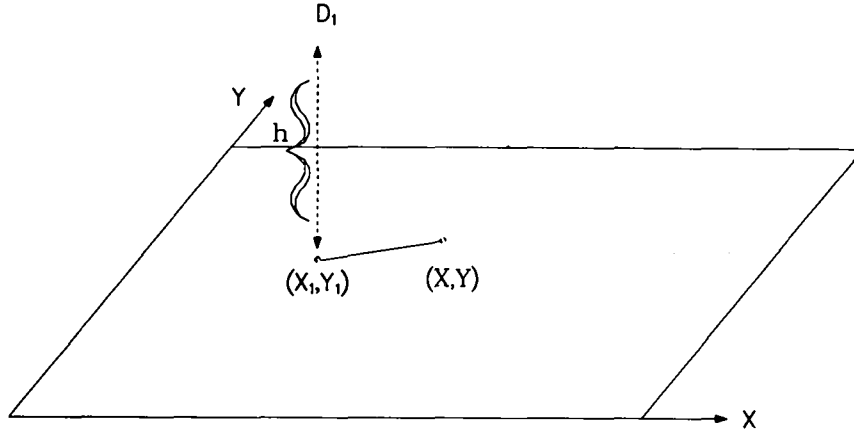


Fig. 13. A single detector over  $(x_1, y_1)$ .

Substitution of Eq. (6) into Eq. (5) yields the relationship

$$\begin{aligned}
 N(t, x_1, y_1) = \alpha t & \left\{ c_1 \iint_{\substack{(x-x_1)^2 + (y-y_1)^2 < r^2 \\ 0 < x < 132 \\ 0 < y < 66}} [h^2 + (x-x_1)^2 + (y-y_1)^2]^{-1} dx dy \right\} \\
 + \beta t & \left\{ c_1 \iint_{\substack{(x-x_1)^2 + (y-y_1)^2 < r^2 \\ 0 < x < 132 \\ 0 < y < 66}} x[h^2 + (x-x_1)^2 + (y-y_1)^2]^{-1} dx dy \right\} \\
 + \gamma t & \left\{ c_1 \iint_{\substack{(x-x_1)^2 + (y-y_1)^2 < r^2 \\ 0 < x < 132 \\ 0 < y < 66}} y[h^2 + (x-x_1)^2 + (y-y_1)^2]^{-1} dx dy \right\}
 \end{aligned}$$

Though nontrivial to compute, the integrals in brackets are constants and  $N(t, x_1, y_1)$  is a linear function of the unknown parameters  $(\alpha, \beta, \gamma)$ . Similarly, integral holdup values  $N(t, x_2, y_2)$  and  $N(t, x_3, y_3)$  are also linear in the parameters.

These observed holdup values are "true" holdup measured with error, and from them can be obtained estimated parameters in the linear model. The estimated density is then

$$\hat{d}(t, x, y) = \hat{\alpha}t + \hat{\beta}tx + \hat{\gamma}ty, \tag{7}$$

which is integrated as in Eq. (4) to provide the holdup estimator  $\hat{h}(t)$ . For this model,  $h(t)$  is a linear function of  $(\hat{\alpha}, \hat{\beta}, \hat{\gamma})$  so that error propagation is straightforward.

As an application, consider data collected from the low-airflow run of the  $U_3O_8$  experiment (Fig. 14). Note the approximately linear increase of the net counts with respect to throughput exhibited at all three locations. Also, the observed holdup appears relatively uniform across locations, in this instance reflecting the smoothing discussed previously.

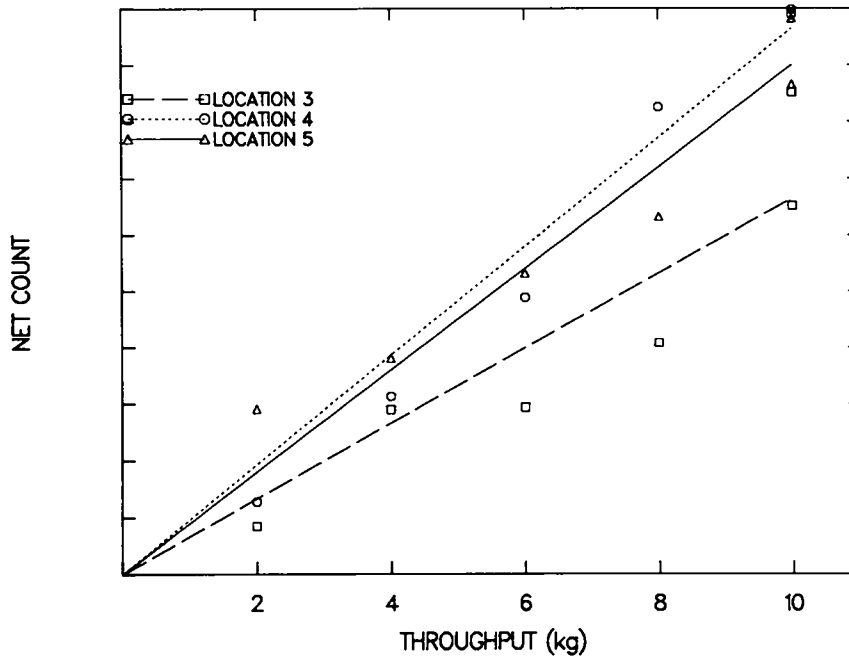


Fig. 14. Measurements on the glove box floor.

Upon fitting the model to the data, a joint hypothesis of  $(\beta, \gamma) = (0, 0)$  is significantly rejected, indicating nonuniform deposition. The estimated density is higher in the region about  $(x_1, y_1) = (13.97, 42.55)$  than in the region about  $(x_3, y_3) = (97.79, 34.29)$ , confirming suspicions based on visual inspection of the glove box. The estimated holdup at the end of the experiment,  $t = 10$  kg, is

$$\begin{aligned} \hat{h}(10) &= \int_0^{66} \int_0^{132} \hat{d}(10, x, y) \, dx \, dy \\ &= 2.68 \text{ g} \end{aligned}$$

which is in good agreement with the cleanout value, 2.71 g.

Use of the predictive Eq. (7) is relatively straightforward and parallels usage of the model developed for the filter. Model-based estimates can be used for estimation of holdup for a brief period into the future, at which point additional measurements are required to validate the model and update parameter estimates. For these purposes, future data need not be collected at the same locations nor with the same frequency as in the initial experiment.

**4. The Vertical and Horizontal Ducts.** Rising from the top of the glove box is a vertical pipe (segments 6 and 7 in Fig. 6). To develop the model for this component, it is necessary to introduce some notation and the mathematical concepts used here.

When measuring holdup that has accumulated on the interior surface of a vertical cylinder (or pipe), the experimenter must deal with the geometrical aspects of the problem. Because the "range of vision" of the detector is a cone emanating from the point of measurement and holdup is deposited on a cylindrical surface, modeling is most easily developed using spherical coordinates.

Consider a set of points in three-dimensional space. In the "usual" coordinate system, a point is described as  $(x,y,z)$  as in Fig. 15.

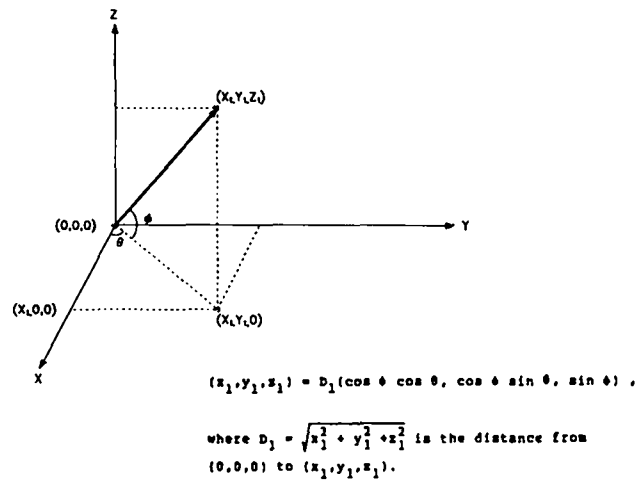


Fig. 15. Spherical coordinates in three-dimensional space.

If we were looking from the point  $(0,0,0)$  toward the point  $(x_1, y_1, 0)$ , we would have to raise (or lower) our sights to see the point  $(x_1, y_1, z_1)$ . Letting  $\phi$  denote the angle through which we raised our sights, it follows that

$$z_1 = D_1 \sin \phi ,$$

where

$$D_1 = \sqrt{x_1^2 + y_1^2 + z_1^2} .$$

If we were looking from the point  $(0,0,0)$  toward the point  $(x_1, 0, 0)$ , we would have to turn our heads to the left (or right) to see the point  $(x_1, y_1, 0)$ . Letting  $\theta$  denote the angle through which we turned our heads, it follows that

$$x_1 = D_1 \cos \theta \cos \phi$$

and

$$y_1 = D_1 \cos \theta \sin \phi$$

because the distance from  $(0,0,0)$  to  $(x_1, y_1, 0)$  is

$$\sqrt{x_1^2 + y_1^2} = D_1 \cos \theta .$$

The three-dimensional coordinate system is thus "transformed" from one involving  $(x,y,z)$  into one involving the distance  $D = \sqrt{x^2 + y^2 + z^2}$  and the angles  $(\phi, \theta)$ .

Now consider material held up on the interior surface of a vertical cylinder that is being measured by J detectors. Let the detectors be located at the points  $\{(x,y,z) = (0,0,z_j)\}$ , and let the center of the cylinder run vertically through the point  $(x,y,z) = (c,0,0)$ . In other words, the detectors are stacked vertically above the point  $(0,0,0)$ , and the center of the cylinder runs parallel to the line of detectors and is a distance  $c$  away (Fig. 16).

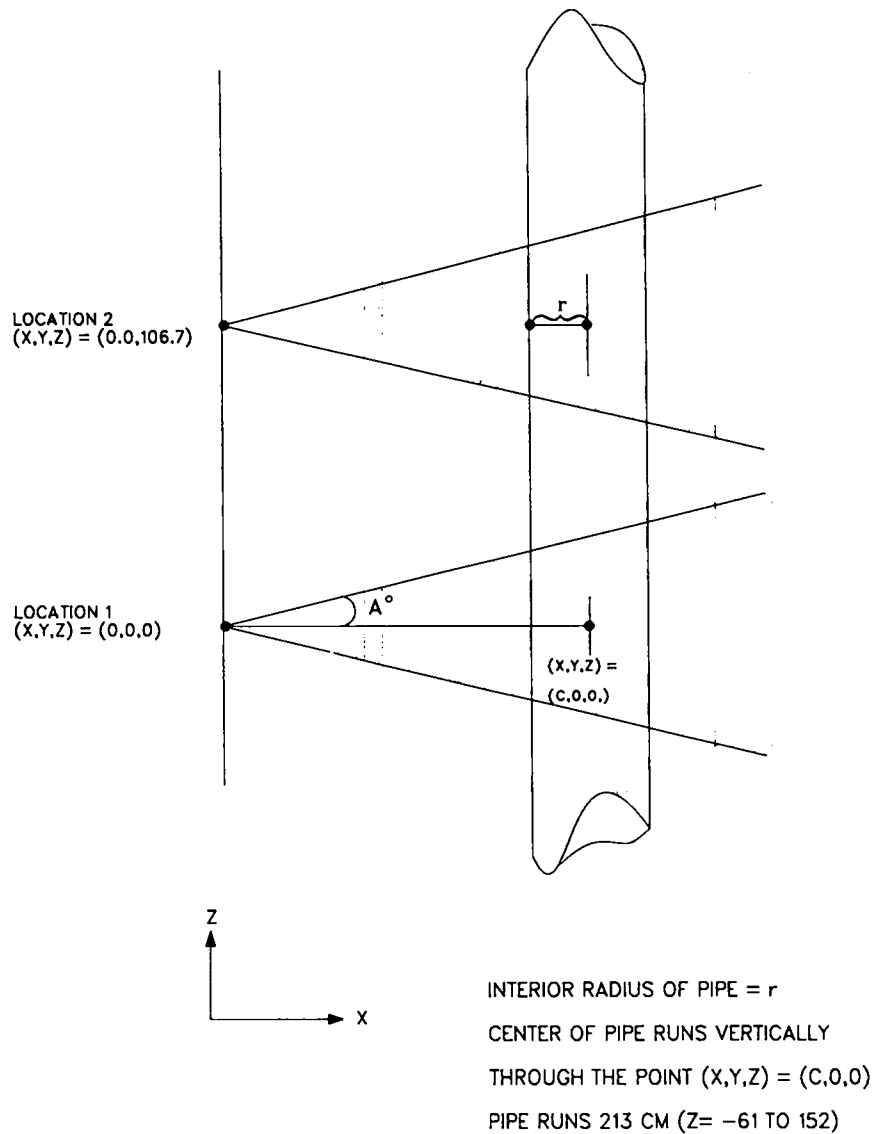


Fig. 16. Side view of detector and vertical cylinder.



If the vertical coordinate  $z$  takes on values from  $a$  to  $b$  and  $r$  is the interior radius of the cylinder, the set of points on the interior surface is

$$S = \{(x,y,z) \mid (x - c)^2 + y^2 = r^2 \text{ and } a < z < b\} .$$

Expressed in the spherical coordinates of Fig. 16, the equation  $(x - c)^2 + y^2 = r^2$  is equivalent to

$$(D \cos \phi \cos \theta - c)^2 + (D \cos \phi \sin \theta)^2 = r^2 ,$$

or

$$[\cos^2 \phi]D^2 + [-2c \cos \phi \cos \theta]D + [c^2 - r^2] = 0 . \quad (8)$$

Note that for fixed line of sight  $(\phi, \theta)$ , this is a quadratic function in the distance  $D$ . The two roots correspond to the points where the line of sight “enters” and “leaves” the cylinder. Call the roots  $D_{\min}(\phi, \theta)$ , and  $D_{\max}(\phi, \theta)$ (Fig. 17).

From its location  $(x,y,z) = (0,0,z_j)$ , the  $j$ th detector can see up/down from angle  $-A$  to  $+A^\circ$ . The same is true from right to left, although it is clear from Fig. 17 that the cylinder lies entirely within the right/left angle  $\theta$  for

$$\theta \in (\sin^{-1}[-r/c], \sin^{-1} [r/c]) .$$

The  $j$ th detector receives nonzero net signals from all locations in the intersection  $S \cap R_j$ , where  $S$  is the interior surface of the cylinder as before and  $R_j$  is the range of vision of the  $j$ th detector. For the detector at location 6,  $(x,y,z) = (0,0,0)$ , we have

$$R = \{(D, \phi, \theta) \mid D > 0, \sin^2 \phi + \sin^2 \theta \leq \sin^2 A\} .$$

The postulated density function takes the form

$$d(t,x,y,z) = \alpha t + \beta t z .$$

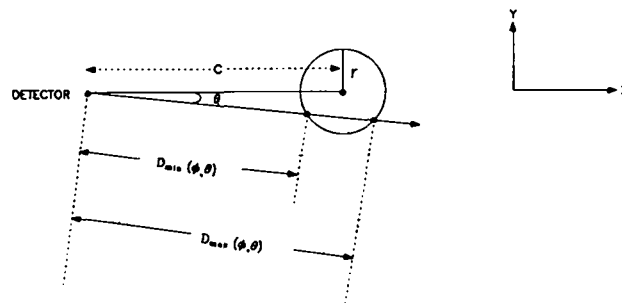


Fig. 17. Overhead view of detector and vertical cylinder.

This is interpreted as follows:

1. At a given location (x,y,z), the amount of material increases proportionally to throughput t.
2. At a given throughput t, the density varies linearly with height z but does not depend on x or y. The difference in air velocity at the top and bottom of the pipe servicing the glove box accounts for the change in material deposition as a function of height.

Expressed in spherical coordinates, the density is

$$d(t,D,\phi,\theta) = \alpha t + \beta t D \sin \phi . \quad (9)$$

Consider the measurement from location 6,  $(D,\phi,\theta) = (0,0,0)$ . For a given line of sight  $(\phi,\theta)$  in the range of vision  $R_6$  of the detector, nonzero net signals are received from two locations at distances  $D_{\min}(\phi,\theta)$  and  $D_{\max}(\phi,\theta)$  as indicated in Fig. 17. The integrated value of the holdup at this location is the collection of all such signals in  $R_6$ ; that is, analogous to Eq. (5) from the modeling of the glove box floor, the value of  $N(t,0,0,0)$  from location 6 satisfies

$$N(t,0,0,0) = c_1 \int \int_{R_6} \left\{ \frac{d[t,D_{\min}(\phi,\theta),\phi,\theta]}{D_{\min}^2(\phi,\theta)} + \frac{d[t,D_{\max}(\phi,\theta),\phi,\theta]}{D_{\max}^2(\phi,\theta)} \right\} d\phi d\theta .$$

The roots of the quadratic Eq. (8) are

$$D_{\min}(\phi,\theta) = \frac{c}{\cos \phi} [\cos \theta - \sqrt{(r^2/c^2) - \sin^2 \theta}] \quad (10)$$

and

$$D_{\max}(\phi,\theta) = \frac{c}{\cos \phi} [\cos \theta + \sqrt{(r^2/c^2) - \sin^2 \theta}] .$$

Substituting  $d(t,D,\phi,\theta)$  as in Eq. (9) and  $D_{\min}(\phi,\theta)$  and  $D_{\max}(\phi,\theta)$  as in Eq. (10) gives

$$\begin{aligned} N(t,0,0,0) = & \alpha t \left( c_1 \int \int \begin{array}{cc} \sin^{-1}(r/c) & \sin^{-1}(\sqrt{\sin^2 A - \sin^2 \theta}) \\ \sin^{-1}(-r/c) & \sin^{-1}(-\sqrt{\sin^2 A - \sin^2 \theta}) \end{array} \right. \\ & \left. \left\{ \frac{\cos^2 \phi}{c^2 [\cos \theta - \sqrt{(r^2/c^2) - \sin^2 \theta}]^2} + \frac{\cos^2 \phi}{c^2 [\cos \theta + \sqrt{(r^2/c^2) - \sin^2 \theta}]^2} \right\} d\phi d\theta \right. \\ & + \beta t \left( c_1 \int \int \begin{array}{cc} \sin^{-1}(r/c) & \sin^{-1}(\sqrt{\sin^2 A - \sin^2 \theta}) \\ \sin^{-1}(-r/c) & \sin^{-1}(-\sqrt{\sin^2 A - \sin^2 \theta}) \end{array} \right. \\ & \left. \left\{ \frac{\sin \phi \cos \phi}{c [\cos \theta - \sqrt{(r^2/c^2) - \sin^2 \theta}]} + \frac{\sin \phi \cos \phi}{c [\cos \theta + \sqrt{(r^2/c^2) - \sin^2 \theta}]} \right\} d\phi d\theta \right) . \end{aligned}$$

The integrals in brackets are constants for fixed values of  $r$ ,  $c$ , and  $A$ . Once these integrals are found, estimation of the parameters  $(\alpha, \beta)$  can be pursued as with the example of the glove box floor. Corresponding integrals exist for the integrated holdup at other locations. This yields an estimated density function and thus estimated holdup.

For the GA Technologies, Inc., data, we have  $r = 5$  cm,  $c = 40.7$  cm., and  $A = 19.2^\circ$ . The detector was placed at locations 6 and 7,  $(x, y, z) = (0, 0, 0)$  and  $(0, 0, 106.7)$  cm, respectively. Data from the low-airflow run of the  $U_3O_8$  experiment are plotted in Fig. 18, and the estimated density function is, in units of milligrams per square centimeter,

$$\hat{d}(t, D, \phi, \theta) = 0.00198t + 0.0000273t D \sin \phi .$$

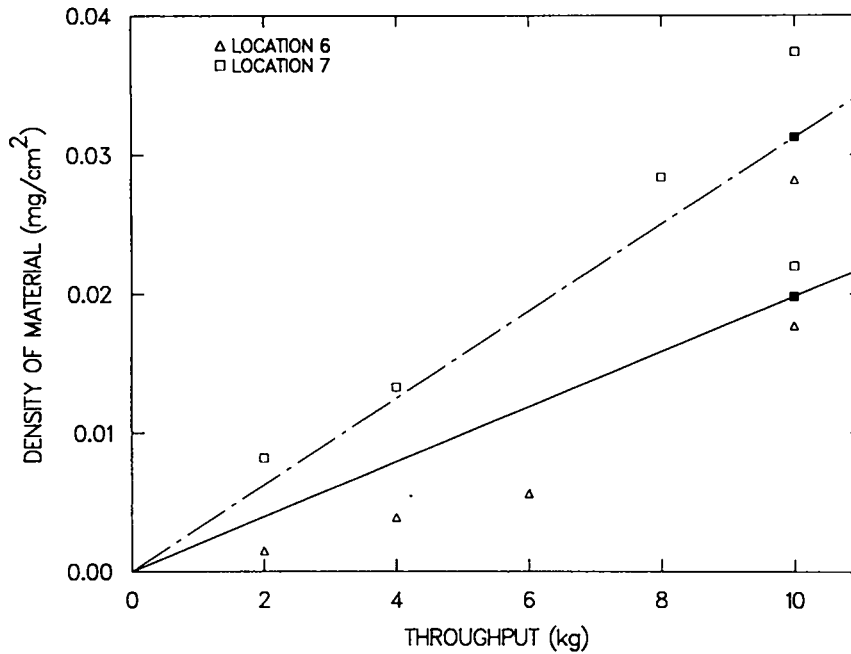


Fig. 18. Measurements on the vertical cylinder.

As expected, the estimated density increases as a function of the height  $D \sin \phi$ . At the conclusion of the experiment,  $t = 10$  kg and the estimated holdup is

$$\begin{aligned} \hat{h}(10) &= \int_s \hat{d}(10, D, \phi, \theta) dD d\phi d\theta \\ &= 0.168 \text{ g} . \end{aligned}$$

This value agrees reasonably well with the NDA measurements.

The horizontal segment of ductwork, roughly 2 m long and covering measurement points 11-13, can be modeled using the same principles. A first step in such modeling is to look for change (or lack of change) in holdup over the segment of ductwork. In contrast to data from the vertical segment, materials deposition here did not appear to differ from location to location, and thus a simpler model can be used. A plot of the measurement histories at locations 11-13 from the low-airflow experiment with  $U_3O_8$  is given in Fig. 19.

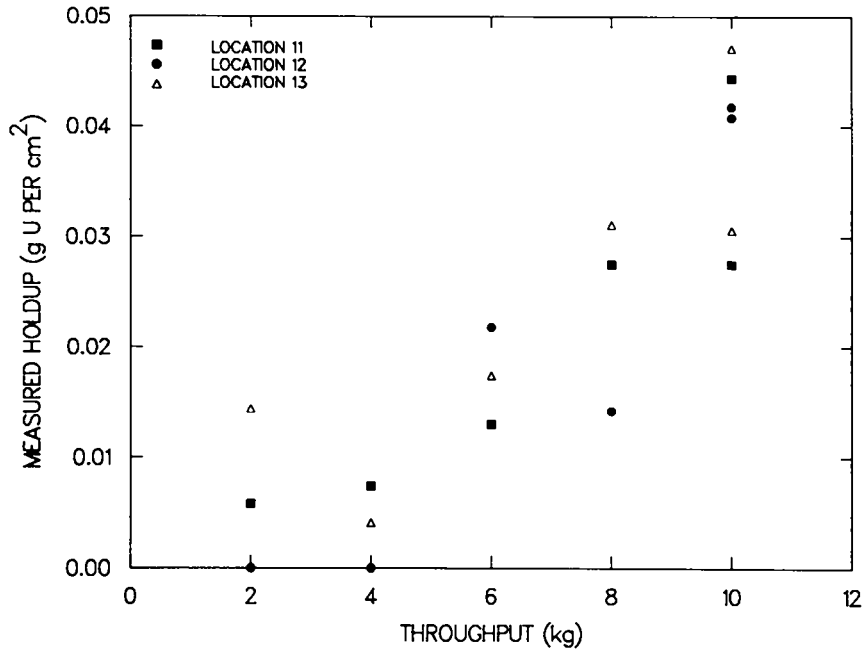


Fig. 19. Holdup measurement history (for low-airflow measurements with  $U_3O_8$ ) at locations 11-13.

If materials deposition were uniform throughout the length of the duct segment, data at each of the measurement points could be used to estimate the total amount of holdup. As at the elbows, a linear increase in materials deposition as a function of throughput is indicated by the data. A model for the density of material (holdup per unit area) at locations  $(x,y,z)$ , where the left end of the horizontal segment is taken for convenience to be at  $(0,0,0)$ , is

$$d_h(t,x,y,z) = \alpha_h t .$$

That is, the density depends on throughput  $t$  but does not depend on the location. The estimated holdup for the segment of ductwork is then

$$\begin{aligned} \hat{h}(t) &= \int_S \hat{d}_h(t,x,y,z) \, dx \, dy \, dz \\ &= A \hat{\alpha}_h t \quad , \end{aligned}$$

where  $S$  again denotes the duct's interior surface,  $A$  is the associated surface area, and  $\hat{\alpha}_h$  is estimated from the data.

**5. Modeling the Glove Box System.** Once models for the components of the glove box system (such as filter, glove box floor, or horizontal duct segment) have been developed, they can be combined to yield a model for the system as a whole. The estimated system holdup is simply the sum of the estimated amounts of holdup in each of the components. A model for the system can be obtained by "adding" the models for the individual components. An example of this for the low-airflow experiment with  $U_3O_8$  is given in Table VIII.

It is important to note that the estimated parameters for a given component may be difficult to obtain, as in the cases of the glove box floor and vertical segment where nonuniform deposition must be accounted for and integration of an estimated density function is involved. Also, when updating the model for the

TABLE VIII. Summary of Modeling Results for Low-Airflow Experiment with  $U_3O_8$ <sup>b</sup>

Component	Measurement Point <sup>a</sup>	Model for Low-Airflow Experiment with $U_3O_8$ <sup>b</sup>	Estimated Holdup (g) Throughput = 10 kg <sup>b</sup>
Glove box sides	1-2	$\hat{h}_s(t) = 0$	0
Glove box floor	3-5	$\hat{h}_f(t) = 0.2677t$	2.677
Vertical segment	6-7	$\hat{h}_v(t) = 0.0168t$	0.168
First elbow	8	$\hat{h}_1(t) = 0.0027t$	0.027
Segment between elbows	9	$\hat{h}_b(t) = 0.0086t$	0.086
Second elbow	10	$\hat{h}_2(t) = 0.0036t$	0.036
Horizontal segment	11-13	$\hat{h}_h(t) = 0.0195t$	0.195
Filter	14	$\hat{h}_f(t) = 0.0232t + 0.0014t^2$	0.372
System total	1-14	$\hat{h}(t) = 0.3421t + 0.0014t^2$	3.561
System weight loss			4.193

<sup>a</sup>See Fig. 6 for details.

<sup>b</sup>The number of significant figures in the tabulated data in columns 3 and 4 of this table is not a representation of the accuracy of modeling estimates. See Table VI for relative errors of estimations.

system (that is, using additional data to check model performance and update parameter estimates), the individual components must be updated separately and re-added to give the revised system model. Perhaps the primary value in developing an overall model for the system is to characterize the system holdup as a function of relevant variables for a given set of operating conditions. For example, results from the low-airflow experiment with  $U_3O_8$  indicated that, beginning from a "clean" state, holdup initially accumulates roughly proportionally to throughput. Of course, the same need not occur under other operating conditions.

6. Comparison of Experiments. The models used in all experimental work are of the same structure as those described in great detail for the low-airflow run with  $U_3O_8$ . Thus, it is not necessary to repeat that model development here. The only (minor) differences in modeling occurred when the cleanout from the previous experiment left a small amount of material for the beginning of the next one. A term was added to the model to account for this when necessary.

The effects on holdup of varying operating conditions were reasonably predictable. Increasing the airflow level deposited additional material into the ductwork and filter. Not only was the amount of material in these locations increased but so was the fraction of the total system holdup residing there. Use of fine  $U_3O_8$  powder generated the most holdup of the three materials, with ash next, and finally the coarse  $U_3O_8$  material.

Throughout the experiments, holdup behavior at the individual measurement locations remained relatively stable. On the face of the glove box (measurement locations 1 and 2 in Fig. 6), there was no indication of appreciable material deposition as a majority of the net count rates obtained were negative. Holdup on the glove box floor (locations 3-5) exhibited nonuniform deposition with the greatest concentration of material usually on the portion of the floor beneath the vertical segment of ductwork rising from the glove box. On the interior walls of the vertical segment (locations 6 and 7), deposition

increased as a function of height. At the two elbows and adjoining segment (locations 8-10), holdup accumulated in an approximately linear fashion with respect to throughput at each measurement point as described in Sec. III.E.2. The horizontal segment of ductwork (locations 11-13) exhibited no evidence of nonuniform deposition; that is, in contrast to the vertical segment, there was no significant difference in accumulated holdup among the three locations. Finally, measurements on the filter (location 14) exhibited a nonlinear increase in holdup in accordance with the model discussed in Sec. III.E.1.

#### IV. EXPERIMENTAL STUDY OF URANIUM HOLDUP IN A LIQUID-LIQUID EXTRACTION PULSE COLUMN

Liquid-liquid extraction processes for the separation of uranium and plutonium from fission products and other impurities are widely used in nuclear fuel-reprocessing plants and scrap recovery operations at nuclear fuel materials preparation and fabrication facilities. The chemical separation processes for the extraction of uranium and/or plutonium are based on the differences in the abilities of the nitrate salts of cations to form neutral complexes with tributyl phosphate (TBP). These neutral complexes are lipophilic and are soluble in an immiscible TBP phase, where they are essentially un-ionized. Actinide elements in the +4 and +6 valences form stronger complexes than almost any other element. Metal nitrate salts in which the metal valence is +1, +2, or +3 are virtually not extractable under these conditions. These features provide the basis for PUREX separation for spent fuel reprocessing and extraction of SNM during scrap recovery operations.

In practice, the separation and purification of uranium and plutonium are achieved using a series of solvent-extraction contactors in which uranium and plutonium are selectively extracted into the organic phase containing TBP through countercurrent aqueous and organic streams. Three common liquid-liquid extraction contactors are mixer-settlers, pulse columns, and centrifugal contactors.

The objective of this investigation was to attempt to develop holdup estimators for a pulse-column liquid-liquid extraction system using concentration profiles developed from extensive sampling and analyses during steady-state operations of the pulse columns. The principles used in developing such estimates of SNM inventories are applicable to estimating materials holdup in liquid-liquid extraction contactors during steady-state operations as well as in valved-off and drained column conditions. Significant quantities of SNM remain in these pulse columns during steady-state operations and plant shutdown conditions. The runout inventories (residual holdup) of the pulse columns after a solution dump are small compared with the in-process inventories. All these inventories are of importance to materials accountability; however, estimating the column inventories in an operating plant is extremely difficult. The method of estimating inventories of SNM in liquid-liquid extraction systems by means of direct NDA techniques is desirable, although such measurements have yet to be fully developed for a processing facility.

In a recent attempt to determine the residual holdup of uranium in pulsed extraction columns, three pulse columns at the Y-12 plant in Oak Ridge were flushed out with 50% HNO<sub>3</sub>, and the uranium contents of the cleanout solutions were determined using a solution-assay system. The results of these measurements<sup>27</sup> indicate that only ~1% of the steady-state inventory of the column remained as residual holdup after column dumps. The average value of the inventories of HEU in the three columns before dumping was 6 kg of HEU, and the average residual holdup of uranium in these columns was <80 g. Attempts to perform *in situ* measurements of this residual amount of uranium in an operating plant with the associated spatial distribution of uranium in the column and radiation background problems caused by uranium inventories in the vicinity would only have been a futile exercise.

The experimental studies described here offer an alternative approach of developing holdup estimation models for the pulse column from known process parameters and a limited number of measurements.

## A. Experimental Study

A pilot-scale pulse-column profile study was sponsored by the Los Alamos National Laboratory at the Allied General Nuclear Services (AGNS) facilities at Barnwell, South Carolina.<sup>28</sup> This experimental study was designed to investigate pulse-column operations using only uranium. The pulse columns of this pilot facility were equipped with samplers along the length of the column to collect samples for uranium analyses and to develop the profile of uranium within the column during steady-state operations. In addition, a few analyses of the column dumps were performed to assess the value of the integrated inventories developed from column profiles. Although the primary purpose of these pilot-scale experiments was to assess computer programs developed for pulse-column profiles, the data obtained during these experimental studies are valuable for developing holdup estimators or column inventories of uranium after steady-state operations are reached. In the following sections, details of the pilot-scale experimental studies are presented with emphasis on two experiments (2A-3 and 2D-2) relevant to this holdup study. The data from these experiments are used in the development of estimators for uranium holdup in the pulse columns.

## B. Equipment and Facilities

The equipment used for the two experiments consisted of two glass pulse columns (1A and 1B) as illustrated in Fig. 20. Auxiliary equipment included circulation pumps as well as stainless steel tanks for feed solutions, product(s), and waste(s). Column 1A, with a diameter of 5 cm, was an extraction/scrub pulse column with a height of ~8 m. Column 1B was a stripping column with a diameter of 7.5 cm and a height of ~6 m. Both pulse columns had 0.15-cm-thick plates spaced 5 cm apart with ~23% free surface area and plate orifice diameters of 0.3 cm each. Both pulse columns had top and bottom disengaging sections made of glass. The top section was vented and the bottom one was connected to a bellows-type pulser. The aqueous and organic interfaces were controlled automatically at the bottom of the disengaging section of column 1A and at the top section of column 1B using two titanium conductivity probes to regulate air-operated control valves at the aqueous-phase outlet.

The pulse columns were provided with sampling ports as shown in Fig. 20 (A1-A11 and B1-B7). There were five sampling ports along the scrubbing section of column 1A and six along the extraction section. The stripping column 1B had a total of seven sampling ports.

## C. Experimental Procedures

Unirradiated uranium was used as the solute in these pilot-plant experiments. The experiments were designed to obtain detailed aqueous and organic concentration profiles and fractional phase volumes as well as the uranium inventory of the entire column. The experimental setup incorporated both of the pulse columns described earlier. The center-fed extraction/scrub column had an aqueous feed (1AF) with the TBP extractant in an organic solvent entering at the base of the column. The organic product from the first column was allowed to enter the second column as a bottom-fed stream, and uranium from the organic phase was stripped into an aqueous stream entering at the top of the second column. The operating conditions of the columns during these experimental runs are summarized in Table IX.

During experimental runs, steadily operating positive displacement pumps were used for feeding each pulse column with corresponding feed solutions. When the pulse columns were at steady state, as determined by uranium assays at the end of the streams, samples of aqueous and organic phases were collected for analysis. The results of these analyses were used to develop the concentration profiles of uranium in the columns. Uranium concentrations were determined by densimetric or titrimetric methods.

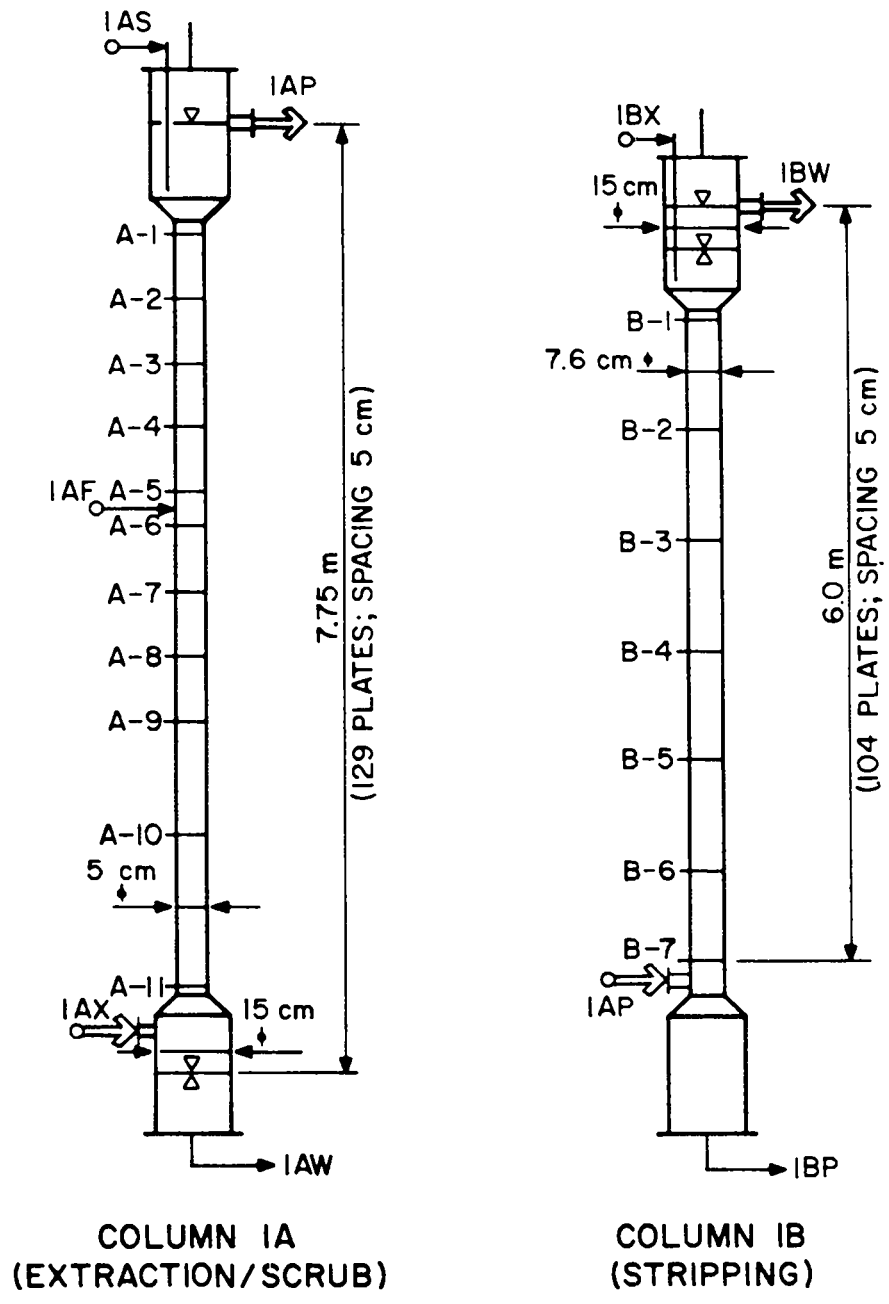


Fig. 20. A schematic representation of the pulse columns used.



TABLE IX. Pulse-Column Operating Conditions

Process Parameters	Column 1A (Extraction/scrub)	Column 1B (Stripping)
Run no.	2A-3 & 2D-2	2A-3 & 2D-2
Feed inlet	650 mL/min	---
Stripping solution inlet	---	1130 mL/min
Pulse frequency	82/min	60/min
Pulse amplitude	2 cm	2 cm
TBP concentration	30%	30%
Original solvent	n-dodecane	n-dodecane
HNO <sub>3</sub> Concentration	2 M	~ 0.01 M

The inventories of uranium in the columns were also determined by analyzing the column dumps by measuring both the volumes and concentrations of uranium in the partitioned phases of the dump solutions.

#### D. Uranium Concentration Profiles of Pulse Columns

Typical uranium concentration profiles of the two columns used in these experiments are as shown in Figs. 21 and 22. Figure 21 shows the concentration profile of the extraction/scrub pulse column (1A) in which the aqueous phase was dispersed. The aqueous uranium concentrations obtained during analyses of samples that had reached equilibrium did not necessarily reflect the actual concentrations of uranium in the column at the time of sampling. Therefore, a method proposed by Gier and Hougen<sup>29</sup> was employed to determine the actual concentrations of uranium at the time of sample withdrawal from each sampling point along the column. Concentration profiles thus developed for experiments 2A-3 and 2D-2 are presented in Tables C-XVI and C-XVII, respectively.

#### E. Pulse-Column Inventory Estimation

The most straightforward method of estimating the amount of material in a pulse column entails a cessation of column operation followed by a cleanout of material. Though useful in providing information for accountability purposes, such an approach is very disruptive and thus could be performed only infrequently. The development of estimates not requiring process disruptions would be of substantial benefit to facility operation as well as to materials accountability.

The quantity of material to be estimated here is the sum of the amounts of uranium in different portions of the column. Consider a hypothetical situation as depicted in Fig. 23. The column's working section has 20 stages, and the amount of uranium in each stage is plotted as a function of stage number. The total amount of uranium is the sum of the 20 values, which is equal to the shaded area under the column's concentration profile.

Given measurements from different stages in the column, acquired either by NDA measurements or by chemical analyses, it is possible to estimate the profile. Mathematical integration of this profile yields the estimate of uranium in the column. The two primary sources of error in this estimate are

- uncertainties in the measured values of uranium for the sampled stages and
- uncertainty resulting from interpolation over any unsampled stages in estimation of the profile.

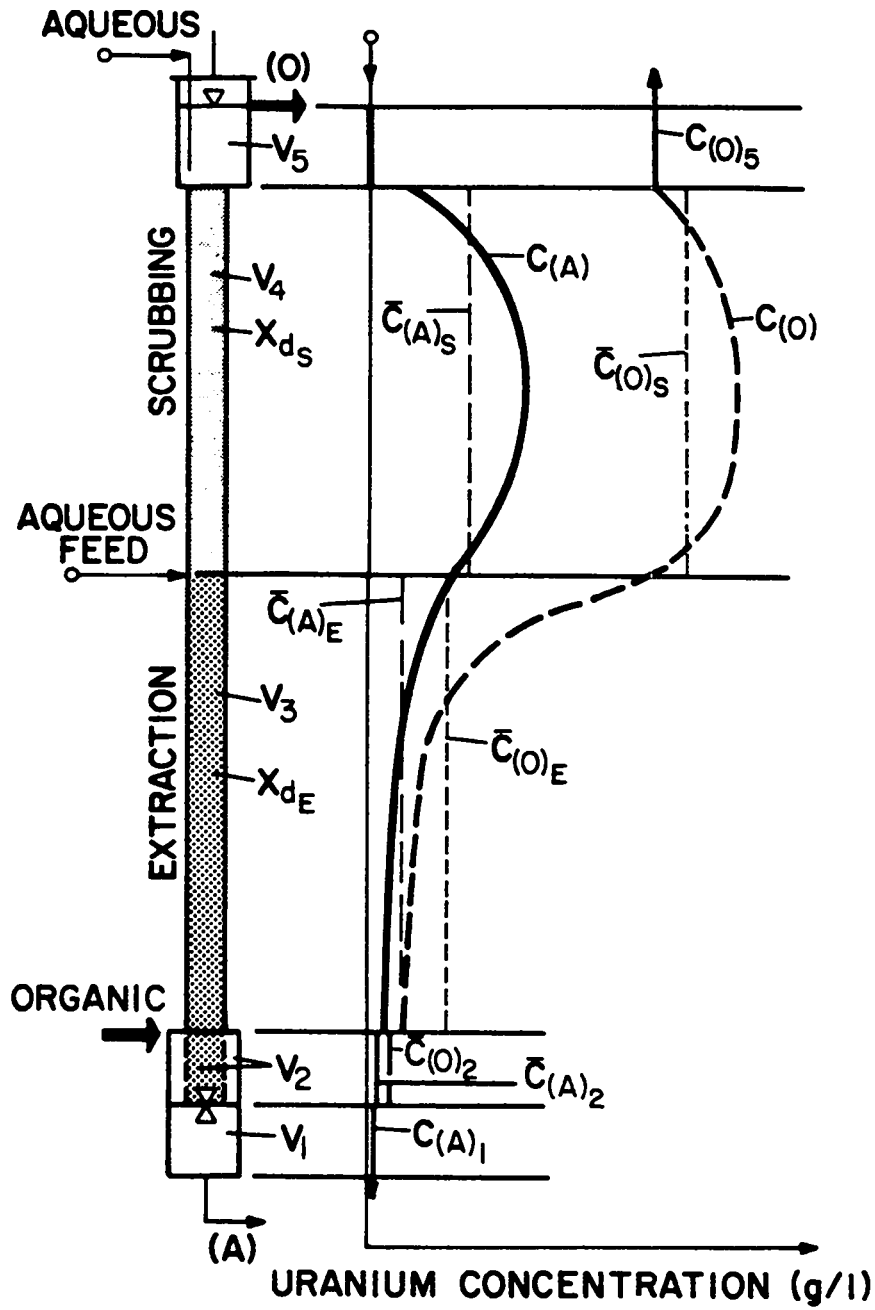


Fig. 21. Uranium concentration profile of the extraction/scrub column.

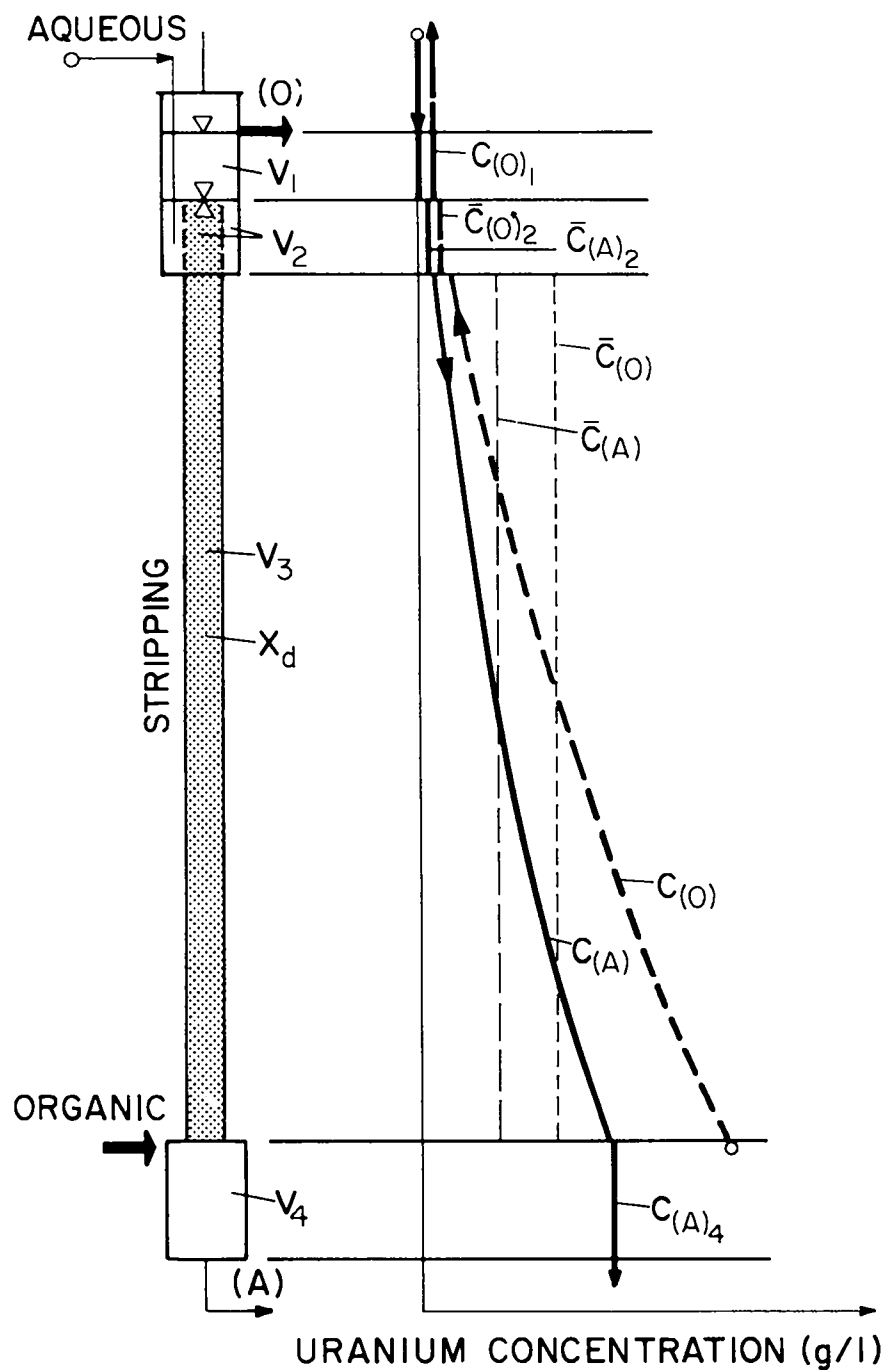


Fig. 22. Uranium concentration profile of the stripping column.

The following paragraphs discuss aspects of pulse-column estimation and illustrate application of the methodology to results from the bench-scale experiments described previously. Although the modeling techniques are presented in the context of estimating the quantity of uranium in a column that has attained steady-state operation, the underlying principles involved are equally applicable to columns that have been either valved off or drained. In all cases the amount of material within the column is the integral of a profile from which data may be obtained.

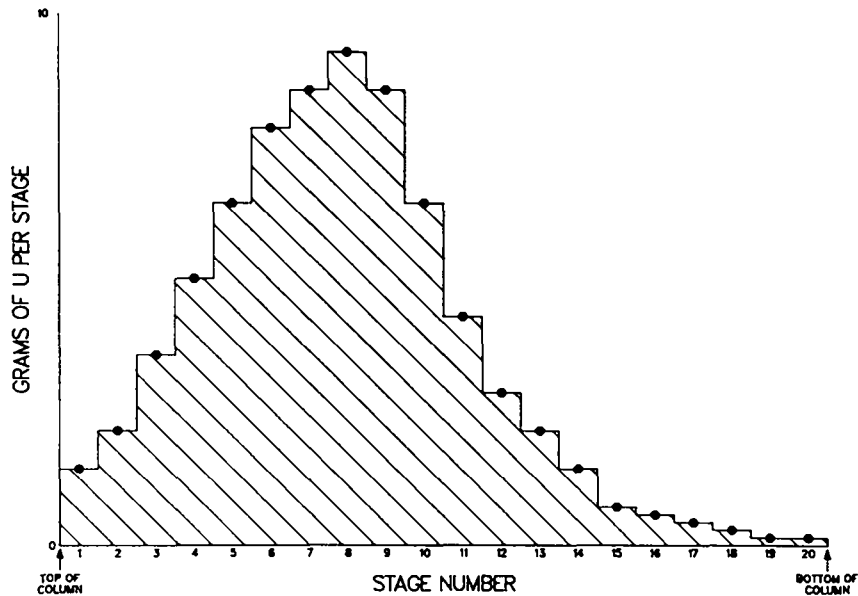


Fig. 23. A hypothetical concentration profile of uranium concentrations.

**1. Model Development.** Three fundamentally different approaches to the problem are introduced here. The first involves the derivation of inventory estimates based solely on the operating conditions of the column, and the second uses only concentration measurements acquired from along the column. The third approach is a combination of the other two. In the following paragraphs, the relative merits of each approach are discussed.

One method of obtaining profile estimates over a wide range of conditions is to use complex computer codes that simulate column operation.<sup>30</sup> These codes do not require "direct" concentration measurements from along the column, and in facility environments where the performance of NDA instrumentation would be marginal because of high background or other limitations, this approach may be the only feasible one. Error propagation for the resulting inventory estimate is not overly difficult, amounting to a sensitivity analysis of the simulation code. In general, this approach has a variety of drawbacks and is not considered in detail here.

A second approach is based on sample data obtained from several locations along the column. Most likely, the data would be collected through use of NDA instrumentation mounted on the column itself, although it may also be possible to physically withdraw solution for destructive analysis as in the AGNS experiments. From the resulting data, the concentration profile can be estimated using standard regression methods, and integration provides an inventory value. This approach is easily understood (in contrast to the black box atmosphere of simulation codes) and is perhaps less vulnerable from a security standpoint than the first approach (it is easier to check that a detector is working properly than to check other instrumentation such as flow meters; also, tampering with an extensive computer code might be difficult to uncover). Error propagation is straightforward and is discussed later. The standard deviation of estimation depends largely on the number of detectors used and the quality of the corresponding measurements.

A third approach to the problem links a simulation code to sample data obtained along the column, attempting to take advantage of knowledge of column operation through use of the code as well as benefiting from the presence of "direct" measurements. This approach is also pursued below and, ideally,

should be the best method of inventory estimation short of a column dump. In the experiments at AGNS, it is not clear whether shortcomings of the simulation code are serious enough to make the second approach preferable.

**2. Profile Approximation by Regression Methods.** In pulse columns, the aqueous and organic profiles are relatively smooth functions, and their integrals can be approximated in a variety of ways. Methods common to elementary calculus can be used to provide somewhat crude approximations. For example, the measured values could be used to determine a step function, similar to that in Fig. 23, but based on sampling only a small fraction of the stages. The integration of a step function is analogous to the Riemann approximation of the integral of a continuous function and is easily computed. An alternative method, illustrated in Fig. 24 using data from the 2A-3 run of the extraction/scrub column, "connects the dots" with line segments. Integration of this type of estimated profile is straightforward, equivalent to summing the areas of a number of trapezoids as indicated in Fig. 24. Though using a piecewise linear function or a step function is somewhat simple-minded, the resulting estimates are not difficult to derive and can be useful.

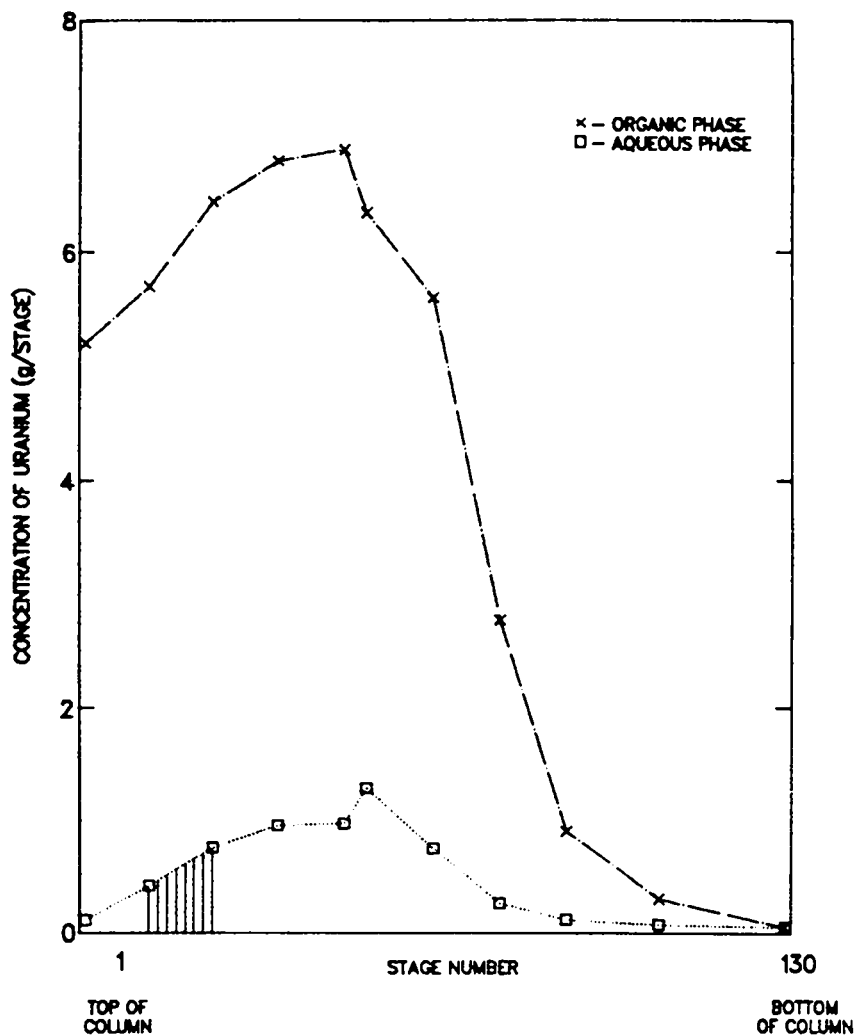


Fig. 24. Estimated profile—piecewise linear approximation.

Perhaps the most practical approach toward profile estimation involves the use of regression techniques to fit smooth curves to the data. Approximation by this method does not require the quantity or quality of measured values needed to obtain good results using more simplistic methods. Propagation of error for the estimated column inventory is straightforward.

In the examples at hand, the profiles are approximated by functions of the form

$$\hat{p}(x) = \exp \left( \sum \beta_i x^i \right) .$$

where  $\hat{p}(x)$  is the estimated concentration of uranium at distance  $x$  from the top of the column's working section and the parameters  $\{\beta_i\}$  are estimated from the data. This model evolves from a Taylor-series expansion of the logarithm of the concentration profile. Figure 25 illustrates application of this approach using the 2A-3 extraction/scrub column data given in Table C-XVI.

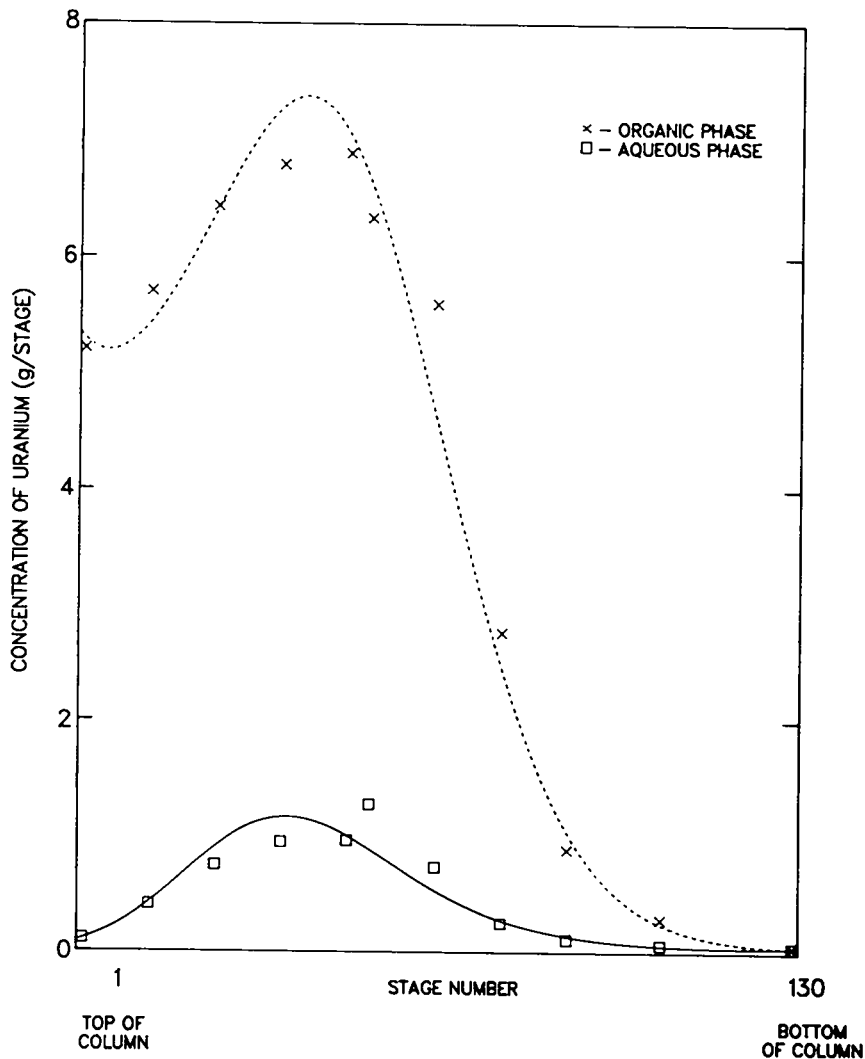


Fig. 25. Estimated profile—regression methods.

In general, the degree of the polynomial providing the best fit depends on the actual profile, which in turn depends on the type of column and the nature of its operation. It should be pointed out that polynomials of low orders (Table II) are used, avoiding any potential difficulties with overfitting the data. For the 2A-3 extraction/scrub column, the estimated aqueous and organic profiles  $\hat{p}_a(x)$  and  $\hat{p}_o(x)$ , respectively, are given by

$$\hat{p}_a(x) = \exp(-2.4009 + 0.1500x - 0.002583x^2 + 0.00001068x^3),$$

and

$$\hat{p}_o(x) = \exp(1.6767 - 0.01165x + 0.001300x^2 - 0.00002407x^3 + 0.00000009682x^4). \quad (11)$$

In any given case, some judgment on the part of the experimenter is necessary to choose the most appropriate model, although formal selection algorithms (for example, backward elimination) are included as options in many statistical package programs. Ideally, column operation would remain sufficiently stable over a period of time to allow the form of the model chosen following a detailed preliminary investigation to be used repeatedly; the parameters  $\{\beta_i\}$  could be re-estimated as new data become available.

Estimated quantities of SNM are obtained by integration of the estimated profile over the length of the column. For example, the top of the working section of the extraction/scrub column corresponds to  $x = 0$  and the bottom corresponds to  $x = 130$  (each stage has unit length). The amount of uranium in the aqueous phase is estimated to be

$$\int_0^{130} \hat{p}_a(x) dx = 59.37 \text{ g} .$$

Similarly, integration of  $\hat{p}_o(x)$  from Eq. (11) yields an estimated 479.31 g in the organic phase. Addition of the measured 394.27 g in the disengagement section yields a final estimate of 932.95 g, which is within 3% of the dump value of 960 g.

Propagation of error is not difficult and provides information for accountability purposes. Suppose a polynomial of degree  $d$  is to be used, that is, the fitted profile has the form

$$p(x) = \exp\left(\sum_{i=0}^d \beta_i x^i\right) .$$

Given concentration measurements  $\underline{y}' = (y_1, y_2, \dots, y_n)$  obtained from along the length of the column, the estimated parameter vector  $\underline{\beta}' = (\beta_0, \beta_1, \dots, \beta_d)$  is a known vector-valued function of the  $\{y_i\}$ , for example,

$$\underline{\beta} = \underline{f}(\underline{y}) . \quad (12)$$

In the example above, the  $\{\beta_i\}$  were obtained from a least squares polynomial regression on the natural logarithms of the  $\{y_i\}$ . For the column length  $L$ , the estimated inventory is

$$I(\underline{\beta}) = \int_0^L \exp\left(\sum_{i=0}^d \beta_i x^i\right) dx .$$

This estimator, viewed as a function of  $\beta$ , is differentiable:

$$\frac{\partial \hat{I}(\beta)}{\partial \beta_j} = \int_0^L x^j \exp\left(-\sum_{i=0}^d \beta_i x^i\right) dx \quad .$$

Let  $a_j = \partial \hat{I}(\beta) / \partial \beta_j$ , where the derivative is evaluated at the observed estimate of the parameter vector, and let  $\underline{a}' = (a_0, a_1, \dots, a_d)$ . For  $\hat{\Sigma}_{\beta}$ , the covariance matrix of  $\underline{\beta}$ , the variance of the estimator, obtained by standard error propagation, is estimated by

$$\text{Var} [\hat{I}(\beta)] \doteq \underline{a}' \hat{\Sigma}_{\beta} \underline{a} \quad . \quad (13)$$

The matrix  $\hat{\Sigma}_{\beta}$  can be propagated following from Eq. (12).

Variance expressions of the form of Eq. (13) are useful for accountability in that the precision of the estimated inventory is evaluated. Also, the dependence of Eq. (13) on the locations  $\{x_i\}$  where data are collected can be examined and alternative measurement schemes can be compared. Indeed, the field of optimal experimental design (a standard reference is Ref. 31) deals with such problems as determining where to locate a given number of detectors to minimize the variance of the subsequent estimator. Similarly, the merits of increasing/decreasing the number of measurements along the column or using different instruments could be studied.

**3. Estimation Based on Theoretical Considerations.** The previous section introduced estimation methods that exploited the continuity of the concentration profile. It is possible to improve on those procedures by taking advantage of knowledge concerning column operation. A major drawback of such an approach relative to regression methods is that lengthy computations are required, which often result in only modest improvements in estimation. Further, a sensitivity analysis is required to propagate errors adequately. Thus, the simpler approaches described earlier are generally recommended when profile measurement data are available. However, some benefits are offered in cases in which insufficient measurement data are available for profile approximation using regression.

A number of computer codes have been written to simulate pulse-column operation and to provide inventory estimates. In a recent survey,<sup>30</sup> L. Burkhart discussed the theoretical basis behind such codes and the present limitations concerning their use. One of these codes, developed by Burkhart and his coworkers, is considered here for illustration. In this code, a discrete-stage model is used, and solute concentration profiles are solved numerically using a Newton-Raphson procedure. Calculations are performed stagewise using finite difference equations that include reaction kinetics, empirical dispersed- and continuous-phase volume relationships, axial eddy current diffusion (or backmixing), and non-equilibrium mass-transfer effects. The Burkhart model can be used to simulate either single- or dual-process pulse columns.

As implemented here, the estimation procedure resembles the general curve-fitting methodology described in the previous section. The mass-transfer and backmixing coefficients, unknown but required for input by the code, are treated as parameters to be estimated. Inventory estimates are obtained by finding the code-generated profile that agrees best (in a least squares sense) with the observed data. This optimization is performed by using the code in conjunction with a standard, derivative-free function minimization routine. When no profile measurements are available, it may be possible to estimate the required coefficients based on information of operating conditions, though this possibility is not considered below.

The estimated profile of the 2A-3 extraction/scrub column obtained through use of the code is shown in Fig. 26. The corresponding estimated quantity of uranium is 932 g, which compares well with the dump value of 960 g (see Table X).



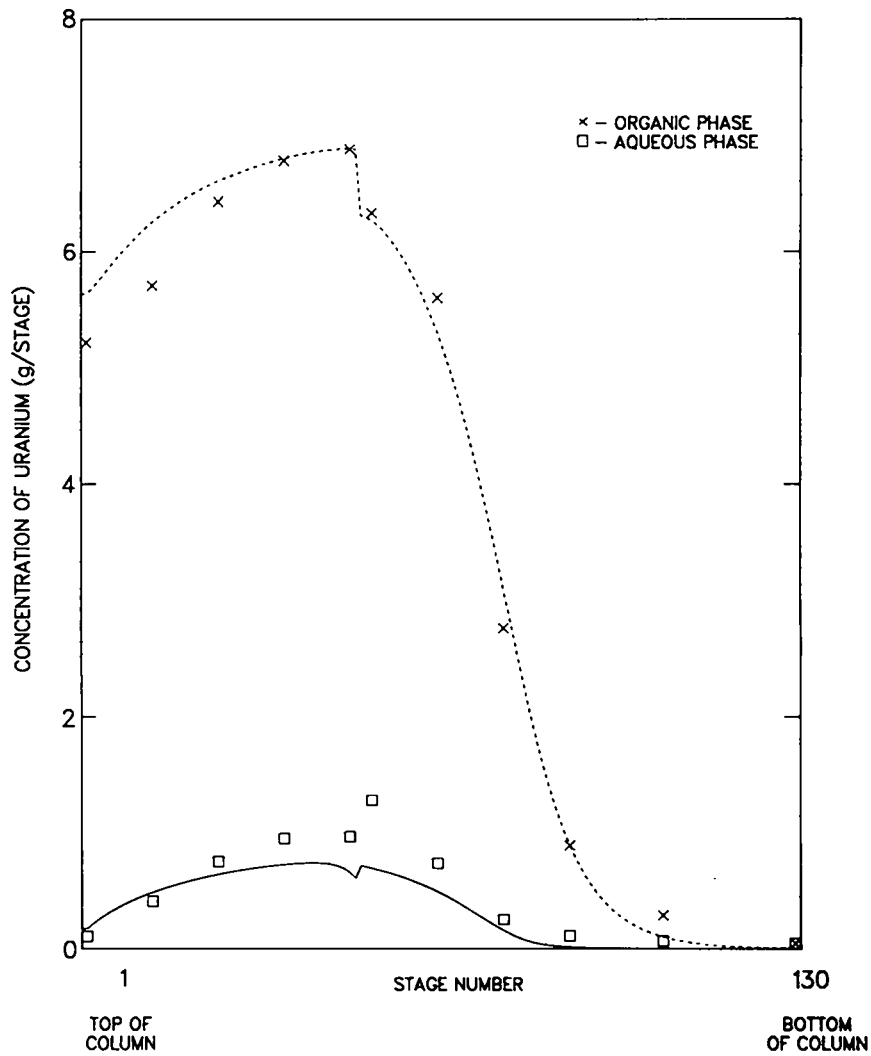


Fig. 26. Estimated profile—Burkhart model.

TABLE X. Summary of Modeling Results

Experimental Run 2A-3			
	Extraction/scrub Column	Stripping Column	Total for Experiment
Inventory estimate using regression methods, g	933	1148	2081
Inventory estimate using Burkhart code, g	932	1184	2116
Dump value, g	960	1090	2050
Experimental Run 2D-2			
	Extraction/scrub Column	Stripping Column	Total for Experiment
Inventory estimate using regression methods, g	1577	1298	2875
Inventory estimate using Burkhart code, g	1609	1304	2913
Dump value, g	1430	1315	2745

The same procedures were applied to data obtained from the stripping column of the 2A-3 experiment. The estimated profiles from the regression approach and from the Burkhardt code are displayed in Figs. 27 and 28, respectively. The corresponding estimated inventories are 1148 and 1184 g compared with the dump value of 1090 g.

Analysis of the 2D-2 experiment followed along the same lines. Figures 29-32 are the counterparts of Figs. 25-28, and the results are summarized in Tables X and XI. Summing results for the extraction/scrub and stripping columns, the dump value of 2745 g is reasonably approximated by the regression estimate of 2875 g (an error of 5%) and the code-generated value of 2913 g (an error of 6%).

Because many data of high quality exist on which to derive estimated profiles, good results can be anticipated from either method. Had fewer measurements been obtained from along the column or if larger measurement errors had been present, poorer performance would, of course, be expected from any approach.

TABLE XI. Estimated Concentration Profiles

1.A Extraction/scrub column

Estimated profiles are of the form

$$\hat{p}(x) = \exp(\beta_0 + \beta_1 + \beta_2 x + \beta_3 x^2 + \beta_4 x + \beta_5 x^2),$$

where  $\hat{p}(x)$  is the estimated concentration of uranium (in grams per unit length of the column) at location  $x$  along the column, and the other parameters have the values tabulated below.

	2A-3 Experiment		2D-2 Experiment	
	Aqueous	Organic	Aqueous	Organic
$\beta_0$	$-2.401 \cdot 10^0$	$1.677 \cdot 10^0$	$-1.645 \cdot 10^0$	$2.063 \cdot 10^0$
$\beta_1$	$1.500 \cdot 10^{-1}$	$-1.165 \cdot 10^{-2}$	$2.186 \cdot 10^{-1}$	$-1.637 \cdot 10^{-3}$
$\beta_2$	$-2.583 \cdot 10^{-3}$	$1.300 \cdot 10^{-3}$	$-8.652 \cdot 10^{-3}$	$9.536 \cdot 10^{-4}$
$\beta_3$	$1.068 \cdot 10^{-5}$	$-2.407 \cdot 10^{-5}$	$1.620 \cdot 10^{-4}$	$-3.620 \cdot 10^{-5}$
$\beta_4$	0	$9.682 \cdot 10^{-8}$	$-1.332 \cdot 10^{-6}$	$5.175 \cdot 10^{-7}$
$\beta_5$	0	0	$3.584 \cdot 10^{-9}$	$-2.618 \cdot 10^{-9}$

1B. Stripping column

Estimated profiles are of the form

$$\hat{p}(x) = \exp(\beta_0 + \beta_1 x + \beta_2 x^2).$$

	2A-3 Experiment		2D-2 Experiment	
	Aqueous	Organic	Aqueous	Organic
$\beta_0$	$3.904 \cdot 10^{-1}$	$-6.158 \cdot 10^{-1}$	$-5.5508 \cdot 10^0$	$-8.615 \cdot 10^0$
$\beta_1$	$3.174 \cdot 10^{-2}$	$1.982 \cdot 10^{-2}$	$1.734 \cdot 10^{-1}$	$1.830 \cdot 10^{-1}$
$\beta_2$	$-1.420 \cdot 10^{-4}$	$-6.887 \cdot 10^{-5}$	$-9.054 \cdot 10^{-4}$	$8.946 \cdot 10^{-4}$

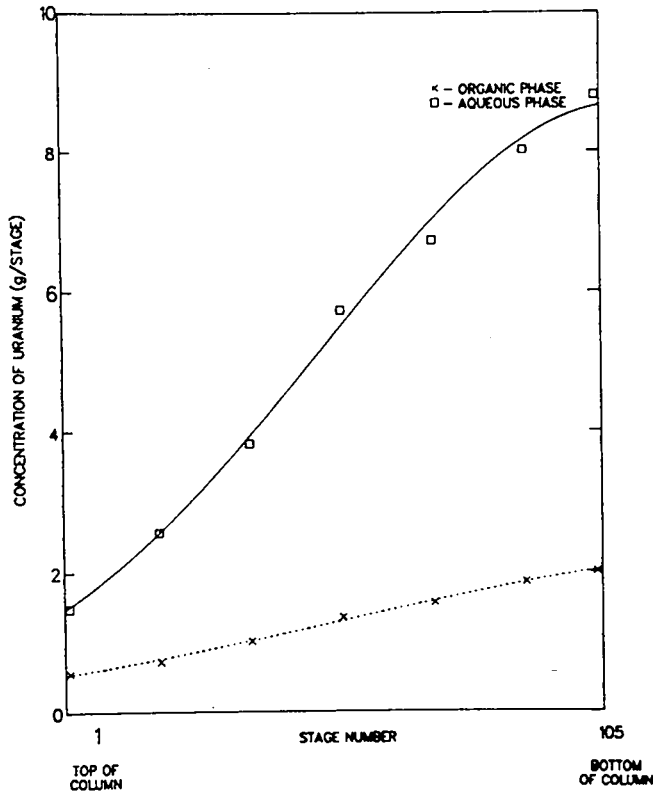
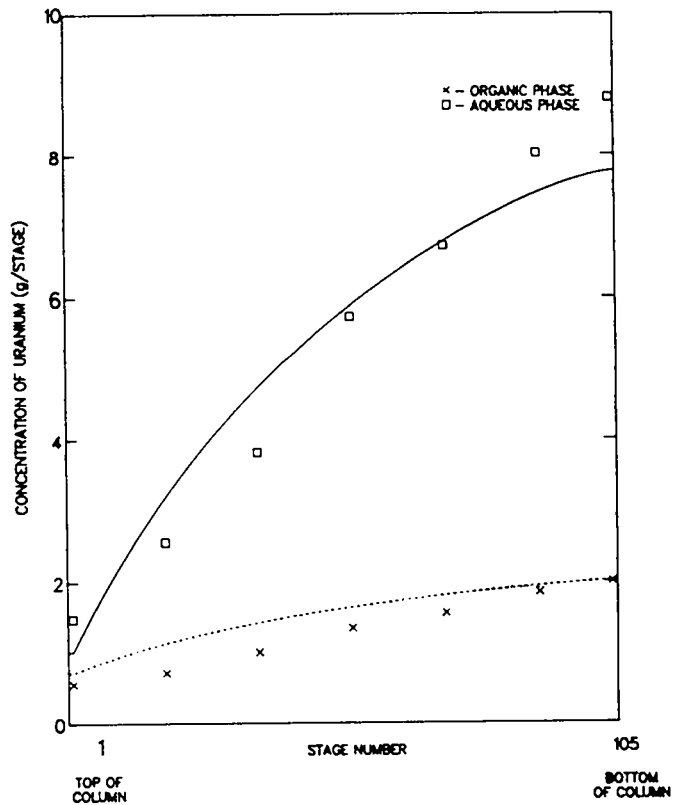


Fig. 27. Estimated profile—regression methods.

Fig. 28. Estimated profile—Burkhart model.



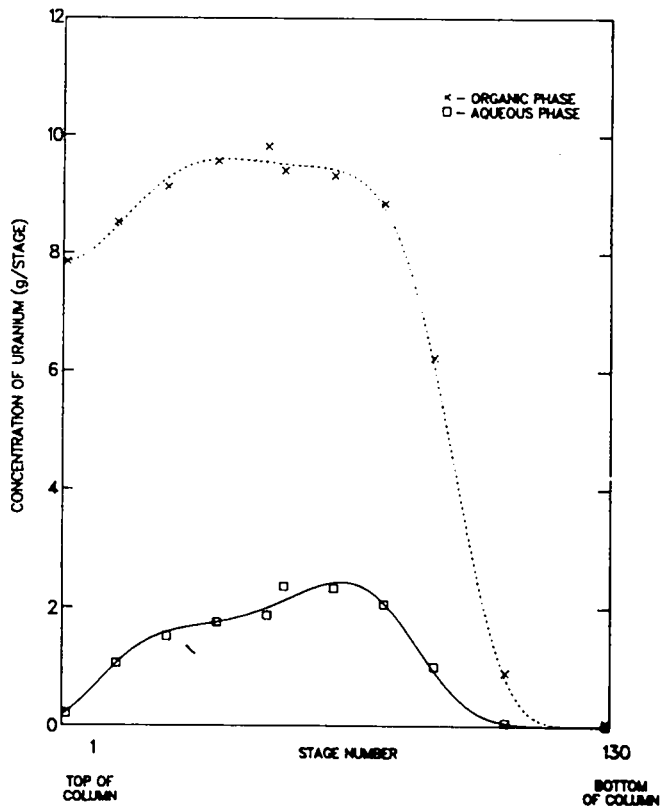
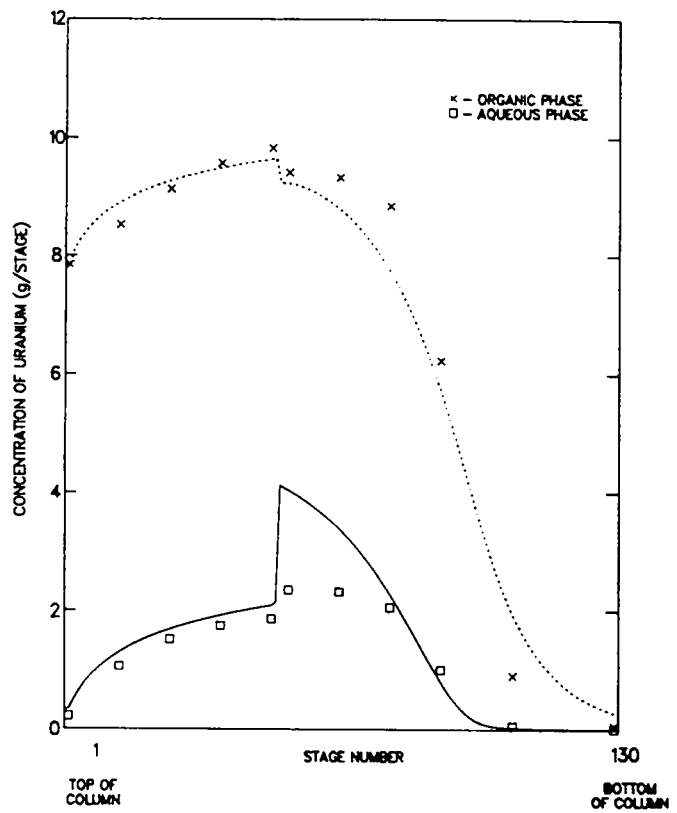


Fig. 29. Estimated profile—regression methods.

Fig. 30. Estimated profile—Burkhart model.



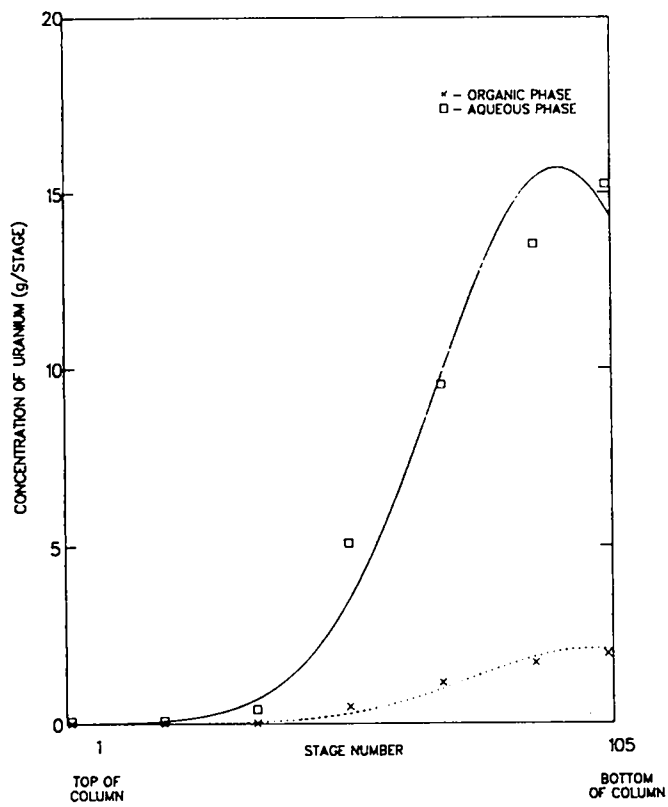
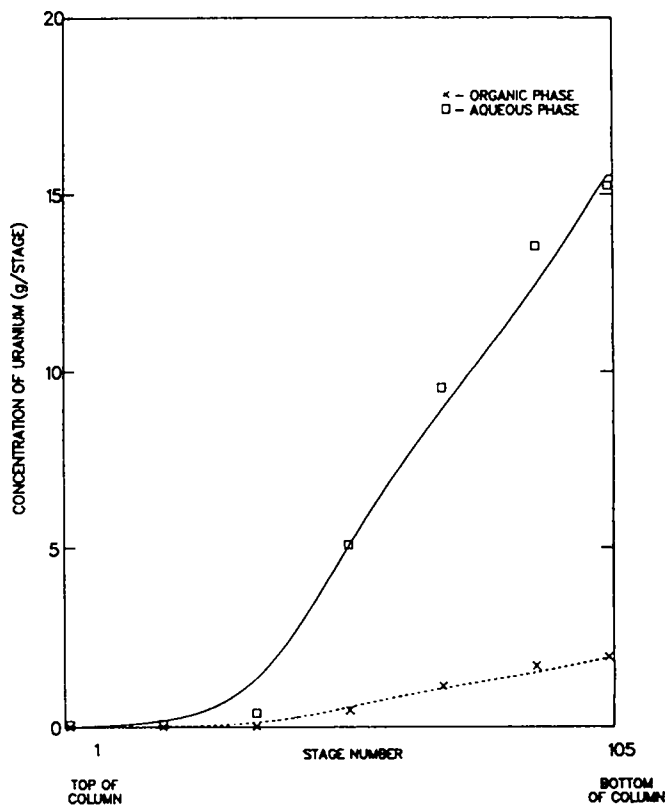


Fig. 31. Estimated profile—regression methods.

Fig. 32. Estimated profile—Burkhardt model.



## V. EXPERIMENTAL STUDY OF URANIUM HOLDUP DURING AMMONIUM DIURANATE (ADU) PRECIPITATION AND CALCINATION

The process of precipitating uranium with  $\text{NH}_4\text{OH}$  is widely used in the nuclear fuels materials preparation industry. Therefore, the materials holdup in this unit process is of concern to the nuclear industry as well as to regulatory agencies. Uranium can be completely precipitated from uranyl solutions provided the matrix does not contain complexing ions such as carbonate, citrate, tartrate, and fluoride. This process serves to separate uranium from many anions, alkali metals, alkaline earths, and cations such as copper, nickel, cobalt, zinc, and others that form complexes with ammonia. Although this procedure itself does not accomplish the necessary purification, it is an essential first step for fuels materials preparation for a variety of nuclear reactors.

In the industrial application of this process, the feed material (usually uranium hexafluoride) is converted into a uranyl solution by hydrolysis. This solution contains  $\sim 4$  moles of hydrofluoric acid per mole of uranium and is used as the feed solution for the precipitation of ADU. The ADU precipitate is filtered and calcined to produce  $\text{U}_3\text{O}_8$ , which is further processed to prepare fuel pellets.

### A. Experimental Study

The objective of this experimental study was to simulate the generic process involved in ADU precipitation and calcination and to measure holdup of uranium as a function of throughput in various parts of the process equipment. In addition, the experimental study of the holdup of uranium in dissolvers was combined at the front end of this process for efficiency of experimental design and data gathering. Several variations of the ADU precipitation and calcination unit process are practiced in the industry. The following procedure was chosen for this study and is commonly used in fuel materials preparation facilities and scrap recovery operations.

A known weight of  $\text{U}_3\text{O}_8$  (1-kg equivalent of uranium) was placed in the stainless steel dissolver. This dissolver vessel was a cylinder of 20-cm diam and 1-m height. The  $\text{U}_3\text{O}_8$  was wetted down with 1 L of distilled water and 700 mL of concentrated  $\text{HNO}_3$ . The mixture was heated for 10 min in a well-ventilated hood to complete the dissolution, then diluted to 4 L with appropriate amounts of concentrated  $\text{HNO}_3$  and water to get the desired acid concentration for the feed solution to the precipitator. A one-time addition of a predetermined amount ( $\sim 10^8$  Bq) of  $^{46}\text{Sc}$  tracer as  $\text{Sc}^{3+}$  was made to the solution, and the mixture was homogenized using a magnetic stirrer. The weight of the solution in the dissolver was recorded, and a 2-mL aliquot of the solution was removed for analysis.

The uranium solution in the dissolver was then transferred to the precipitation column using a vacuum transfer technique illustrated in Fig. 33. The vacuum line was disconnected, the  $\text{NH}_4\text{OH}$  metering pump was connected (Fig. 34) to the inlet of the column, and the circulation pump was started. This circulation pump was maintained at a flow rate of  $\sim 5$  L/min, which allowed for vigorous mixing of the contents of the precipitator. Ammonium hydroxide was added to the precipitator at a rate of  $\sim 300$  mL/min while the solution was mixed by the circulation pump. After the addition of the predetermined amount of  $\text{NH}_4\text{OH}$ , the mixing of the contents of the precipitator was continued for another 15 min. A sample removed from a side port next to the pump was used to measure the pH of the final mixture. This pH was maintained at 9-10 for most of the runs in this series of experiments.

Four large (15-cm diam) polyethylene filter funnels were placed on 4-L vacuum flasks and fitted with double layers of Whatman #2 filter paper. The slurry of ADU in the precipitation column was drained into these filtration devices, and the vacuum was maintained for 1-2 h to remove most of the residual liquid from the ADU. The ADU cakes were then transferred to two shallow Inconel-600 trays ( $35 \times 20 \times 2$  cm) and weighed to determine the wet weight of the ADU cake. The trays containing the moist cake were carefully loaded into the Lindberg furnace, preheated to the calcining temperature ( $700\text{-}900^\circ\text{C}$ ), and calcination continued for 10 h. After calcination, the furnace was allowed to cool to room temperature, and the contents of the Inconel trays were again weighed to determine the amount of  $\text{U}_3\text{O}_8$  recovered. This

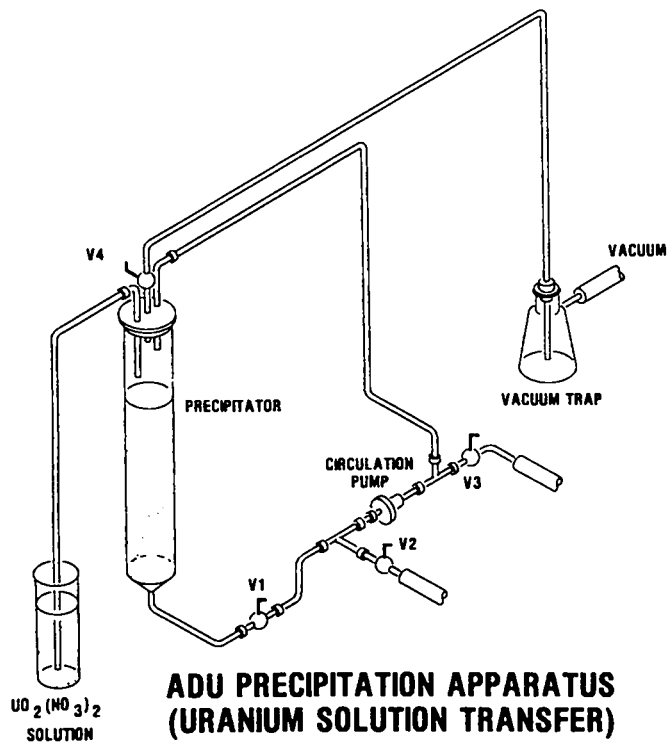


Fig. 33. An isometric view of the precipitator during solution transfer.

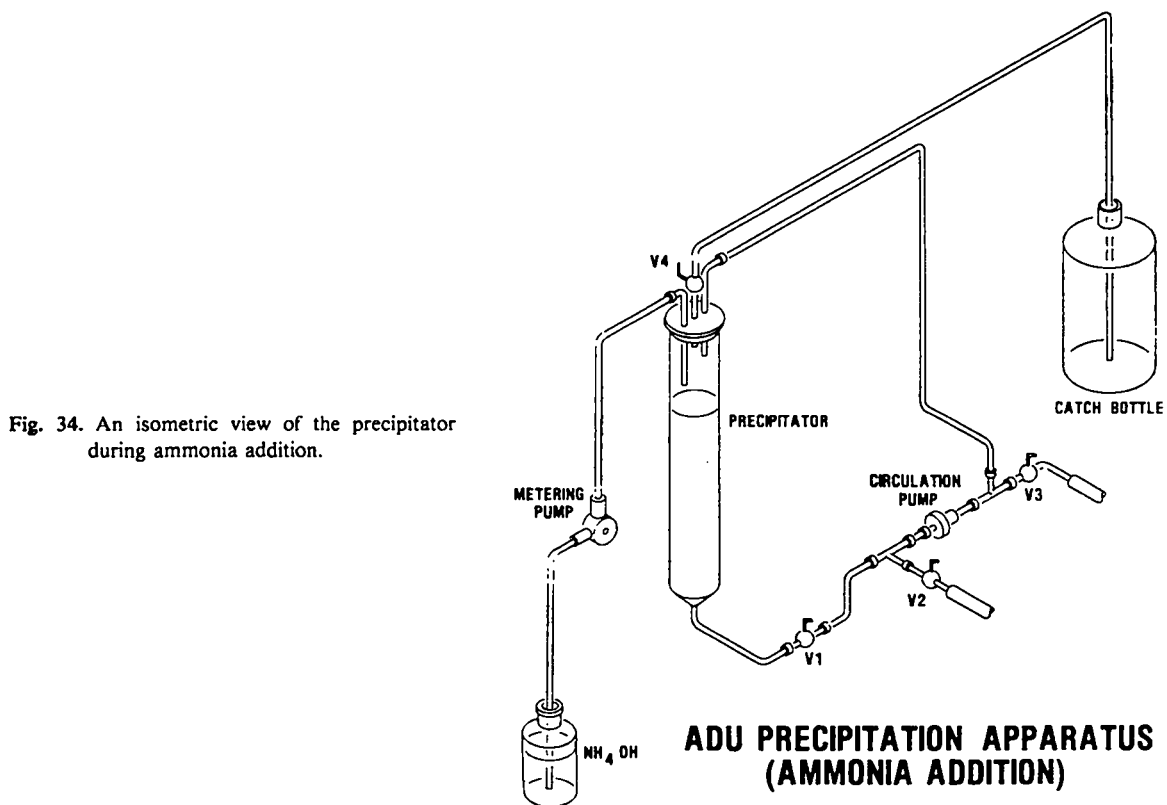


Fig. 34. An isometric view of the precipitator during ammonia addition.

$U_3O_8$  was transferred to the tared dissolver once again, and the weight of  $U_3O_8$  to be dissolved for the next batch was determined. This cycle was repeated 52 times during this experimental study with a cumulative throughput of  $\sim 52$  kg of uranium.

Scandium, a chemical analogue of uranium with a unique neutron activation product, was used as a tracer to measure the holdup by nondestructive gamma-assay techniques. In the case of ADU precipitation and calcination, uranium went from a homogeneous solution to a precipitate and then to a calcined solid. The scandium also followed the physical changes of uranium concomitant with chemical changes.

Between each batch operation, the holdup of uranium in the dissolver, the precipitation column, filter funnels, the calciner, and the calciner trays were carefully measured using the NaI(Tl) detector system described in Sec. V.C. After each run, materials balance computations were made by analyzing the feed solution and the combined filtrate from the filtration flasks and using the weighings and NDA measurement results of that run.

Acid concentrations of the feed solution, quantities of excess  $NH_4OH$  added to the precipitation column, duration of the vacuum filtration step, and temperature of the calcining furnace were varied to determine whether these parameters had any influence on the holdup characteristics of uranium.

## B. Facility Description

This experiment was performed at one of the research facilities of the Los Alamos National Laboratory. This facility is normally used for processing and characterizing depleted and low-enrichment uranium in various physical and chemical forms. Generally, this location has large inventories of uranium, which contribute to the background radiation levels and are undesirable for the NDA of small amounts of uranium. The ADU precipitation column and associated equipment were located in two of the large hoods in this laboratory. The calciner, a Lindberg muffle furnace, was located in such a manner that the effluents from the furnace could be safely vented. The ventilation duct, maintained at a negative pressure, was extended to the top of the furnace to prevent the dispersal of fumes from the furnace.

## C. Holdup Measurement

All the holdup measurements of this experiment were made using the  $^{46}Sc$  radioactive tracer, carefully chosen to be compatible with the chemical and physical changes of uranium during this unit process. The desirability and advantages of using tracers for holdup measurement are discussed in detail in Appendix A. The  $^{46}Sc$  tracer has a half-life of 83.8 days and two high-energy gamma emissions with energies of 889.3 and 1120.5 keV. These gamma emissions were readily measurable in a location having significant background radiations from enriched and depleted uranium. Furthermore, it was possible to make these measurements using a 5- x 5-cm NaI(Tl) scintillation detector and a single-channel analyzer and a scaler. A commercially available stabilized single-channel analyzer (Ludlum model 2218 dual-channel analyzer) was the instrument used in day-to-day measurements. The detector was shielded by a 1.5-cm-thick lead shield with a 5-cm-long collimator. The shielded detector was mounted on a mobile, vertically adjustable and horizontally rotatable pedestal (Fig. 35). This mounting was versatile enough to make all the required measurements of uranium holdup in the dissolver, precipitator, filter funnels, calciner, and calciner trays. Of these NDA measurements, the most difficult one was the holdup in the 1-m-long precipitator column. Access to this column was limited to one side of the hood, where there was a glass shutter. Some details of the strategy used in accomplishing this measurement are given in the following paragraphs. All the other measurements were relatively simple and used specially fabricated standards to match the geometry of the holdup in the process vessel or equipment.



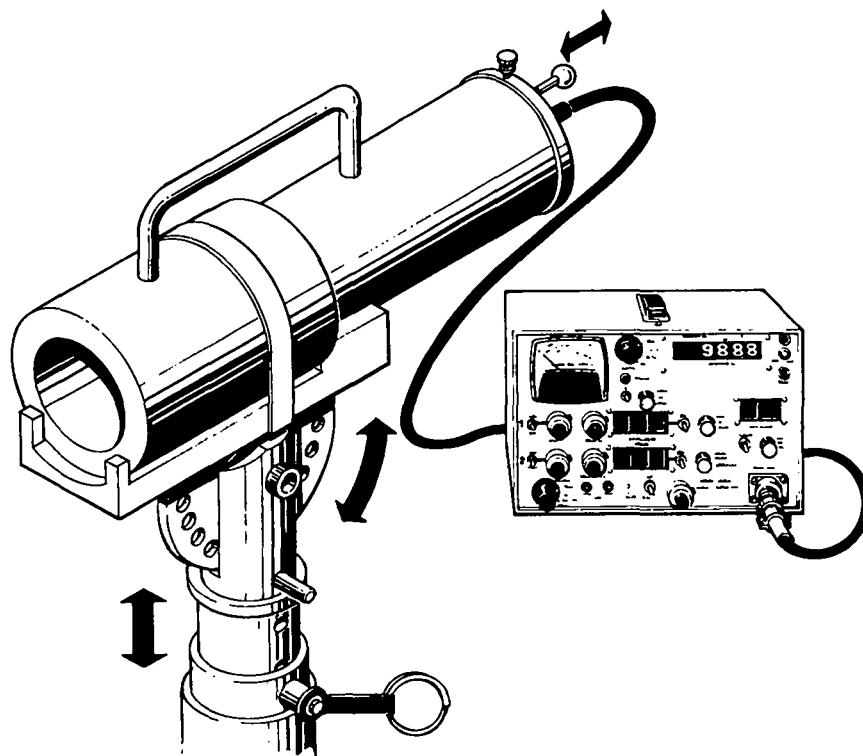


Fig. 35. Detector assembly and its pedestal.

As described earlier, the precipitator column consisted of a 20-cm-diam, 1-m-long, stainless steel column with a wall thickness of 3.5 mm. This column was mounted vertically inside the hood and had a flat top and a 45° conical bottom, which was attached to piping as shown in Fig. 33. In principle, the holdup could be distributed with an arbitrary time-varying profile along the length of the column. The objective was to make the holdup measurements in a simple and reproducible manner, with only one or two measurements, locating the detector at predetermined positions. Because of the background levels in the area, close coupling of the detector with the column was desirable. Close coupling of a detector with an extended source leads to a nonuniform response to materials at different positions within the source. Therefore, it was decided to make the measurements from two vantage points of the detector (Fig. 36). Measurement A was made in a geometry (15° upward from the horizontal plane of the detector) such that holdup at the top and bottom of the precipitator had the same response (counts/time/unit holdup) and the center section had a response approximately twice as large. This response profile was experimentally determined using a source of known strength, which had been fabricated into a ring that fit snugly into the column. Count rates were obtained from the source at 17 equally spaced positions along the column.

If the holdup profile was uniform along the length of the column, the calibration constant relating the count rate to the holdup would simply be the average value of the response function. However, if the material was not held up uniformly, which was the actual case, the calibration constant had to be calculated by averaging the response function at each location weighted by the fraction of the total holdup at that location. Because the holdup profile varied with some of the parametric changes in the precipitation process, new holdup measurement profiles were periodically obtained to determine calibration constants. The holdup profiles were measured by a small, essentially unshielded NaI(Tl) detector setup ("Samson," manufactured by Eberline Instrument Co.) to count the high-energy gamma rays. The spatial resolution of the detector used was about 6-cm FWHM for the column geometry.

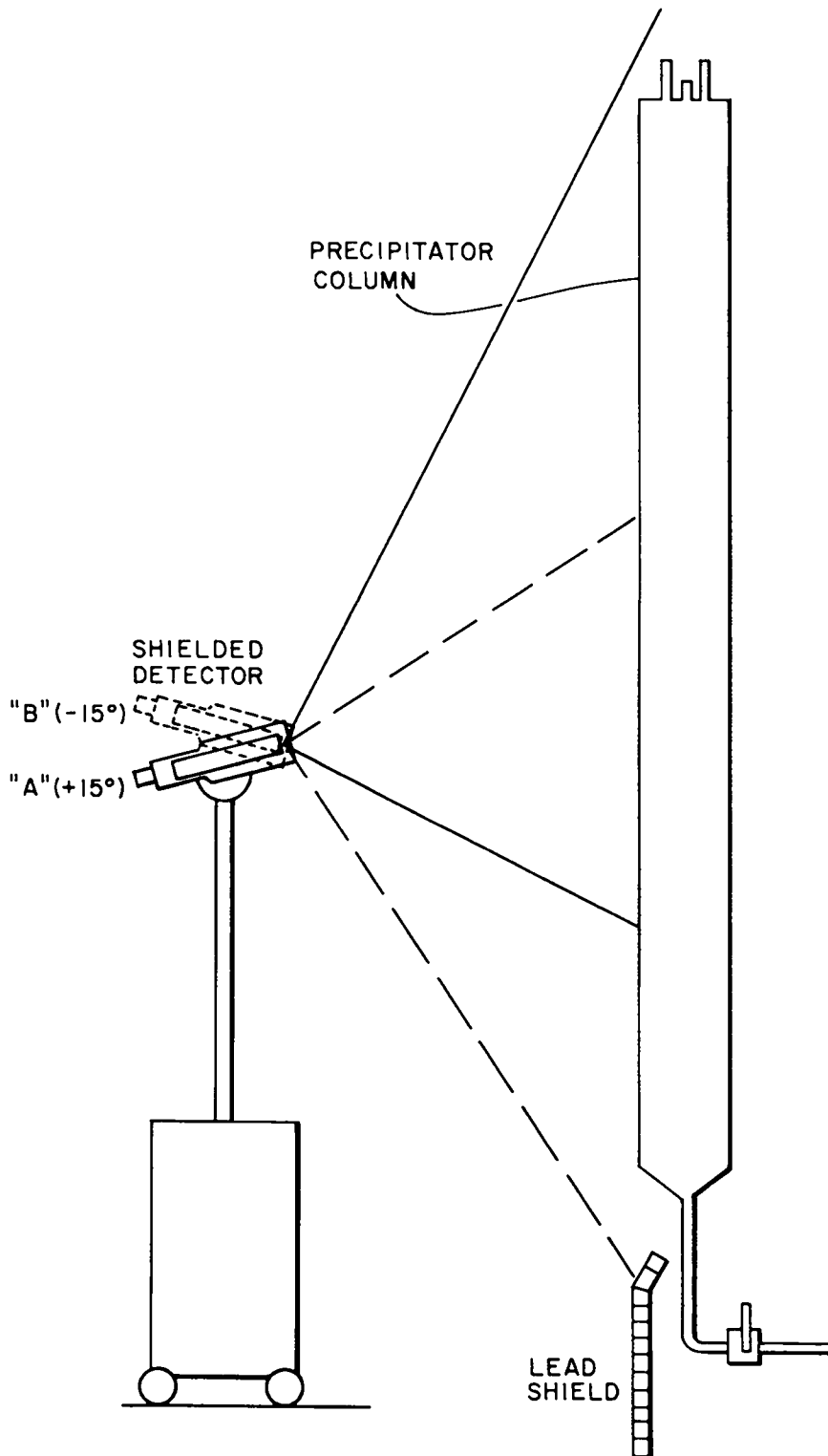


Fig. 36. Detector positioning in front of the precipitator for measurements A and B.

One additional measurement (B) was made with the detector tilted 30° downward from the first measurement position. In this position, the whole column was viewed with quite a different response function; the bottom of the column had a weighting factor ~2.5 times that of measurement A. As with measurement A, the calibration constant was calculated by averaging the response function, weighted by the actual holdup profile determined periodically during the experiment using the small NaI(Tl) detector. Ideally, the two measurements would indicate the same holdup, and any disagreement between the two is an indication of the potential measurement error. Such disagreements were realized few times during these measurements, and they were caused by unusually large holdup in the valves and pump located next to the column. An attempt was made to minimize these interferences by placing shadow shielding as shown in Fig. 36, although it was difficult to fully shield the detector from 1-MeV gamma rays by 2.5-cm-thick lead plates.

The measurement of the holdup of uranium in the calciner furnace was done by placing the detector in a reproducible position in front of the open furnace and measuring the gamma emission of the tracer in the residual uranium. The calibration constant was developed in a manner similar to that for the precipitator column using specially fabricated rectangular sources that fit snugly inside the furnace. Because of the reasonably stationary profile for deposition of uranium within the furnace, one measurement per run was adequate for good results.

#### D. Experimental Results

This investigation of the holdup of uranium during ADU precipitation and calcination employed various combinations of experimental conditions (Table XII) to examine whether these changes had any influence on the holdup of uranium in the equipment used. Five pieces of equipment selected for holdup measurements were the precipitator, filter funnels, calciner, calciner trays, and dissolver vessel. The measured holdup of uranium in each of these items, as a function of throughput, is tabulated in Tables C-XVIII through C-XXII. Detailed examination of these results for estimation model development are presented in Sec. V.F. Some qualitative observations derived from continually monitoring the results as the experiments progressed are presented here; they are also apparent from detailed results tabulated in Appendix C.

TABLE XII. Experimental Parameters of ADU Precipitation and Calcination Experiments

Experiment Nos. <sup>a</sup>	Concentration of HNO <sub>3</sub> in Feed Solution (moles/L)	Volume of Concentrated NH <sub>4</sub> OH (mL)	pH of ADU Slurry	Duration of Filtration (h)	Calcining Temp. (°C)
1-8	0.1	950	7.9-8.4	0.5-3.0	700
41-44	0.1	950	7.8-8.0	0.5-1.0	900
9-16	1.0	1600	7.8-8.2	0.5-2.0	800
45-48	1.0	1900	8.5-9.2	0.5-1.0	900
17-24	2.0	2300	7.8-8.2	0.5-1.0	800
49-52	2.0	2500	8.3-9.2	0.5-1.0	900
25-32	2.0	5000	9.9-10.2	0.5-2.0	800
33-40	2.0	5000	10.0-10.2	0.5-2.0	800

<sup>a</sup>The throughput of uranium was ~1 kg/batch.

In general, the holdup of ADU in the precipitation vessel accounted for 20-80% of the total holdup of uranium in this unit process. There were changes in the holdup of ADU that were attributable to the excess acid in the feed solution and the large excess of  $\text{NH}_4\text{OH}$  added to the precipitation vessel. This appears to have influenced the physical characteristics of the ADU precipitate. However, this property of the precipitate was not quite controllable or quantifiable. During the initial addition of  $\text{NH}_4\text{OH}$  to the highly acidic uranyl solution, a violent reaction takes place at the interface of the uranyl solution, and this splatters the product to the upper surfaces of the precipitator above the liquid interface. This slurry had a tendency to adhere to the surface and remain in the upper regions of the precipitator column even after the bulk of the ADU slurry was drained out of the column. The unusual shift in the ADU profile with very large depositions at the lower regions of the column may be caused by the physical characteristics of the ADU, which was very slimy and viscous. This occurrence was less frequent than the occurrence of profiles with large depositions at the top and middle sections of the precipitator column.

There was significant holdup of ADU in the filter funnels, and the changes in holdup in the funnels are generally attributable to the physical characteristics of the precipitate. It was difficult to maintain a uniform quality of the precipitate from batch to batch even when the experimental conditions were not deliberately altered. The filtration time of ADU was varied from 0.5 to 3 h with several intermediate stages to observe changes in the moisture content of ADU as a function of vacuum retention on the filtration system. The surface of the ADU cake almost always cracked  $\sim 0.5$  h after the supernatant liquid layer filtered through the cake. As a result, the ADU cake reached a moisture content of  $\sim 50$ - $53\%$  and remained almost unchanged irrespective of retaining the vacuum for various periods up to 3 h. The variations in filtration time did not show any marked influence on holdup in the funnels.

The holdup in the calciner and the calciner trays showed steady increases as a function of throughput, although the quantities of these holdups were small fractions of the total holdup for the unit process. Calcining the ADU to convert it into  $\text{U}_3\text{O}_8$  was usually done at temperatures of  $700$ - $900^\circ\text{C}$ . Two step changes in calcining temperature were examined during this investigation to study the influence of calcining temperature on the holdup of uranium in the calciner and calciner trays. There was no observable influence of calcining temperature on the quality of the calcination product. A marked change in holdup in the calciner was observed when the calcining temperature was increased to  $900^\circ\text{C}$  after experiment 40. There may have been small unmeasured losses of uranium from the furnace through the ventilator terminal near the door of the furnace. This loss was not significant as evidenced by the overall materials balance calculations for each batch processed.

The holdup of uranium in the dissolver vessel was only  $\sim 2\%$  of the total holdup in the ADU precipitation and calcination process equipment. The holdup remained reasonably constant throughout because of the redissolution and transfer of residues from previous batches, and the maintenance of a constant volume of solution within the dissolver. The changes in experimental conditions examined during this study did not seem to have any significant influence on the holdup of uranium in the dissolver vessel.

Of the various parameters examined, the  $\text{HNO}_3$  concentration of the precipitator feed solution and the final pH of the ADU slurry appeared to influence the holdup pattern of uranium in the precipitator. Careful measurements of the holdup profile inside the precipitator column, using a small collimated  $\text{NaI}(\text{Tl})$  scintillator-based detector, showed different profiles of ADU residue distributions in the column (Fig. 37). The procedure for generating these profiles from measurements using the thin  $\text{NaI}(\text{Tl})$  detector is mentioned in Sec. V.C. The deposition of ADU along the length of the precipitator column was monitored at 17 positions 5 cm apart, and the relative count rates observed are plotted on this illustration. The changes in the deposition patterns of ADU in the inner surfaces of the precipitation vessel during experiments 33-52 cover the entire range of parametric changes listed in Table XII. These profile changes are attributable to the changes in experimental conditions. Detailed examination of the results (Table C-XVIII) shows intermittent rapid changes in the holdup of uranium in the precipitator, although the experimental conditions were not altered. It was not possible to associate these changes in total holdup within the precipitator to any of the combinations of experimental conditions listed in Table XII.

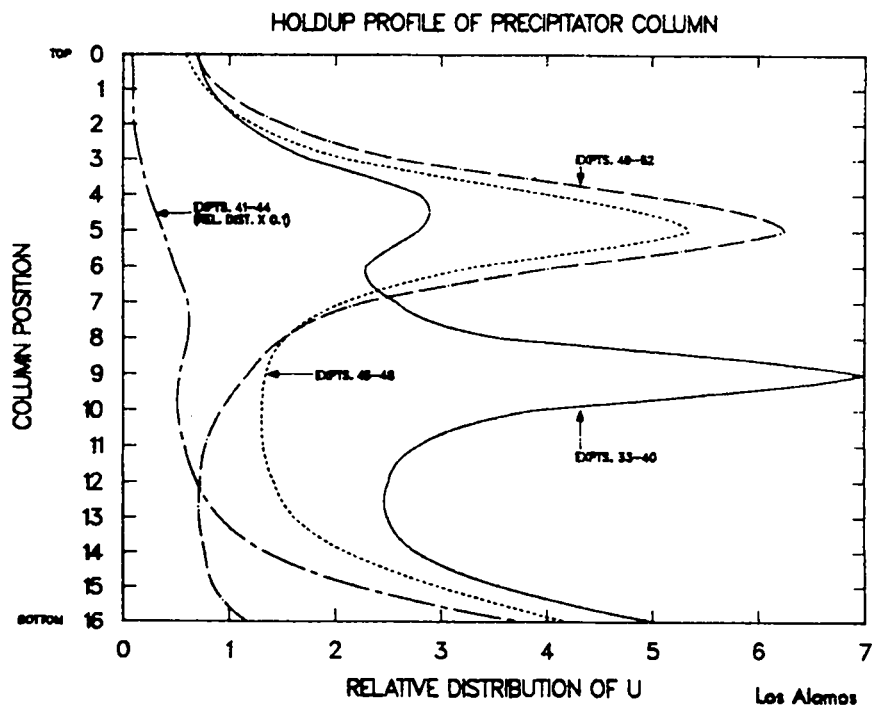


Fig. 37. Different profiles of ADU holdup along the precipitator column.

#### E. Materials Balance and Cleanout Measurements

Gravimetric measurements of  $U_3O_8$  before dissolution and the weighings of recovered  $U_3O_8$  from calcination of ADU provided two reliable measurements to estimate the total loss of uranium during each batch operation of the ADU precipitation and calcination experiment. The loss of uranium from the system in the discarded filtrate was determined by spectrophotometric analysis using Arsenazo-III. These measurements were conducted on filtrates from each of the batch operations. In general, the quantity of uranium lost from the system through filtrates was  $<100$  mg/batch. The uranium content of the dissolver solution was periodically measured by either isotopic dilution mass spectrometry or Davies-Gray titration. Figure 38 compares the sum of the NDA measurement values of holdup of uranium in the dissolver, precipitator, filter funnels, calciner, and calciner trays with the inventory difference (difference in gravimetric measurements) described above. Ideally, a  $45^\circ$  line through the origin would indicate complete agreement between these two sets of residual holdup measurements. The data presented in Fig. 38 show the deviation from the ideal and the reasonably good agreement between NDA measurements and gravimetric estimation of inventory difference. The discrepancies at the higher values of inventory difference (or total holdup) are caused by (1) the major contribution by the holdup in the precipitation vessel and (2) the adhesion of large quantities of material in the upper regions and the lid of the precipitator vessel. This nonuniform deposition of ADU causes the NDA measurements to show lower values because of the use of uniformly distributed thin sources for calibration of the measuring instruments. Further lowering of the "holdup-NDA" value is caused by the very small losses of uranium ( $<100$  mg/batch) through discarded filtrates and unaccounted losses of uranium through the furnace ventilation duct. At the same time, the gravimetric inventory differences plotted here are not influenced by any of these factors.

Several cleanout measurements were performed during this investigation to compare the results of NDAs using  $^{46}Sc$  tracer with destructive chemical analyses. Again, the cleanout measurements were done by spectrophotometric analysis mentioned earlier. The results of these measurements (Table XIII) once again show good agreement between NDA measurements and the cleanout measurements.

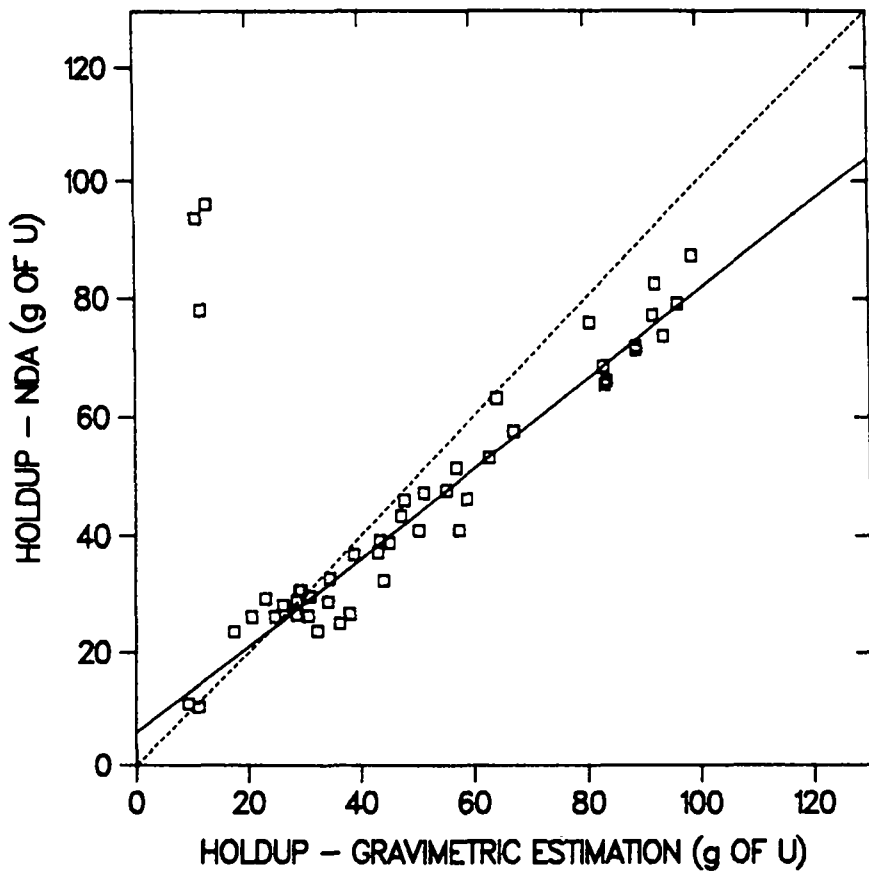


Fig. 38. A comparison of inventory differences with NDA-measured total holdup.

TABLE XIII. Comparison of NDA Measurements of Holdup with Cleanout Measurements (in Grams of Uranium)

Equipment/Parts	NDA Measurement	Cleanout Measurement
ADU precipitation vessel (after experiment 32)	12.6	14.6
ADU precipitation vessel (after experiment 40)	8.8	9.8
ADU precipitation vessel (after experiment 52)	9.3	10.5
Calcining furnace (after experiment 52)	1.7	1.5
Calcining trays (after experiment 52)	1.4	1.3
Filter funnels (after experiment 52)	10.1	9.8

## F. Residual Holdup Estimation

1. **Calciner Trays.** Holdup measurements on the accumulation of material in the calciner trays were made as described in the previous section. The measurement history (Fig. 39) shows a steady increase in observed holdup over time.

As was the case in the analysis of results from ductwork in the dust-generation experiments (Sec. III), material deposition on the calciner trays is (approximately) linearly related to throughput. Modeling thus proceeds similarly to that discussed in Sec. III, where a simple and very useful approach is to obtain the least squares fit of the simple linear regression. This is superimposed in Fig. 39 (the measurement corresponding to a throughput of 48 kg was discarded as an outlier) and can be used for purposes of estimation. The fitted equation is

$$\hat{h}_c(t) = 0.122 + 0.024t, \quad (14)$$

where  $\hat{h}_c(t)$  denotes the estimated holdup in the calciner trays at throughput  $t$ . For  $t = 52$  kg, the end of the experiment, the estimate is  $\hat{h}_c(52) = 1.37$  g uranium. The corresponding cleanout value is 1.26 g, an error of roughly 10%.

If the calcination process were to continue using the same trays, holdup could be predicted for future throughputs by substituting the desired value of  $t$  into Eq. (14). Note, however, that the standard deviations of such estimates increase as a function of the difference between the throughputs corresponding to the predicted values and the last observed measurement. Thus, maintaining good accountability requires that additional data be obtained periodically and used to update the fitted model.

In a final note of general interest, the usual least squares approach can be modified to account for heteroscedasticity or correlation among the observed measurements should such issues arise. When amounts of material do not change considerably over time and errors caused by instrument calibration and process variability are small (as in the present experiment involving the calciner trays), there is little need for such modification or the software required for its implementation.

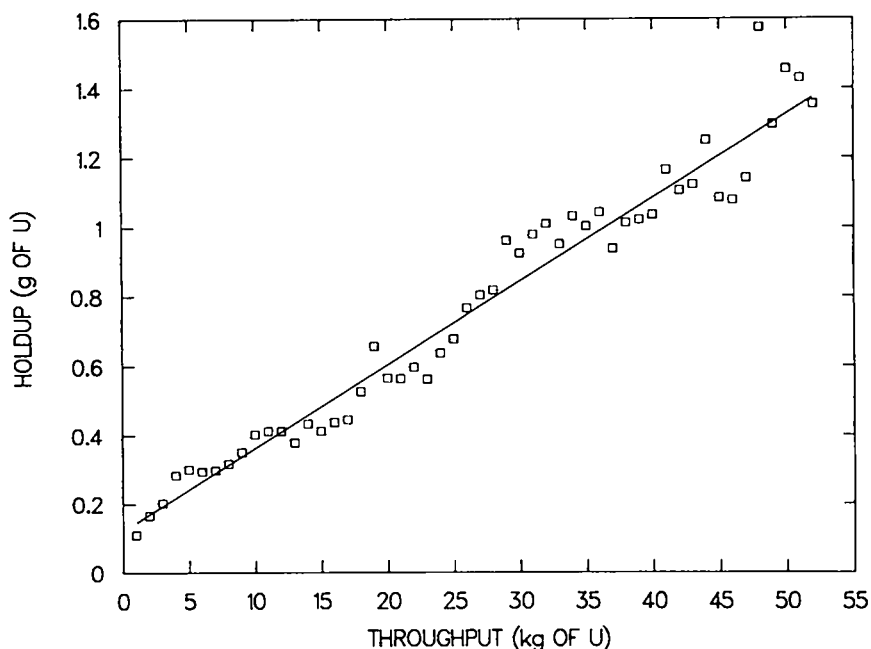


Fig. 39. Linear regression fit to calciner data.

2. Feed Dissolver. The measurement history of the dissolver (Fig. 40) is very unlike the histories observed from the calciner trays or from the dust-generation experiments (Sec. III). Beginning from a clean state, material does not continue to accumulate with time. Instead, a very brief initial increase in deposition is followed by long-term fluctuation about steady-state conditions. Furthermore, process variability plays a major role in estimation; other information concerning the measured values indicates that the observed differences over time are caused primarily by changes in the amount of material held up instead of being largely the consequence of measurement errors while holdup remains constant.

Modeling a steady-state process is not difficult and typically involves the use of Kalman filtering (Appendix B). This methodology was originally developed in Refs. 32 and 33, and more recent presentations of an elementary nature are included in Refs. 34-36. The Kalman filter has been applied to a variety of engineering problems as well as to nuclear materials safeguards work (see Ref. 37) and is not limited to steady-state situations.

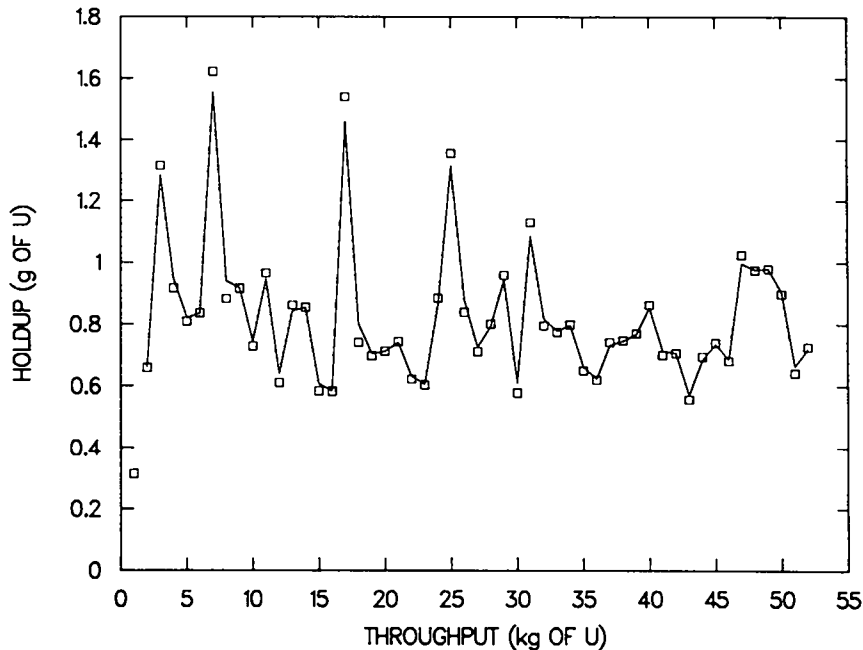


Fig. 40. Application of Kalman filter to the feed dissolver data.

The model is described by two equations, called the measurement and state (or system) equations. These equations reflect the dynamics of the measurement process. The first equation captures the measurement variability (that is, errors exist in all holdup measurements), and the second equation captures the process variability (that is, the "true" amount of material deposited in the feed dissolver varies over time). Estimation of holdup depends crucially on the magnitudes of these variabilities. For example, the measurement history from a poorly measured but very stable process might strongly resemble the history from a well-measured but unstable process. The Kalman filter resolves the contributions of the two sources of variability and produces holdup estimates. Letting  $x(t)$  denote the measured value corresponding to a throughput of  $t$  kg, the measurement equation here is

$$x(t) = h(t) + e(t), \quad (15)$$

where  $h(t)$  is the (unknown) amount of holdup and  $e(t)$  represents the measurement error. It is assumed that  $e(t)$  has mean zero and variance  $\sigma_m^2$ . An estimate of the measurement variability  $\sigma_m^2$  is available from



previous work with the instrumentation involved. In practice, a facility's measurement control program can provide information to help quantify such errors.

The state equation here is

$$h(t) = h(t - 1) + \epsilon(t). \quad (16)$$

This equation captures the steady-state character of the process. The difference in actual holdup between throughputs  $t$  and  $t - 1$  is  $h(t) - h(t - 1) = \epsilon(t)$ , which is assumed to act as a random variable with mean zero and variance  $\sigma_p^2$ . Past experience generally provides an estimate of the process variability  $\sigma_p^2$ . Note that Eqs. (15) and (16) together with the stated distributional assumptions yield a model analogous to the ARIMA (0,1,1) structure described by Box and Jenkins.<sup>38</sup>

The mathematical development of successive holdup estimates  $\{\hat{h}(t)\}$  using Kalman filtering, though relatively straightforward, involves the introduction of some notation and is detailed in Appendix B. Put simply, at each step of the filtering process, the newly observed measurement  $x(t)$  is combined with previous information to update the estimated holdup. Implementation of this methodology to data from the dissolver is illustrated by the solid line in Fig. 40, which connects the filtered estimates. Because measurement errors are small compared with process variability, the filtering has little effect in this particular case, although this is certainly not always the case. At the conclusion of the experiment,  $t = 52$  kg and the filtered estimate is  $\hat{h}(52) = 0.72$  g uranium.

Despite the established value of Kalman filtering in the solution of a variety of engineering problems, there have been relatively few applications in the materials accountability literature. It has been suggested (Ref. 39, p.279) that the (supposedly) esoteric qualities of modeling have precluded widespread use by nonmathematical audiences. This situation may improve in the future as the usefulness of filtering in near-real-time accounting becomes more apparent.

**3. Filter Funnels.** The measurement history for the filter funnels (Fig. 41) bears a strong resemblance to the history of the feed dissolver. That is, an initial accumulation of material is followed by long-term fluctuation about nominally steady-state conditions. Thus, the modeling and estimation proceed as in the case of the dissolver beaker with the use of Kalman filtering.

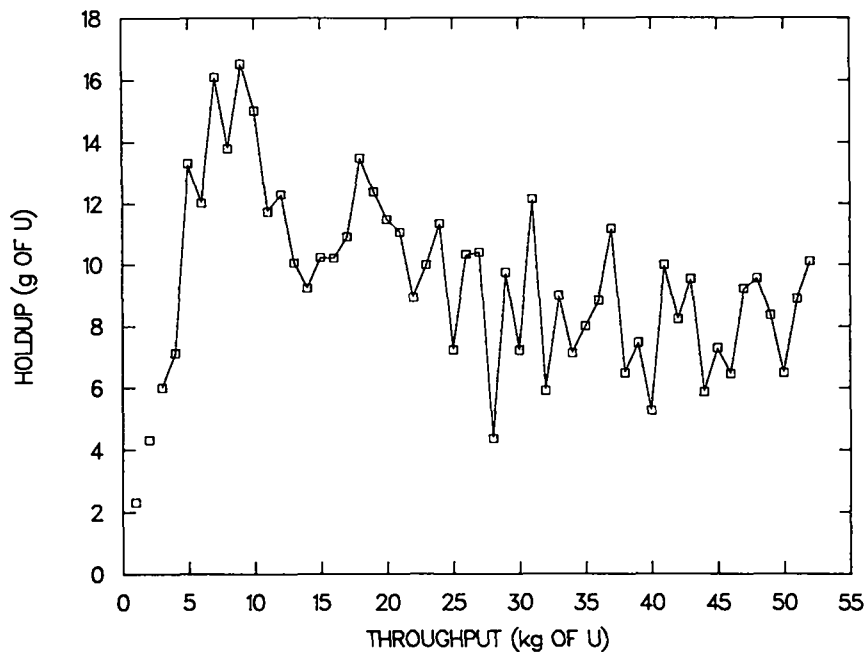


Fig. 41. Application of Kalman filter to filter funnels data.

Filtered estimates, plotted in Fig. 41, are connected by line segments. The amounts of holdup involved are roughly an order of magnitude greater than those observed for the dissolver beaker, and measurement errors are smaller relative to process variability. Consequently, the degree of smoothing is again slight and Fig. 41 appears to connect the measured values, though this is not strictly the case. For example, the estimated holdup at the end of the experiment is 10.099 g uranium, but the associated measured value is 10.11 g uranium.

Use of filtered estimates to serve as near-real-time values for occasions when no measurements are taken presents some interesting issues. Suppose that holdup measurements exist up to a past throughput  $t_0$  and it is desired to obtain a near-real-time estimate of the holdup  $h(t_0 + d)$  at the current throughput  $t_0 + d$ . Because of the presumed steady-state nature of the process, there is no more reason to believe that the actual amount of holdup increased during the interval  $(t_0, t_0 + d)$  than there is reason to believe that actual holdup decreased during that interval. It follows that  $\hat{h}(t_0 + d) = \hat{h}(t_0)$  or that the estimated holdup at throughput  $t_0 + d$  is the same as the estimate at throughput  $t_0$ . Because of the role of process variability, however, errors in estimation increase as a function of  $d$ . Following from Eq. (16) of the model,

$$h(t_0 + d) - h(t_0) = \sum_{t=t_0+1}^{t_0+d} \epsilon(t) \quad .$$

Thus, the increment  $h(t_0 + d) - h(t_0)$  in actual holdup, which depends on process variability, acts as a random variable with mean zero and variance  $d\sigma_p^2$ , where  $\sigma_p^2$  is the process variability. Letting  $\sigma_0$  denote the standard deviation of  $\hat{h}(t_0)$ , the variance in estimation of  $h(t_0 + d)$  using  $\hat{h}(t_0)$  is

$$\text{Var} [h(t_0 + d) - \hat{h}(t_0)] = \sigma_0^2 + d\sigma_p^2 \quad . \quad (17)$$

If, as in the case with observed data from the filter funnels, measurement errors are quite small, the variance in Eq. (17) is roughly  $d\sigma_p^2$ . Maintaining good accountability requires that  $d$  not be allowed to become too large, and thus measurements must be obtained periodically and used for updating.

As an example, consider data from the filter funnels. At  $t = 52$ , the estimated holdup is 10.1 g with a standard deviation of 0.2 g. If the process continued to run and no measurements were made at  $t = 53$  or  $t = 54$ , the predicted holdup for these throughputs would remain 10.1 g because of the steady-state nature of the process. However, the standard deviations of the errors of prediction would rise to 2.4 and 3.5 g respectively. This rise reflects the fact that, primarily because of process variability, the actual amounts of material at  $t = 53$  and  $t = 54$  will likely differ from the predicted values by a few grams. If, at  $t = 55$ , another measurement of high quality were made, the holdup estimate would be updated based on this information, and the associated standard deviation would then return to roughly 0.2 g. Through such periodic measurement, errors in estimation are not allowed to become too large.

**4. Calciner.** The measurement history for the furnace (Fig. 42) exhibits features common to both the calciner trays and the feed dissolver. There is a fairly lengthy period, from the start of the experiment until roughly 10 kg of throughput, during which material continues to accumulate and process variability is quite small. Such behavior resembles the nature of deposition on the calciner trays. Following the period of increase, the process then settles into a steady-state mode from roughly 10-40 kg of throughput and is similar to holdup behavior in the dissolver beaker. Finally, from 41 kg of throughput to the end of the experiment, there is relatively erratic deposition and an overall increase of material.

Data of this nature are commonly analyzed through the use of "changepoint models" as illustrated by the solid line in Fig. 42. Unlike cases in which the transition from one type of behavior (for example, increasing holdup) to another (for example, steady state) is gradual, here the changes occur abruptly. The times of change are not difficult to identify, and modeling proceeds by treating separately each distinct period of holdup behavior. Thus, classical regression techniques are used on the data from the initial increase, and Kalman filtering is implemented for the intermediate period of steady-state operation. The apparent erratic behavior toward the end of the experiment is discussed later.

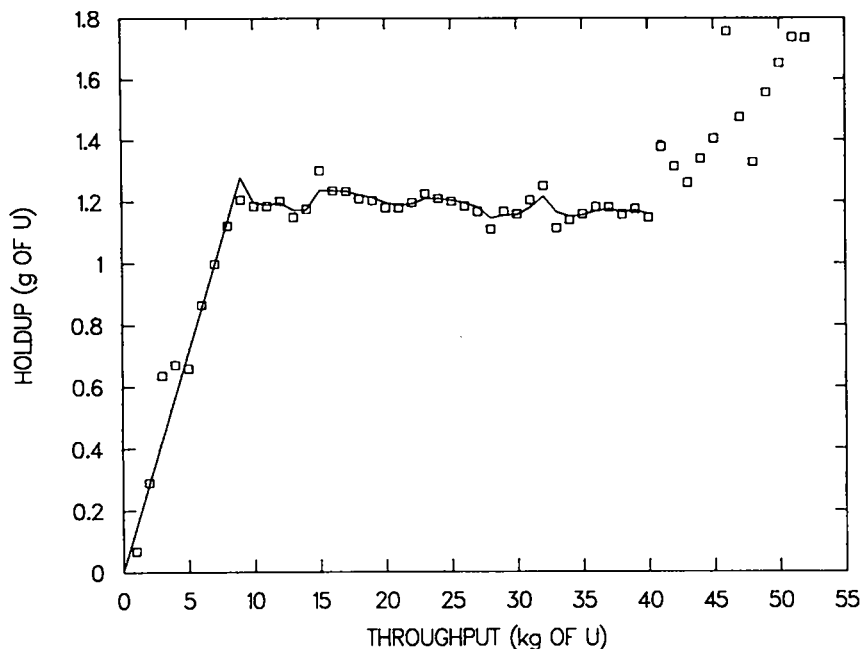


Fig. 42. Change-point model for the calciner data.

Beginning from a clean state, the initial buildup is well characterized by a simple linear regression through the origin, a model used with success in the earlier dust-generation experiments (see Sec. III). The fitted equation is

$$\hat{h}_f(t) = 0.1423t \quad , \quad 0 \leq t \leq 9 \quad (25)$$

where  $\hat{h}_f(t)$  is the estimated holdup in the furnace at throughput  $t$ . From this regression, the predicted value for  $t = 9$  (1.28 g) and its standard deviation (0.078 g) are used to initialize the Kalman filter. Over the interval  $10 \leq t \leq 40$ , where operation is nominally steady state, the filter is used as for the feed dissolver data. Figure 42 illustrates the filtered estimates for this period.

At  $t = 41$ , an apparent anomaly occurs, likely because of changes in experimental conditions (Table XII). Based on information through  $t = 40$ , the predicted holdup for  $t = 41$  under an assumption of continued equilibrium is 1.16 g. The estimated standard error of prediction of the next measurement is 0.045 g. However, the next measured value (1.38 g) is nearly five standard deviations away, indicating perhaps the presence of an outlier or that the process is no longer in steady state. Subsequent measurements confirm the latter hypothesis, and a new model is needed to describe the "new" material deposition. Although several candidate models suggest themselves as possibilities, the data are too erratic and too few in number for a final determination to be made. Thus, no model-based estimates are plotted in Fig. 42 for the period  $41 \leq t \leq 52$ .

Had the experiment continued, collection of additional data would have likely allowed for the construction of a useful model. Worthy of consideration is a Kalman filter application with an assumed linear trend, a model that would capture the overall increase in holdup as well as account for the substantial process variability that apparently existed. Further investigation, however, is required to place adequate confidence in this choice.

5. **Precipitator.** The measurement history for the precipitator is plotted in Fig. 43. Note that the quantities of material involved often greatly exceed those for the other individual pieces of equipment. Over time, the portion of total system holdup residing in the precipitator varies between 40 and 85%. Measured values are of high quality, reflecting the use of tracers as well as the efforts to overcome the potential adverse effects of nonuniform material deposition. Errors resulting from counting statistics are low, and comparisons of the measurements following 32, 40, and 52 kg of throughput with the corresponding cleanout values indicate good agreement.

Besides the large quantities of material that may accumulate, other aspects of holdup in the precipitator are unique. This piece of equipment is the only one in which violent chemical reactions take place during the experiment. The contents of the column undergo dynamic phase changes as a result, and the potential exists for dramatic gains and/or losses of holdup over brief times.

An examination of the measurement history (Fig. 43) exposes some interesting behavior. The early portions of the history are characterized by high variability in the volatile deposition process and unpredictable behavior. This high variability decreases toward the end of the experiment, and measured values tend to be much more stable. It is possible that a learning process took place and is responsible for the improved stability. A facility with stable operations of the precipitator column employing experienced personnel can produce data that will resemble the last part of this experiment. Such data would be amenable to statistical modeling.

Deposits in the upper region of the column contribute to the unusual measurement history before the first cleanout at  $t = 32$ , where an overall increase in holdup is followed by an overall decrease. Figure 44 superimposes a smooth curve over this portion of the data. With the erratic early deposition, material adheres to the upper region of the column as described in Sec. V.D. This material is gradually dissolved with the onset of more stable operation, and amounts of holdup return to more "typical" levels.

Following the first cleanout, steady-state conditions appear to become established. Modeling proceeds as for the feed dissolver and filter funnels with application of the Kalman filter. The estimated holdup at  $t = 40$  is in reasonable agreement (13% error) with the value obtained from the second cleanout (Table XIV).

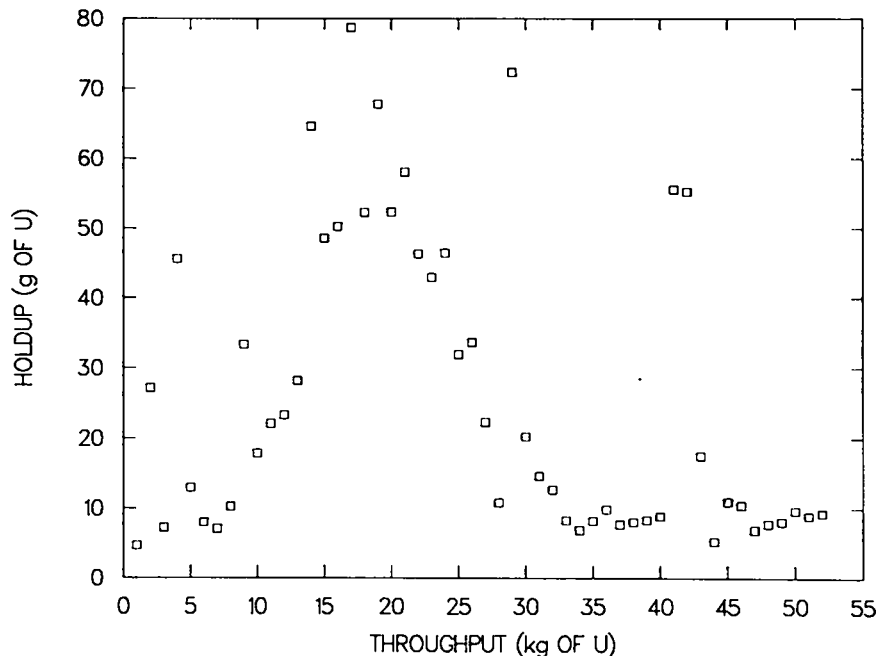


Fig. 43. Measurement history of holdup in the precipitator.

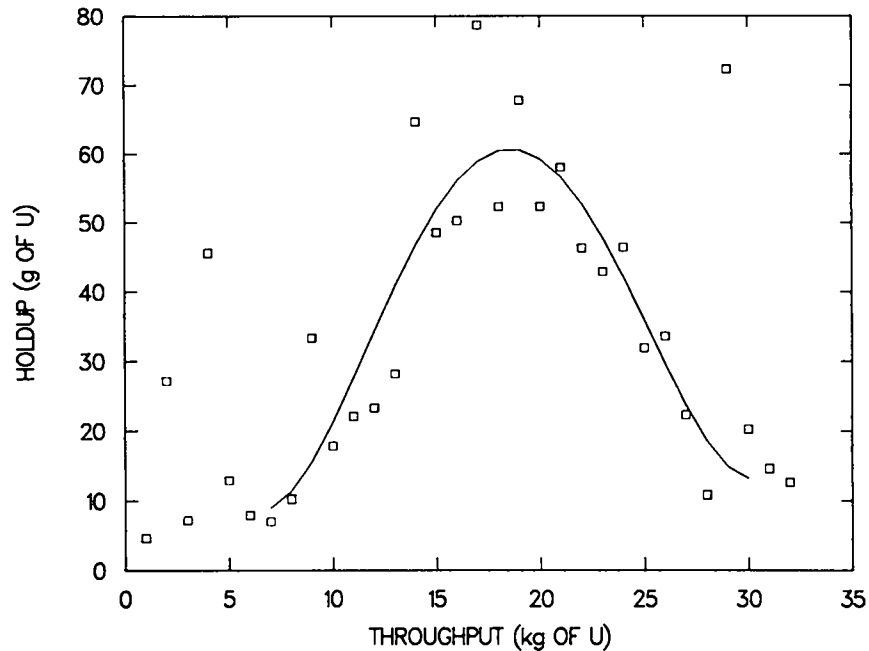


Fig. 44. A smooth curve superimposed on early portions of the precipitator data.

TABLE XIV. Holdup Estimates and Cleanout Values for the ADU Experiment

Equipment	Estimate (g)	Cleanout (g)	Error <sup>a</sup> (%)
Calciner trays (t = 52)	1.37	1.26	9
Feed dissolver (t = 52)	0.72	---	---
Filter funnels (t = 52)	10.10	9.79	3
Furnace (t = 52)	1.76	1.47	20
Precipitator (t = 40)	8.50	9.82	13
Precipitator (t = 52)	9.07	10.53	14

<sup>a</sup>The error is the difference between the estimate and cleanout value expressed as a fraction of the cleanout value.

After the second cleanout, the deposition process is erratic. This is no doubt related to the changes in experimental conditions that took place at  $41 \leq t \leq 44$  (Table XIII). Recall that such changes were also apparent from inspection of the measurement history of the furnace (Fig. 42). Beginning at  $t = 45$ , experimental conditions returned to "normal," and deposition of behavior on  $45 \leq t \leq 52$  again resembled steady state. Applying the Kalman filter to data from this region (Fig. 45) again yields good estimation, and the estimated holdup at the end of the experiment,  $t = 52$ , is in good agreement with the value from the third (and final) cleanout of the precipitator.

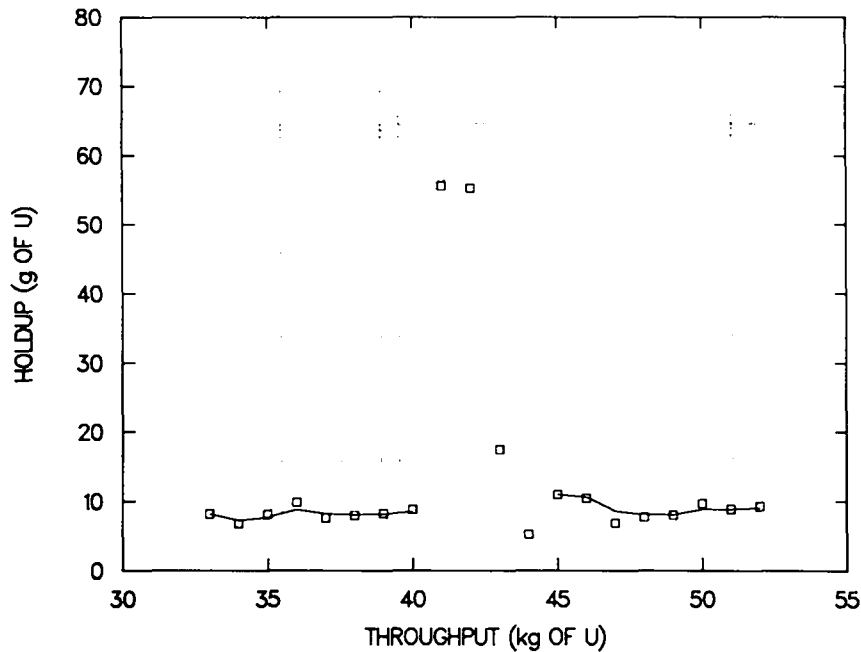


Fig. 45. Application of Kalman filter to steady-state portion of precipitator data.

## VI. EXPERIMENTAL STUDY OF URANIUM HOLDUP IN SOLUTION LOOPS

In uranium-processing facilities and scrap recovery operations, a variety of uranium solutions are transferred from one location to another continuously and/or intermittently through various types of pumps, valves, flow meters, pipes, and pipefittings. Because extensive piping and transfer systems are an essential part of a large processing facility, the residual amounts of HEU in these solution transfer systems can be an important part of the residual holdup of the plant. The potential for developing holdup estimators for these solution transfer systems was examined in an experiment that circulated two types of uranyl solutions through two solution loops. These loops had several components that are often found at an HEU-processing facility, such as pumps, valves, pipes of various dimensions, elbows, tees, pipe unions, and flow meters. The objective of these experiments was to obtain experimental data useful for developing holdup estimators for each component of the solution loop. Because the accumulation of residues inside a solution loop is a relatively slow process, the measurement of the buildup of uranium in these components offered considerably more challenges than any of the other measurements undertaken during these experimental studies. Here again, the use of a carefully chosen tracer, the design of a layout specially suited for measurement reliability, and calibration standards specially fabricated to simulate the parts measured allowed the gathering of experimental holdup data as a function of throughput.

### A. Facility Description

This experimental facility was designed to simulate the component assembly of a solution transfer system at an HEU-processing facility and an HEU scrap recovery operation and to generate data useful for the development of holdup estimators. Two types of materials—stainless steel and chlorinated polyvinylchloride (CPVC)—were chosen for the construction of the solution loops. Also, two types of solutions—uranyl nitrate and uranyl fluoride—that are often found at HEU fuel materials preparation

facilities were chosen for this experimental study. Two independent circulating systems (Figs. 46 and 47) were designed and built incorporating a large storage tank, a surge tank, a pump, ~50 m of pipes of various shapes and sizes, several valves and terminal valves, a variety of pipe unions and clamps, two types of flow meters, elbows, tees, and pressure relief valves.

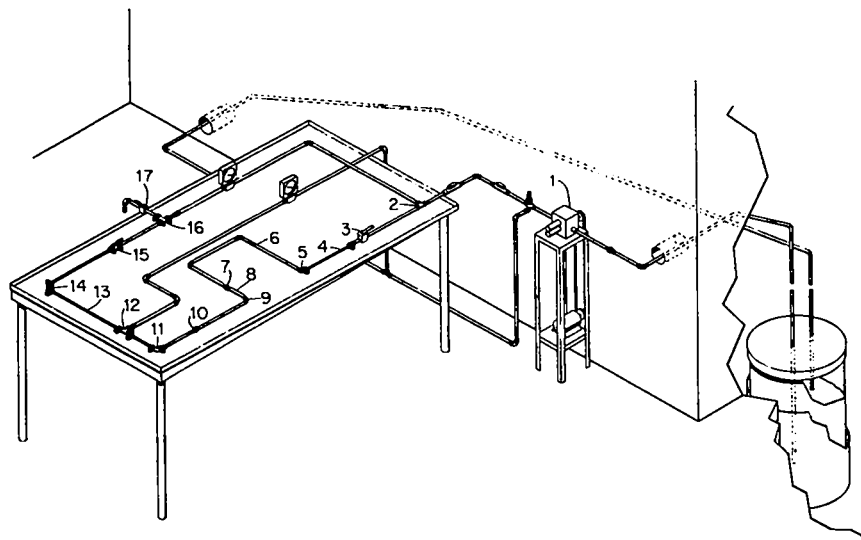


Fig. 46. An isometric view of the stainless steel loop for uranyl nitrate solution.

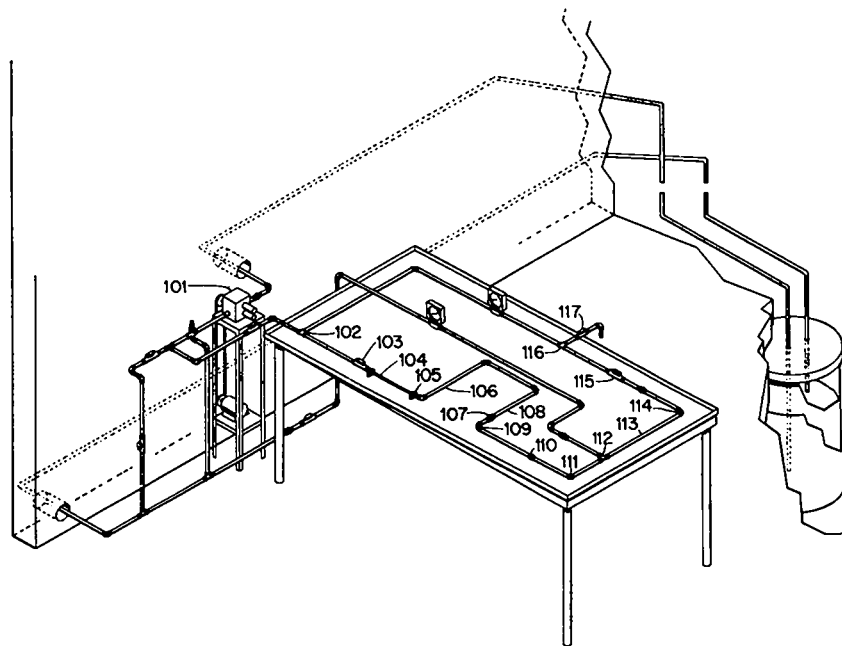


Fig. 47. An isometric view of the CPVC loop for uranyl fluoride solution.

## B. Experimental Procedures

The stainless steel loop was used for the circulation of a uranyl nitrate solution containing 100 g/L of uranium with an excess amount of  $\text{HNO}_3$ . A uranyl fluoride solution containing  $\sim 90$  g/L of uranium was circulated through the CPVC loop system using a hastelloy-C pump and relief valve and all the other components fabricated out of CPVC, Teflon, titanium, graphite, and polyethylene. The system was designed to change the flow rates from 1-2 kg/min of uranium at solution flow rates of  $\sim 10$ -20 L/min. Details of the component descriptions and experimental parameters are summarized in Table XV.

Two different chemical forms of  $^{46}\text{Sc}$  tracer had to be used for the two solutions used in the loops. For the uranyl nitrate solution, scandium in the form of  $\text{Sc}^{3+}$  was used. This species, however, was not suitable for the uranyl fluoride solution as it readily precipitates scandium as  $\text{ScF}_3$ . A complex ion of scandium as  $[\text{ScF}_6]^{3-}$  was prepared by dissolving  $\text{ScF}_3$  in excess  $\text{NH}_4\text{F}$ ; this chemical species was stable in the uranyl fluoride solution and followed uranium stoichiometrically in the solution loop.

Seventeen locations on each of the loops (Figs. 46 and 47) were measured periodically for uranium holdup using the instrumentation and measurement techniques described earlier. Similar measurements were performed on both loops twice a week for the entire duration of the experiment. Before each set of measurements, the pump was turned off, a terminal valve was opened, and the solution in the loop was allowed to drain for  $\sim 30$  min so that only the residual holdup of uranium in the loop components was measured. The measurement regimen included measuring residual uranium in the pump, the terminal valve, and in at least two units each of the pipes, tees, elbows, and unions. The solution in the storage tank was periodically monitored to maintain the concentration level of uranium in the solution reasonably constant throughout the experiment. A set of cleanout measurements was conducted on selected components of both loops before they were dismantled. The storage tank contained  $\sim 55$  L of solution, and this was circulated through the loop using a positive displacement pump. The flow rates were monitored using two flow meters on the inlet and outlet sides of the loops. The flow rates through the loops were changed by changing the gear ratio between the motor and the pump. As far as possible, the circulation of the solution continued for 24 h/day, 7 days/week. The throughput of uranium through the loops between holdup measurements was calculated from known flow rates, the elapsed time between measurements, and the concentrations of uranium solutions in the feed tanks.

TABLE XV. Component Description and Experimental Parameters of Circulation Loop

Components/ Parameters	Stainless Steel Loop	CPVC Loop
Pipe, i.d.	1.9 and 2.5 cm	1.9 and 2.5 cm
Loop length	50 m	50 m
Pump	Stainless steel gear pump	Hastelloy-C gear pump
Relief valve	Stainless steel	Hastelloy-C
Ball valves	5	6
Terminal valve	1	1
Elbows	20	20
Tees	2	2
Flow meters	2	2
Storage tank	Polyethylene 200-L capacity	Polyethylene 200-L capacity
Surge tank	Polyethylene 200-L capacity	Polyethylene 200-L capacity
Flow rates	10 L/min & 20 L/m	11 L/min & 22 L/min
Uranium	100 g/L as $\text{UO}_2(\text{NO}_3)_2$	91 g/L as $\text{UO}_2\text{F}_2$
Excess acid	4 moles of $\text{HNO}_3$ / mole uranium	4 moles of HF/ mole uranium
Throughput	59.5 t uranium	49.0 t uranium



### C. Holdup Measurements

Residual holdup of uranium in various components of the solution loop was measured using a specially fabricated NaI(Tl) detector assembly (Fig. 48). A 5- × 5-cm sodium iodide detector with a collimator and shield was mounted on a pivot with very long horizontal arms, capable of both vertical and horizontal extensions. The detector mounted on the horizontal arm was rotatable in a plane 90° to the horizontal arm. A spring guide extending from the front of the detector assembly allowed careful repositioning of the detector at marked measurement points on the solution loop components. A stabilized single-channel analyzer system was used to process the detector output signals. The measurement system was calibrated with standards carefully prepared to resemble the components to be measured and with uniform material deposition on the interior surfaces in contact with the solution. The standards were assembled using known amounts of  $^{46}\text{Sc}$  tracer uniformly distributed on Teflon films or capillary tubes that can be shaped to fit the interior surfaces of pumps, valves, tees, elbows, and unions and pipes.

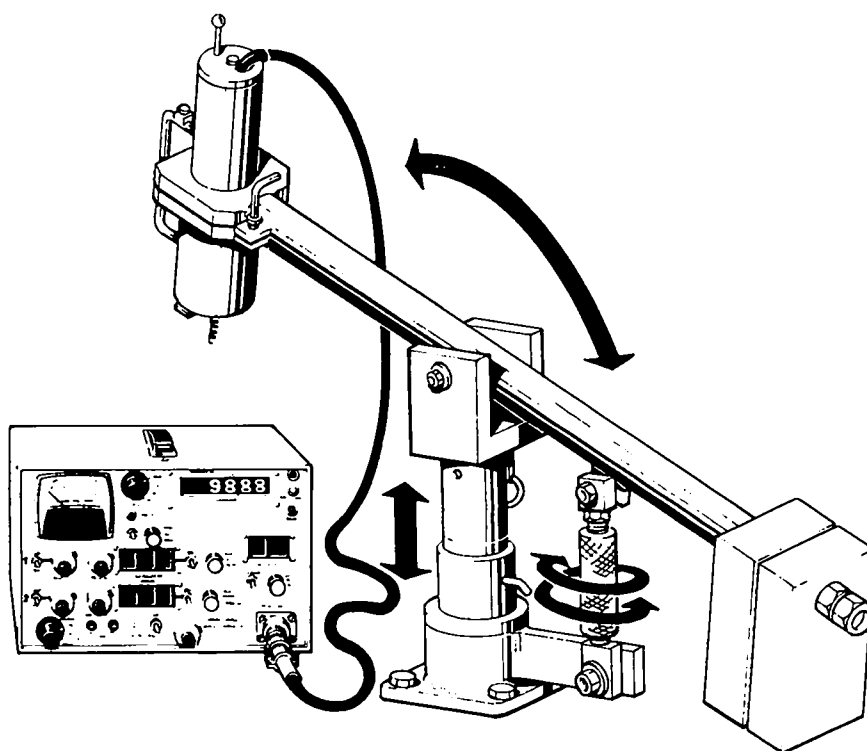


Fig. 48. Shielded NaI(Tl) detector mounted on a long arm with a designed capability to reproduce measurement locations on the solution loop.

### D. Experimental Results

Details of the holdup of uranium in the components of the two solution loops described above are given in Tables C-XXIII through C-XXVII. Graphical presentations of these data are included in Sec. VI.E. Except for the pumps, all the components of the two loops remained the same during the two flow rates. New pumps were installed in both the nitrate and fluoride loops when the flow rates were changed. In general, the uranium holdup in pipes, valves, tees, elbows, and unions showed an initial rapid increase with a subsequent leveling off until termination of the experiments. Increasing the flow rates from 10 to 20 L/min resulted in an initial washout of residues followed by a slow build-up and leveling off. An exception to these observations was that the pumps used in the loops showed a slow but steady increase in holdup

during most of the measurement period. The hastelloy pumps used in the fluoride loop showed an increased rate of build-up, probably caused by an increase in the corrosion of the internal surfaces of these pumps.

The solutions in the storage tanks were continuously monitored to maintain a constant volume. In addition, twice a week during the time of holdup measurements, the circulating solution was sampled and analyzed to determine the concentration of the tracer. The concentration of the solutions in the storage tank remained almost the same throughout the experiment. Small changes (if any) in the concentration of the solution were not identifiable by the radiochemical procedures used in measuring the concentrations of uranium and the tracer.

A number of cleanout measurements conducted at the termination of the experiments confirm that the NDA measurements used in day-to-day measurement of holdup using a NaI(Tl) detector system were highly reliable. The results summarized in Table XVI show very good agreement between NDA measurements and cleanout measurements. These NDA results are not the same as the last holdup measurement, while the component was an integral part of the loop, because of the loss of material during the disassembly of the components. The NDA-measured values reported in Table XVI were obtained after disassembling the loop component and making measurements in place.

TABLE XVI. Cleanout Measurements—Uranium Solution Loop Experiments

Part No. in Illustrations <sup>a</sup>	Parts Description	NDA Measurement (g of U)	Cleanout Measurement (g of U)
6	Pipe	0.50	0.50
11	Elbow	0.025	0.033
11-12	Pipe	0.37	0.40
12	Tee	0.28	0.35
13	Pipe	0.16	0.15
14	Elbow	0.02	0.03
15	Valve	0.40	0.37
15-16	Pipe	0.04	0.07
16	Tee	0.08	0.08
17	Term. valve	0.08	0.07
101 (1)	Hastelloy pump	13.7	11.9
101 (3)	Hastelloy pump	9.4	7.0
102	Tee	0.086	0.099
103	Ball valve	0.36	0.40
104	Pipe	0.014	0.016
105	Elbow	0.074	0.10
107	Union	0.024	0.028
110	Union	0.036	0.041
115	Ball valve	0.29	0.36
117	Term. valve	0.40	0.49

<sup>a</sup>See Figs. 46 and 47.

## E. Modeling

Modeling the data from the solution loops proceeds in much the same fashion as for the ADU precipitation and calcination experimental results of Sec. IV. In most instances, holdup in the equipment reaches steady-state conditions rather quickly (compared with the intervals of measurement) and remains roughly constant for the duration of the experiment. The exceptions to the rule are the pumps when operated at low flow rate, where periods of increasing deposition are apparent.

For each of the 66 cases—16 pieces of equipment under 4 sets of operating conditions plus the 2 pumps at high flow rate—the onset of steady state is deemed to be observed with the second measurement. The first measurement was obtained shortly following start-up and after the “fine tuning” required to attain desired flow rates and other operating conditions. A more lengthy period of stable operation then preceded collection of the second measurement. It is interesting that of the 66 cases, the final measurement exceeds the second one in 33, the converse is true for 29, and equality holds for the remaining 4. Further, inspection of the data from the individual pieces of equipment reveals that consecutive increases (or decreases) in observed holdup over four or five successive time periods are rare. Such behavior is consistent with data from steady-state processes.

The equations and distributional assumptions that define the steady-state model resemble those from the ADU experiment. They are reviewed here for completeness and because the acquisition of data at unequally spaced throughputs adds some minor mathematical complications to the Kalman filtering. Letting  $x(t)$  denote the measurement at throughput  $t$  of the actual quantity  $h(t)$  of holdup, the measurement equation is

$$x(t) = h(t) + e(t),$$

where  $e(t)$  is the associated measurement error. Here the errors  $\{e(t)\}$  are assumed to be independently distributed with mean zero and variance  $\sigma_m^2$ . Values of the measurement variability  $\sigma_m^2$  used in the filtering are given in Table XVII. In general, such values will be condition-specific and may be estimated from calibration and cleanout data.

TABLE XVII. Values of Measurement Variability ( $\sigma_m^2$ ) and Process Variability ( $\sigma_p^2$ ) Used in Filtering the Solution Loop Data

Equipment	Flow Rate	Location <sup>a</sup>	$\sigma_m^2$	$\sigma_p^2$
Pump	High	1, 101	0.0010	0.0100
Tee	Low, high	2, 102	0.0001	0.0004
Tee	Low, high	12, 112, 16, 116	0.0001	0.0001
Valve	Low	103	0.0003	0.0020
Valve	High	103	0.0075	0.0050
Valve	Low, high	3, 15, 115, 17, 117	0.0003	0.0020
Pipe	Low, high	6	0.0020	0.0020
Pipe	Low, high	4, 104, 106, 8	0.0010	0.0005
		108, 13, 113		
Elbow	Low, high	5, 105, 9, 109, 11	0.0001	0.0003
		111, 14, 114		
Union	Low, high	7, 107, 10, 110	0.0001	0.0001

<sup>a</sup>See Figs. 46 and 47.

The state equation in the model reflects the change in actual holdup over time and captures the steady-state character of the deposition process. When the associated measurements are to be obtained at throughputs  $t_1, t_2, t_3$ , and so on up to  $t_n$ , the state equation is

$$h(t) = h(t_{i-1}) + \epsilon(t_i), \quad i = 2, 3, \dots, n,$$

where the  $\{\epsilon(t_i)\}$  are independently distributed with mean zero and

$$\text{Var} [\epsilon(t_i)] = (t_i - t_{i-1})\sigma_p^2. \quad (18)$$

That the  $\{t_i\}$  are unequally spaced means that some of the  $\{\epsilon(t_i)\}$  are more variable than others. A simple interpretation is that over an interval of throughput  $[t_{i-1}, t_i]$ , the change  $h(t_i) - h(t_{i-1})$  in actual holdup is likely to be small if  $t_{i-1}$  and  $t_i$  are close together but may be larger if  $t_{i-1}$  and  $t_i$  are farther apart. That the variance [Eq. (18)] is proportional to the interval width  $t_i - t_{i-1}$  evolves from viewing the "larger" interval  $[t_{i-1}, t_i]$  as a collection of small, independent subintervals. That is, holdup may change in each subinterval, and the variance of the sum of such independent changes acts in an additive manner. Values of the process variability parameter  $\sigma_p^2$  used in the filtering are listed in Table XVII.

Given the measurement and state equations together with the stated distributional assumptions, it is straightforward to generate filtered estimates  $\{\hat{h}(t_i)\}$ . See Appendix B for details. The filtered estimates are superimposed in Figs. 49-60 and provide a very good fit to the data.

Each component of the solution loop system is modeled separately. In some systems (usually "closed" ones with extensive measurement histories), it is advantageous to model any recognized dependencies between responses at distinct individual locations using either multivariate Kalman filtering or time series methodology. In the solution loop experiments, there is no apparent multivariate structure, nor would it have been feasible to collect the many data required for adequate investigation of the more complex model forms.

Because holdup appears to conform to the usual steady-state model, the filtered values for any particular piece of equipment are, in and of themselves, relatively uninteresting. Final holdup estimates for the low and high flow rates are provided in Table C-XXVII. Filtered values are superimposed on Figs. 50-60, and the degree of smoothing is slight because the data are of high quality. Perhaps the most useful lesson here is the confirmation that the steady-state model applies over each of the experimental conditions.

Some of the more interesting results are of a comparative nature, that is, evaluating the effects on holdup attributable to differences between high vs low flow rate, stainless steel vs CPVC, and so forth. Though such comparisons might be of little value to a given facility that has its own equipment and operation (and thus might not be overly concerned about what would happen under *other* conditions), a number of comments are noteworthy.

One of the interesting aspects of this experiment is that holdup on similar types of equipment is similar and is not greatly affected by position within the solution loop. If differences in holdup caused solely by position were small in an operating facility, this would have implications for future measurement plans and the reduction of sampling error. For example, it may be impractical to measure every section of pipe every inventory period. This is especially true if data of very high quality are required. Thus, a portion of the pipe sections can be sampled and the observed values used as a basis for estimating the total holdup. Even if there were no measurement error, the estimated total would not be exact because it is derived from a sample.

The subject of sampling error has been treated extensively in the literature on survey sampling (for example, Refs. 40 and 41). Basically, the usual methods divide the items to be measured (the "population") into a number of relatively homogeneous groups (or "strata"). In the solution loop example, perhaps the different types of equipment, such as tees and unions, could be used to define the strata. Within each stratum, items are selected and measured. Often the selection is made completely at random, though

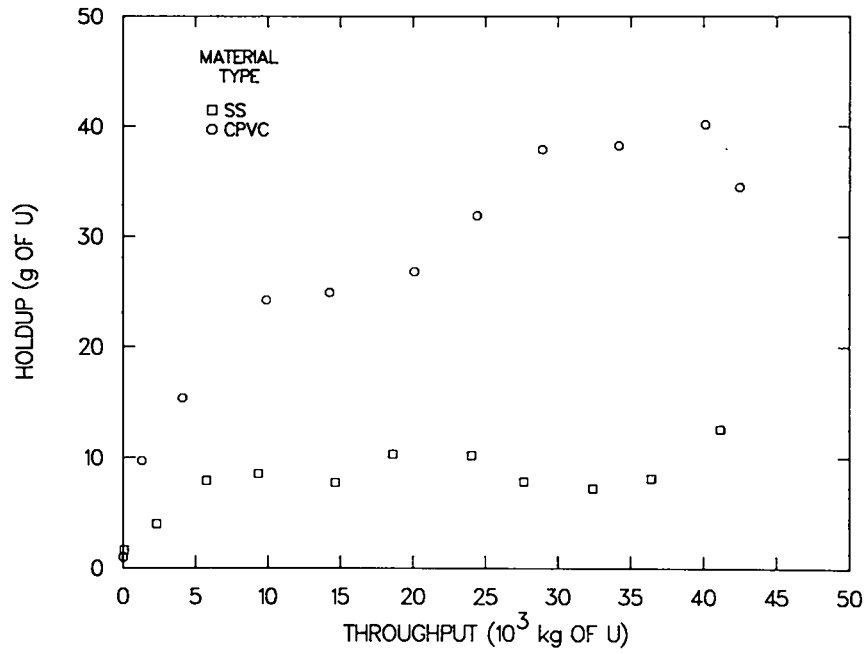


Fig. 49. Measurement history and filtered values for pumps at low flow rates.

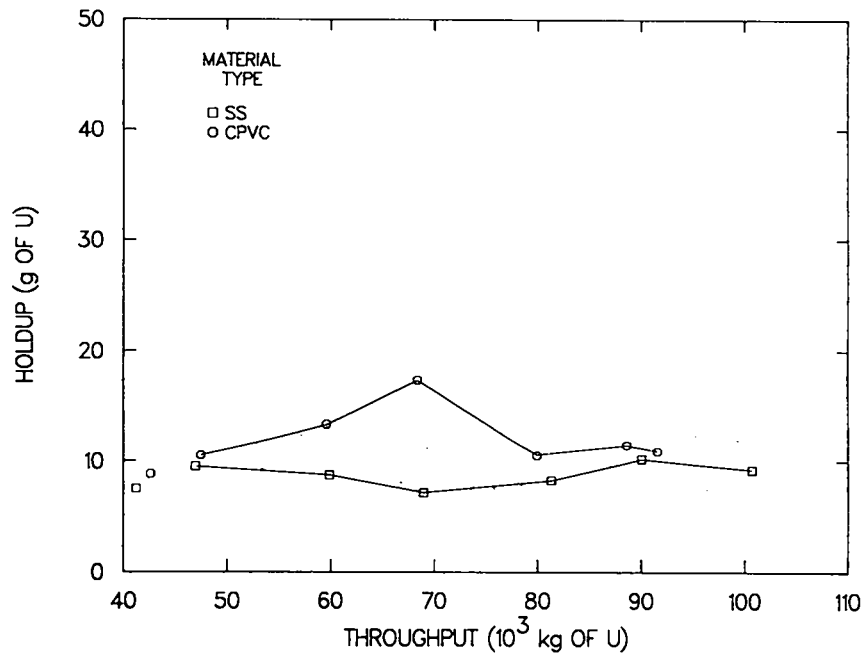


Fig. 50. Measurement history and filtered values for pumps at high flow rates.

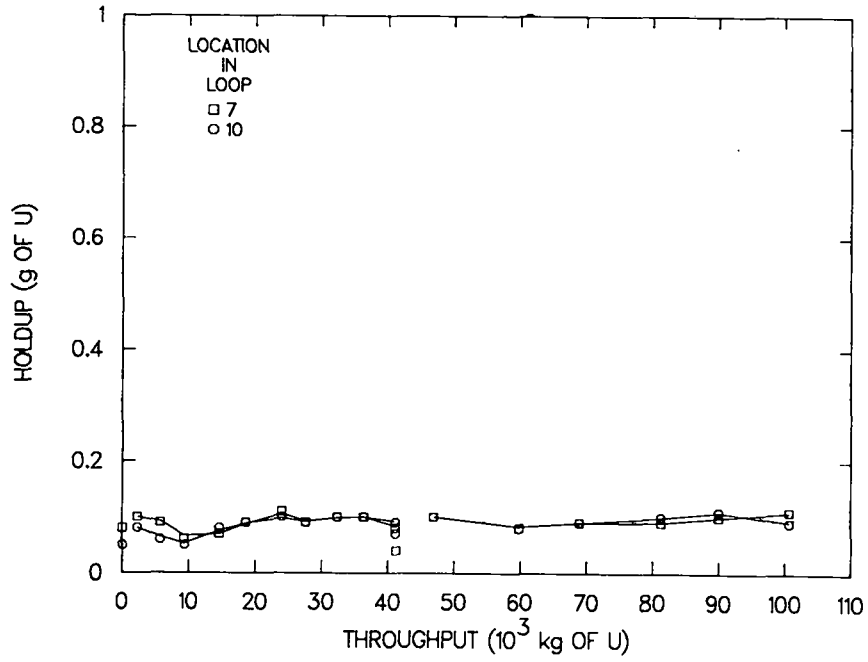


Fig. 51. Measurement history and filtered values for stainless steel unions.

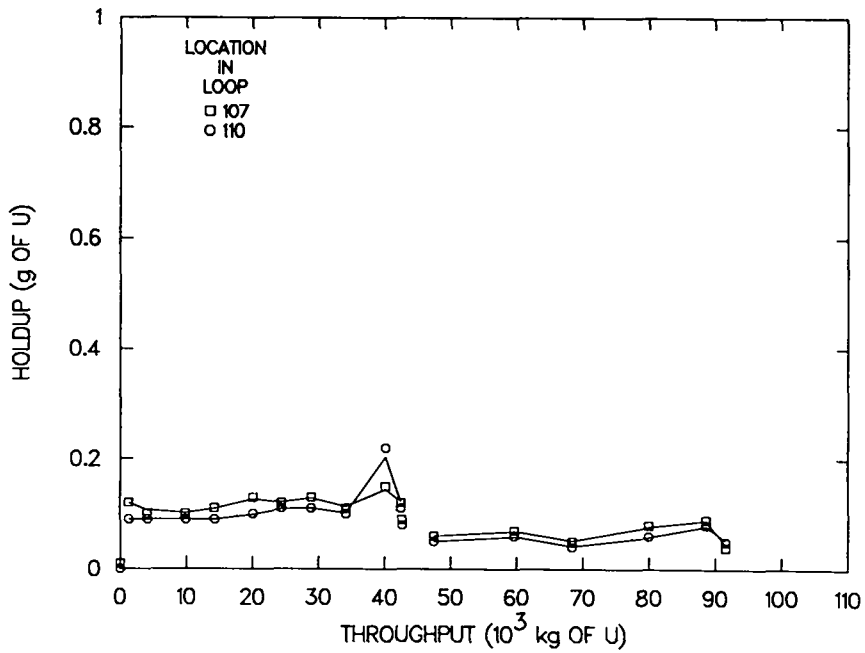


Fig. 52. Measurement history and filtered values for CPVC unions.

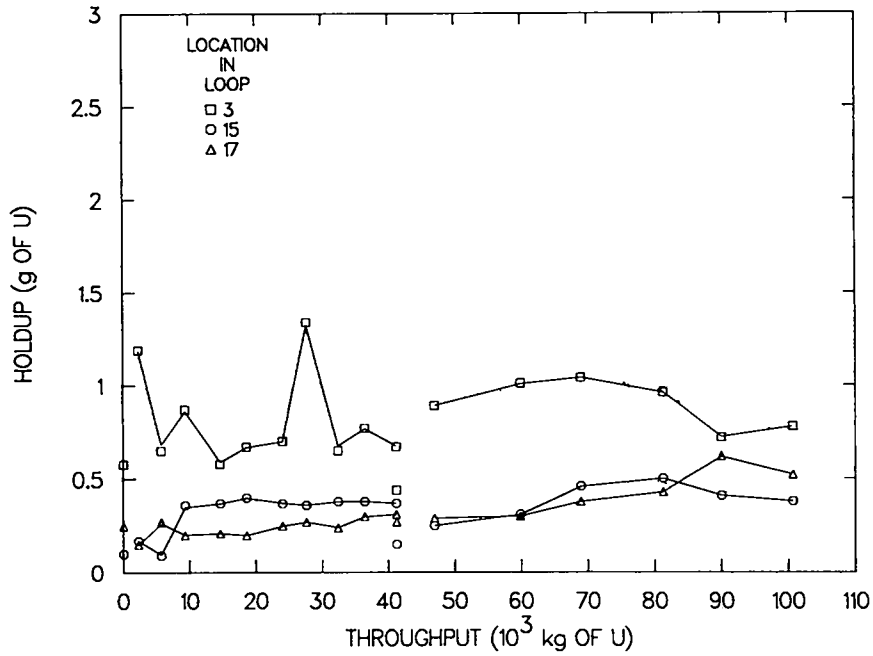


Fig. 53. Measurement history and filtered values for stainless steel valves.

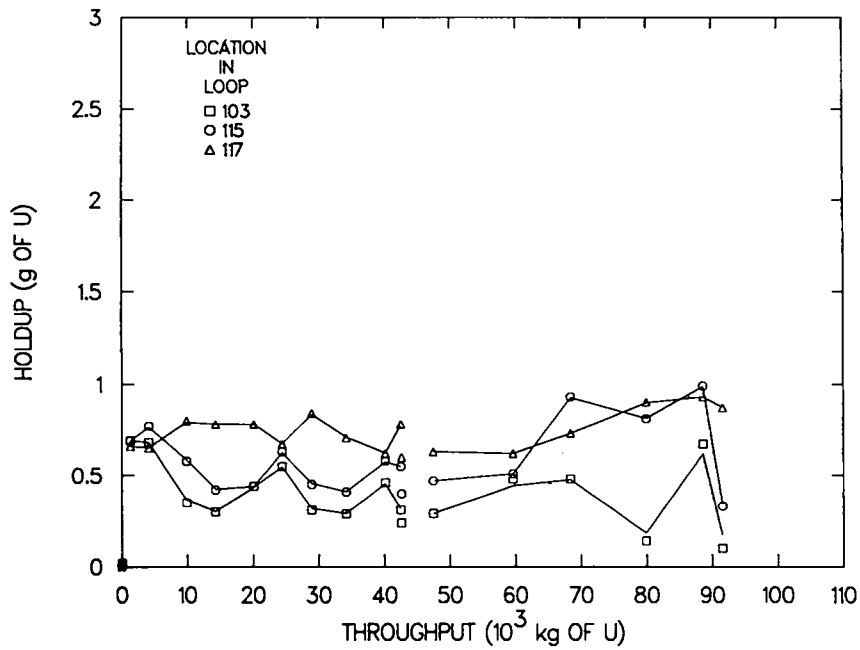


Fig. 54. Measurement history and filtered values for CPVC valves.

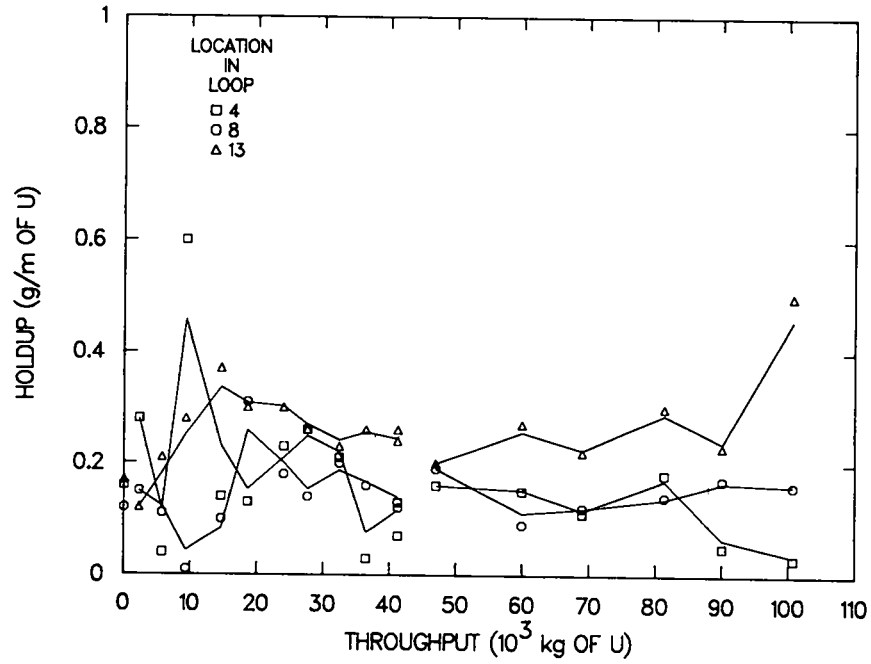


Fig. 55. Measurement history and filtered values for stainless steel pipes.

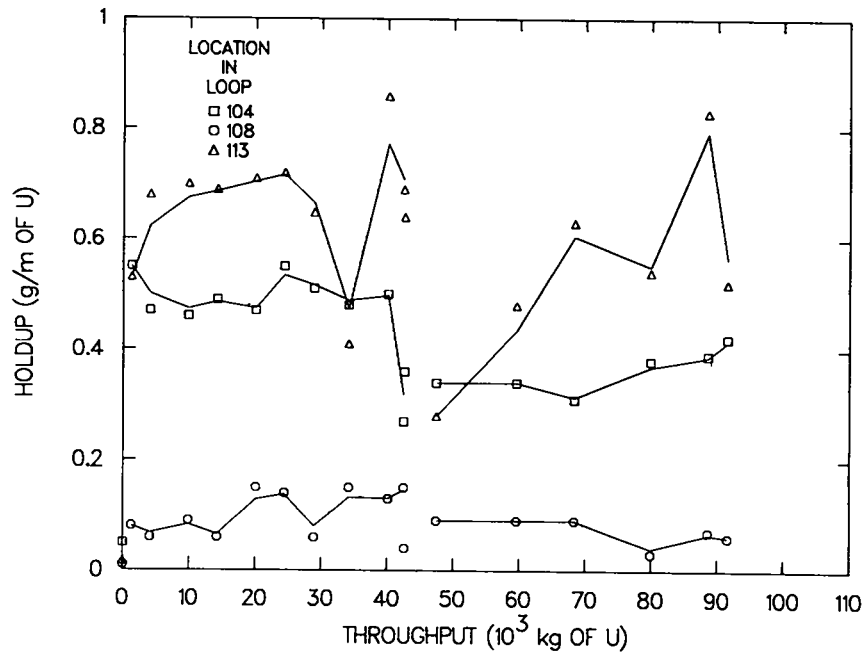


Fig. 56. Measurement history and filtered values for CPVC pipes.



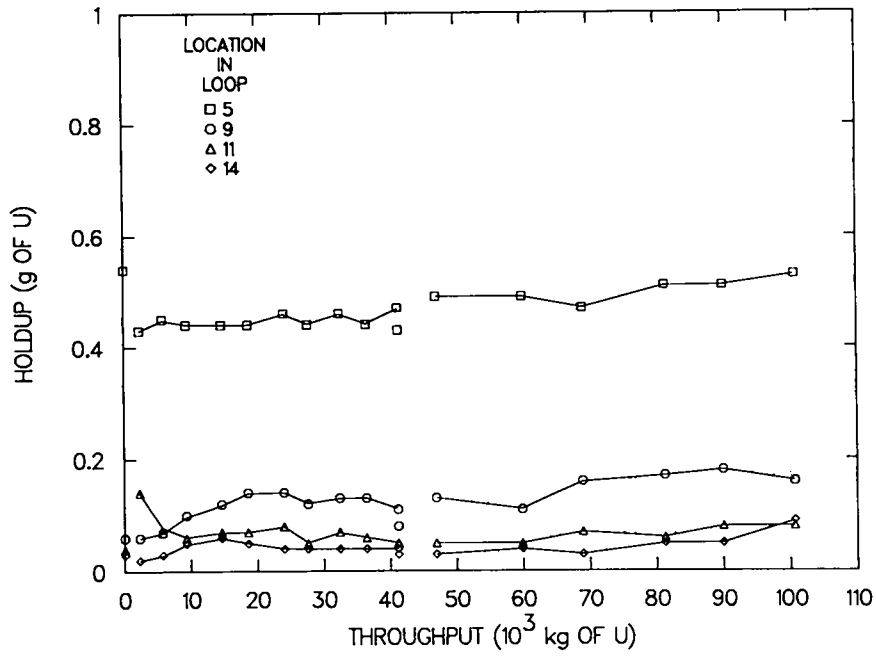


Fig. 57. Measurement history and filtered values for stainless steel elbows.

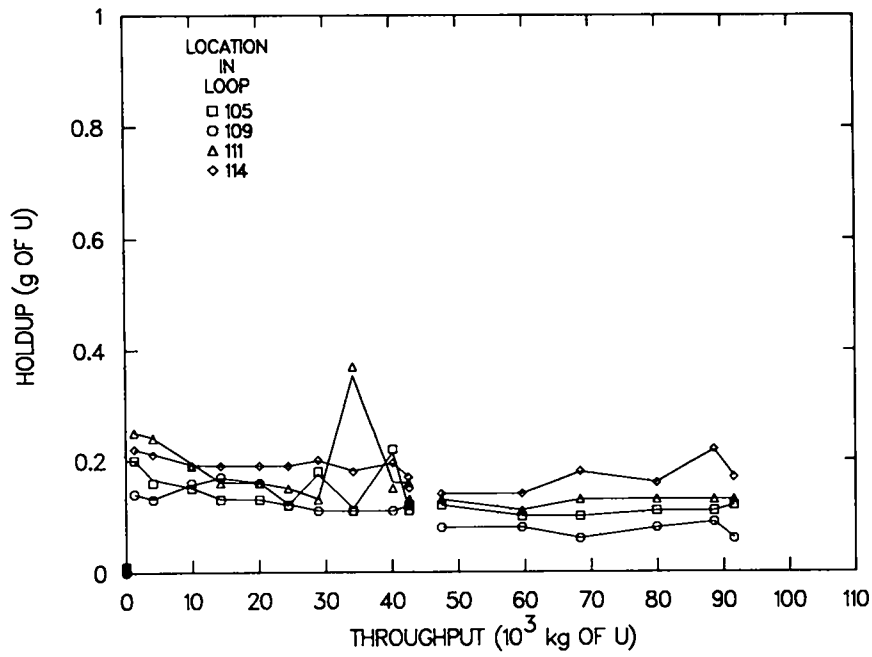


Fig. 58. Measurement history and filtered values for CPVC elbows.

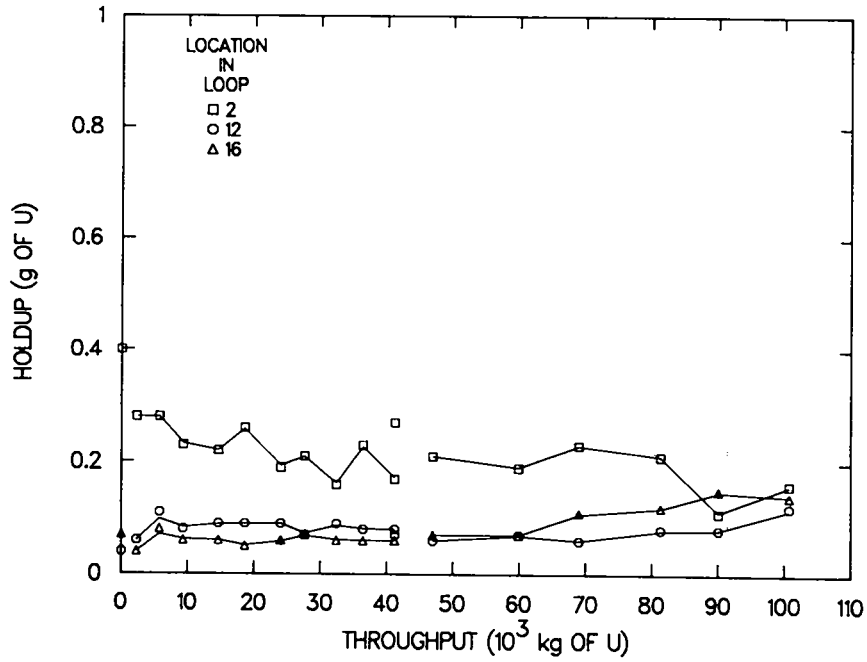


Fig. 59. Measurement history and filtered values for stainless steel tees.

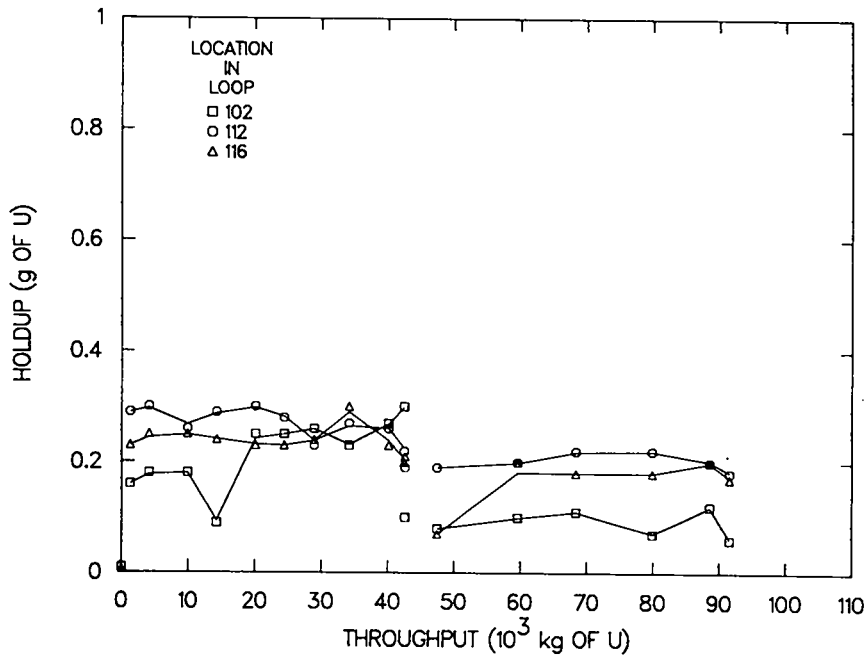


Fig. 60. Measurement history and filtered values for CPVC tees.

alternatives such as clustering may be used to reduce measurement effort. A total for each stratum is then estimated from sample results, and the totals are combined to yield a final estimate for the population.

The magnitude of the sampling error is influenced by the number of items measured within each stratum and by the mode of selection (for example, simple random sampling), but it is largely dependent on the degrees of homogeneity present among items within the various strata. If within-stratum variability is sufficiently small, the stratum total might be much better estimated from a handful of very good measurements than from many more measurements of poorer quality. If, on the other hand, within-stratum variability is large, then it is likely better to obtain a larger number of poor-quality measurements than a few very good ones. When considering the allocation of measurement resources, the tradeoff between measurement error and sampling error is an important factor.

The most dramatic effect observed in the experiment was an unanticipated one. Holdup in one section of stainless steel pipe (location 6) was nearly 10 times that in the other three sections of pipe (locations 4, 8, and 13). The holdup also was nearly 10 times that of its counterpart in the CPVC loop (location 106). Increased accumulation in the suspect section also was apparent following visual inspection and cleanout measurement when the loop was dismantled after the experiment. Furthermore, the elbow adjacent to the suspect section, at location 5, exhibited much greater deposition than any of the other elbows (Figs. 57-58). The cause of this occurrence was the construction of the stainless steel loop. To allow for drainage before measuring residual holdup, it was necessary that the loop be slightly (at least 1° from the horizontal) tilted. The angle of inclination for the portion of the loop covering locations 5 and 6 was not the same as elsewhere, and the uranyl solution clearly did not drain to the same extent. Though unintended, this "flaw" in loop construction illustrated that effects of material type and flow rate may be small in comparison with other factors that were nominally held constant in the experiment. More generally, such factors are one cause of the sampling error as discussed above.

The effect of the change in flow rate was negligible relative to other effects and, often, to process variability. After the 11th measurement on each piece of equipment, the flow rate was doubled as indicated in Table XVII. In Figs. 51-60, filtered values for the low-flow-rate data are connected starting with the second measurement, as are those for the high-flow-rate data. By comparing the results for low throughput (below roughly 42 000 kg) with those for high throughput, the effect of the flow rate change can be observed at each measurement location. As is apparent, no pronounced trend exists over the whole of the experiment.

The effect of material type—CPVC vs stainless steel—is relatively small. Measurement locations 2-9 are directly comparable in this regard, and Table XVI lists the estimated holdup for each location at the conclusion of the low- and high-flow-rate experiments. The portion of the stainless steel loop covering measurement locations 10-17 was constructed of 3/4-in. piping rather than the 1-in. piping used in the first part of the loop and in all of the CPVC loop. Thus, for locations 10-17, the interior surface area in which holdup accumulated was less for the stainless steel than for the CPVC. Accordingly, it can be seen that less material was present for the latter half of the stainless steel loop.

## VII. DISCUSSION AND CONCLUSIONS

During this investigation, we measured holdup in a variety of equipment common to HEU-processing facilities. This equipment included a glove box, a ventilation air duct system, several filters and prefilters, a number of calciners, two types of precipitators, a rotary drum filter, four Buchner funnel-type filters, a dissolver, two pulse columns, several pumps, pipes, elbows, tees, unions, valves, and terminal valves. In most cases, the controlled measurements using properly designed NDA instruments and calibration standards provided good data useful for statistical model development.

## A. Value of Controlled Measurements

The primary objective of the controlled experimental studies performed during this investigation was to demonstrate that well-designed, controlled experiments carried out at large facilities combined with reliable measurements can be used to develop holdup estimation models. The quality of the holdup data being the key to the successful development of estimation models, it is important to invest sufficient effort to minimize the uncertainties in the measurements. Poorly characterized materials, nonuniform depositions, improper calibration standards, and high background interferences generally compound the problems of NDA measurements of large, irregularly shaped process equipment and facilities. One of the methods of enhancing the quality of the holdup data is the use of tracers as stand-ins for materials that are difficult to measure directly. The use of radioactive tracers during these experiments enabled us to generate very reliable holdup data on uranium, which would not have been possible by nonintrusive direct measurement of uranium. From the data generated during limited experimental runs, the value of modeling to holdup estimation was demonstrated.

The applications of these tracer techniques to an actual operating plant would require planning and a recognition that the use of tracers in concentration levels of parts per million or less would not have any influence on the process or the products of the process line. *In vivo* measurement of radionuclides for diagnostic purposes in medicine is a well-established and widely accepted procedure in the human health services industry.<sup>42,43</sup> The application of radioactive tracers for holdup measurements is a rather simple application of this procedure. There is no scientific reason why the tracer techniques cannot be used in a large plant. However, safety-related problems must be addressed and resolved before large-scale applications of radioactive tracers are undertaken. Radioactive tracer applications for holdup measurements have not yet been attempted at a large processing facility, although the unique value of radioactive tracers to the study of process kinetics and material flow in large facilities has been well recognized and demonstrated.<sup>12,17,18</sup>

The results of controlled experiments performed during this investigation have been extremely satisfactory and have been valuable to demonstrating the concept of developing holdup estimators from long-term measurement data. In the dust-generation experiments for determining holdup of uranium in a glove box, duct system, and a prefilter, the variations in particle size, material composition, and airflow through the duct system all played a part in the holdup of uranium. This points to the need for better control of process parameters and better characterization of materials in the applications of statistical models to estimate holdup as a function of material throughput.

In the ADU precipitation and calcination experiments, the holdup of uranium in the dissolver and the filters was not seriously influenced by process parameters such as acidity of the solution and pH of the ADU slurry produced. On the other hand, the holdup of uranium in the calciner was influenced by the final calcining temperature when the temperature was raised from 800 to 900°C, although an earlier step change of temperature from 700 to 800°C did not show any marked influence on the holdup of uranium in the calciner. The holdup of uranium in the precipitator reached a steady state after the process operation became routine. The initial large fluctuations in the holdup of uranium in the precipitator can only be explained by the difficulty in establishing repeatability of such an operation. This process involved a violent liquid-phase chemical reaction producing a precipitate at the interface where the two reactants came into contact with each other and later produced a slurry, whose viscosity varied as the process of precipitation proceeded to completion. Although the operation became routine after a number of experimental runs, it still showed the potential for large fluctuations in holdup. Therefore, in cases such as the precipitation column, where the process variability is considerable, the steady-state models for holdup estimators are of marginal value.

The development of holdup profiles of uranium in a liquid-liquid extraction pulse column used data from steady-state operations of two pulse columns. There have been no reported successful attempts at measuring residual inventories of uranium in pulse columns by NDA; measuring in-process material is difficult enough.<sup>44</sup> The experimental study reported here used periodic removal of materials from sampling

ports along the length of the pulse column and analysis of the uranium contents of the samples by destructive chemical analyses. The data obtained have been valuable for developing a condition-specific concentration profile of uranium along the length of the column, which in turn was used for estimating the total amount of uranium in the column during steady-state operation. The same principles can be used to develop data required to estimate the residual inventory of pulse columns in "run-out" conditions. The "run-out" condition measurements would offer considerable challenges because of small amounts of residual SNM distribution over large surface areas, and modeling could be nontrivial because of difficulties in the estimation of profiles that are not "smooth." The use of appropriate NDA and/or tracer techniques can go a long way toward accomplishing this goal.

The controlled experiments to develop data on uranium holdup in pipes and pipefittings clearly demonstrated the value of high-quality data to develop statistical models, even though the quantities of holdup as a function of throughput were extremely small compared with other measurements conducted during this investigation. A unique observation made during these experiments, using two types of materials for solution loop construction, two chemically distinct uranyl solutions, and two different flow rates through each of the two loops, is that the steady-state model applies over each of the experimental conditions over a wide variety of solution loop components. In addition, this type of measurement has the potential value for developing integrated models of holdup of SNM in facilities containing large assemblies of pipes and pipefittings. The NDA measurement of holdup of HEU in pipes and pipefittings is extremely difficult, and it is the considered finding of this investigation that major influences on holdup in pipes and pipefittings are facility layout, chemical characteristics of the solutions being transferred, and the potentials for interactions between the components of the solutions and their environment.

## B. Motivation for Modeling

The motivation for considering the use of modeling to improve estimation is quite natural. For example, consider the holdup in a segment of ductwork or piping at a particular time. A single measurement of the holdup provides an estimate of the quantity of material involved, but this estimate ignores other information that may be available. Previously collected data from the location are often useful as holdup may accumulate in a predictable manner over time. Also, data from nearby locations, or from locations elsewhere at the facility known to behave similarly, may be relevant. Combining all such information in the right way (formalized through use of the model) leads to improvement in estimation over use of an individual measured value.

The models developed in the previous sections fall into three general categories:

1. modeling over time (such as for the filters discussed in Secs. II and III and for the solution loop components of Sec. VI),
2. modeling over space (such as for the pulse columns of Sec. IV), and
3. modeling over both time and space (such as for the glove box floor of Sec. III).

Each of these categories of modeling is described briefly as it relates to the various holdup experiments.

Modeling holdup over time in various pieces of process equipment is often relatively simple. Basically, process operation is held (nominally) constant and holdup is continually monitored. When measurements are of good quality, often a predictable trend emerges. For the filters discussed in Secs. II and III, process variability was small, and ordinary regression methods proved quite useful in capturing the increasing deposition. Had process variability been large, this factor could have been incorporated into the model using the general Kalman filtering framework.

In the ADU precipitation and solution loop experiments, steady-state models were used successfully. Unlike holdup on a filter, which undergoes a "life cycle" from the time a clean filter is installed until it becomes inefficient and is replaced, quantities of holdup in many pieces of equipment appear to fluctuate about a long-term equilibrium. Modeling such steady-state data is straightforward, and estimation depends crucially on the magnitudes of the holdup data and process variabilities. At one extreme, if no

measurement error exists, the estimated values of holdup would coincide exactly with measured values at points where measurements are obtained. If, at the other extreme, no process variability exists so that  $h(t) = c$ —that is, the true holdup never changes over time—then the smoothed estimate of holdup  $\hat{h}(t)$  takes the form  $\hat{h}(t) = \hat{c}$ . In practice, neither extreme is attained, and both measurement and process variabilities are present. Thus, a plot connecting estimated holdup values at times of measurement exhibits a degree of “smoothing” between one extreme (connecting observed points) and the other [the line  $\hat{h}(t) = \hat{c}$ ]. The extent to which such a plot resembles either extreme depends on the relative magnitudes of measurement and process variabilities.

When using models to estimate present or future holdup, an important point to keep in mind concerns the distributional properties of prediction error. The variance of this error is not only a function of the quality and quantity of data used to derive the predictive equation but is also a function of the degree of extrapolation. A simple measure of the degree of extrapolation is the difference in throughputs corresponding to the holdup to be estimated and to the last observed measurement. If the difference is large, then the model is being used to project well beyond the range of the existing data and accountancy clearly suffers. To avoid such a problem, it is mandatory to obtain periodic measurements of holdup and use that information to update the model. Accountability goals determine the minimum frequency of updating.

To this point, the discussion has involved modeling holdup over time. In some cases, it is necessary to model holdup over space since nonuniform deposition is present in many large pieces of processing equipment. A good example is the pulse column, the modeling of which was described in Sec. IV. Here the basic idea is to formally incorporate the nonuniformity in the model and then integrate the estimated profile to obtain an estimate of the holdup.

Finally, modeling over both time and space may be considered. This was done with respect to the glove box floor in the dust-generation experiments (Sec. III) and the precipitator in the ADU experiment (Sec. V), to name two examples. In both instances, the nonuniform deposition was characterized using measurements from various locations. For the precipitator, the estimated profile was then used to convert subsequent counting information to estimated holdup, and Kalman filtering was implemented for the steady-state modeling. For the glove box floor, response-surface methodology (essentially regression) was used to estimate the time-varying density function (or profile), and integration then provided the final holdup estimate. The approaches to modeling holdup over time and space in these two pieces of equipment are quite general and can be applied in many other situations.

### C. Applications to Fuel Cycle Facilities

The primary objective of this investigation was to demonstrate the development of holdup estimators (for specific process equipment) with potential value to NRC in their license evaluation of current and future fuel cycle facilities. However, this objective is different from demonstrating how to obtain quality data without which meaningful estimation models are difficult to develop. There are several ways of improving the quality of SNM holdup measurements. One approach used during the controlled experimental studies of this investigation involved the use of specially designed instrumentation and calibration standards along with carefully chosen radioactive tracers. Although the use of improved instrumentation and specially fabricated standards are valuable to all holdup measurements, the use of tracers has to be undertaken only after careful evaluation of the advantages and limitations to a particular process or facility. The application of techniques described in this report, for holdup measurement and to develop estimation models of holdup, to a process facility would require

1. a careful evaluation of the needs of the facility in terms of holdup estimation;
2. allocation of resources to undertake good-quality measurements for the development of holdup estimators;

3. identification of regions of a plant where there is significant holdup of SNM and an evaluation of safety-related issues of these residual inventories;
4. a classification of equipment into a few categories and the selection of a representative number from these categories for detailed evaluation;
5. development of accurate base levels of holdup for each of these facilities;
6. use of reliable instrumentation specially designed to meet the requirements of holdup measurements and the use of calibration standards that are representative of material type, equipment geometry, and the material distribution within the equipment;
7. gathering holdup data as a function of SNM throughput for a reasonable length of time when the process operation is stable;
8. use of cleanout measurements of representative equipment to determine the validity of nonintrusive, nondestructive measurements and to develop proper calibration parameters;
9. use of appropriate statistical techniques to develop prediction models of holdup from the good-quality data; and
10. updating of the estimation models on a periodic basis through a limited number of good-quality measurements.

#### D. Conclusions

The findings of this investigation suggest that there are considerable difficulties associated with the measurement as well as the development of reliable estimates of the holdup of SNM in large processing facilities. Materials accumulating on the surfaces, cracks, pores, and zones of poor circulation of process equipment are not easily measurable by conventional methods. The requirements of instrumentation, measurement methods, and calibration standards for NDA have a rather limited range of options depending on the geometry of the facility, the deposition pattern of residues, background interferences to radiation measurement, the characteristics of the SNM, and the quantity of the holdup.

This examination of the potential value of developing statistical models that are useful to holdup predictions leads us to conclude that there are many instances in which modeling can be beneficial to developing estimates of residual inventories of SNM. The value of a statistical model, however, is very much dependent on the quality of the holdup data used in the development of such a model. If the measurement errors are very large and/or operating conditions are subject to frequent changes, it is unrealistic to expect the development of useful estimation models under such conditions. On the other hand, if the process operation is stable and the holdup data gathered are of good quality, the models developed can be very valuable to making present and future estimates of holdup.

Our early attempts during this investigation to use available historical data on uranium holdup to develop estimation models suffered from poor quality of the data and a lack of knowledge regarding process variables that may have influenced the holdup. A careful examination of available historical data on uranium holdup from Los Alamos National Laboratory and GA Technologies, Inc., indicate that there is very limited value to much of the existing holdup data, gathered by nonintrusive passive assay techniques, for developing estimation models of residual inventories of uranium. Another task undertaken during this investigation was to conduct specially designed NDA measurements of SNM holdup at operating facilities. This effort had limited success, and it was recognized that such an approach to develop holdup data can be valuable only when these measurements are properly coordinated with plant operating personnel. In operating facilities, it is not practical to obtain measurements analogous to those in controlled experiments. The process of gathering holdup data at such facilities necessarily will have to involve some disruptions in the routine operations of the process, although such measurements can be conveniently scheduled to minimize impact on plant operations.

The difficulties associated with holdup measurements at SNM-processing facilities are the results of both facility- and measurement-related problems. Neither of these problems has a simple short-term solution, although improvements over the present situation can be accomplished to meet the objectives of nuclear material safeguards and accountability by incorporating carefully designed measurements as part of inventory records development and the judicious use of statistical prediction models.

There are several limiting factors to accomplishing the goals of regulatory requirements of holdup estimation. They include the layout of the plant and equipment, the need for calibration standards, limitations of NDA instruments, and the lack of priorities for holdup measurement at SNM-processing facilities. The layout of many of the existing facilities is a major hindrance to holdup measurement. Although it is difficult to make major changes in existing facilities, it is an important factor that should be considered in the design and construction of new facilities. There is considerable room for innovations in the development of standards specially suited for materials holdup measurement, and this is an area that can be stressed in regulatory guidelines on holdup measurements. The developments in NDA instrumentation of the last decade has yet to address the needs of holdup measurement. Thus, there is a dearth of specially designed NDA instruments that are readily adaptable to meet the needs of a variety of holdup measurements. Finally, and most important, an increased awareness of the importance of holdup measurements for materials accountability, process safety, and efficient plant operations can make a significant contribution to meet the goals of regulatory requirements of residual holdup estimations.

## ACKNOWLEDGMENTS

The authors wish to acknowledge the technical assistance of C. C. Thomas, Jr., N. Ensslin, T. Marks, Jr., R. Siebelist, M. C. Tinkle, T. M. Foreman, C. A. Ostenak, and J. T. Markin of Los Alamos National Laboratory during various phases of this investigation. In addition, we wish to acknowledge the assistance of J. Razvi and R. Wadham of GA Technologies, Inc., in helping to conduct the uranium dust-generation experiments described in Sec. III, and the assistance of A. F. Cermak of Allied-General Nuclear Services in performing the pulse-column experiments described in Sec. IV. We acknowledge the valuable computer services provided by J. Hafer and graphics assistance provided by K. Woodward of Los Alamos throughout this project. We are thankful to J. P. Shipley, E. A. Hakkila, D. B. Smith, and J. W. Tape of Los Alamos for their contributions to this investigation through constructive suggestions and criticisms. Our special thanks to S. Hurdle for the word-processing services in preparation of this document.

## REFERENCES

1. H. J. Kouts and J. M. Williams, "U.S. Safeguards Systems Studies," in "Safeguards Systems Analysis of Nuclear Fuel Cycles," US Atomic Energy Commission report WASH-1140 (October 1969).
2. "Selected Measurement Methods for Plutonium and Uranium in the Nuclear Fuel Cycle," C. J. Rodden, Ed., US Atomic Energy Commission report TID-7029, 2nd Ed. (1972).
3. R. L. Bramblett, "Passive Nondestructive Assay Methods," in *Handbook of Nuclear Safeguards Measurement Methods*, D. R. Rogers, Ed. (US Nuclear Regulatory Commission, Washington, DC, 1983: NUREG/CR-2078, MLM-2855), Chap. V.
4. Regulatory Guide 5.37, "In-Situ Assay of Enriched Uranium Residual Holdup," US Atomic Energy Commission (April 1974) and proposed revision to Regulatory Guide 5.37, Rev. 1 (November 1983).
5. Regulatory Guide 5.23, "In-Situ Assay of Plutonium Residual Holdup," US Atomic Energy Commission (May 1974) and proposed revision to Regulatory Guide 5.23, Rev. 1 (February 1984).



6. C. H. Kindle, "In Situ Measurements of Residual Plutonium," Nucl. Mater. Manage. V(III), 540-549 (1976).
7. A. R. Anderson, R. H. James, and F. Morgan, "Hidden Inventory and Safety Considerations," Nucl. Mater. Manage. V(III), 525-532 (1976).
8. M. S. Zucker, "Standards for Holdup Measurement," Brookhaven National Laboratory report BNL-31549 (1982).
9. N. H. Trahey, "Reference Materials for Nuclear Safeguards Measurements—A Forecast for the 1980's," Nucl. Mater. Manage. IX (Proceedings Issue), 697-707 (1980).
10. R. Abedin-Zadeh, T. Beetle, G. Busca, S. Guardini, E. Kuhn, D. Terrey, and S. Turel, "Preparation of Plant-Specific NDA Reference Material," in Nuclear Safeguards Technology 1982, Vol. II, 57-63 (IAEA, Vienna, 1983).
11. W. D. Reed, Jr., J. P. Andrews, and H. C. Keller, "A Method for Surveying for  $^{235}\text{U}$  with Limit of Error Analysis," Nucl. Mater. Manage. II, 395-414 (1973).
12. T. Gozani, "An Evaluation of Hold-Up Measurement," Nucl. Mater. Manage. VI(III), 424-433 (1977).
13. B. F. Disselhorst, J. E. Glancy, and D. S. Brush, "Survey Techniques for Measuring Uranium-235," Nucl. Mater. Manage. VI(III), 411-423 (1977).
14. J. W. Tape, D. A. Close, and R. B. Walton, "Total Room Holdup of Plutonium Measured with a Large-Area Neutron Detector," Nucl. Mater. Manage. V(III), 533-539 (1976).
15. M. C. Moxon and E. W. Lees, "Non-Invasive Determination of the Uranium Content in a Centrifuge Plant Dump Trap," in Nuclear Safeguards Technology 1982, Vol. II, 57-63 (IAEA, Vienna, 1983).
16. Regulatory Guide 5.13, "Conduct of Nuclear Material Physical Inventories," US Atomic Energy Commission (May 1973).
17. R. S. T. Shaw, "The Investigation of Industrial Plant Process Using Radioactive Tracer," J. Radioanal. Chem. 64, 337-349 (1981).
18. "Evaluation of Minor Isotope Safeguard Techniques (MIST) in Reactor Fuel Reprocessing," US Atomic Energy Commission report WASH-1154 (February 1970).
19. K. K. S. Pillay, "Use of Tracers in Materials Holdup Study," Nucl. Mater. Manage. XII (Proceedings Issue), 182-186 (1983).
20. Regulatory Guide 5.8, "Design Considerations for Minimizing Residual Holdup of Special Nuclear Material in Drying and Fluidized Bed Operations," US Atomic Energy Commission (May 1974).
21. D. D. Cobb, L. E. Burkhart, and A. L. Beyerlein, "In-Process Inventory Estimation for Pulsed Columns and Mixer-Settlers," *Proceedings of the 2nd Annual Symposium on Safeguards and Nuclear Material Management* (European Safeguards Research and Development Association, 1980), ESARDA 11, pp. 145-151.

22. R. W. Hass, "Development and Verification of a Mathematical Model for a Pulsed Extraction Column," M. S. Thesis in Chemical Engineering, Iowa State University, Ames, Iowa (1983).
23. A. M. Krichinsky, "NUMATH: A Nuclear Material Holdup Estimator for Unit Operations and Chemical Processes," Oak Ridge National Laboratory report ORNL/TM-8175 (February 1983).
24. F. T. Wright, "Estimating Strictly Increasing Regression Functions," *J. Am. Stat. Assn.* **73**, 636-639 (1978).
25. R. R. Picard and R. S. Marshall, "Uranium Holdup Modeling," Los Alamos National Laboratory report LA-9853-MS, NUREG/CR-3448 (November 1983).
26. R. H. Myers, *Response Surface Methodology* (Allyn and Bacon, Boston, Massachusetts, 1971).
27. P. A. Russo, "Estimation of Holdup in Solvent Extraction Columns Based on Data Obtained at Y-12," Los Alamos National Laboratory memorandum Q-1-83-427/0665D to Sam Pillay (June 7, 1983).
28. A. F. Cermak, "Pilot-Scale Pulsed Column Profile and Holdup Studies," Allied-General Nuclear Services report AGNS-35900-3.1-111 (November 1980).
29. T. E. Gier and J. O. Hougen, "Concentration Gradients in Spray and Packed Extraction Columns," *Ind. Eng. Chem.* **45**, 1362-1370 (1953).
30. L. Burkhart, "A Survey of Simulation Methods for Modeling Pulsed Sieve-Plate Extraction Columns," Ames Laboratory report UCRL-15101 (March 1979).
31. V. V. Fedorov, *Theory of Optimal Experiments* (Academic Press, New York, 1972).
32. R. E. Kalman, "A New Approach to Linear Filtering and Prediction Problems," *Journal of Basic Engineering* **82**, 34-45 (1960).
33. R. E. Kalman and R. S. Bucy, "New Results in Linear Filtering and Prediction Theory," *Journal of Basic Engineering* **83**, 95-108 (1961).
34. R. J. Meinhold and N. D. Singpurwalla, "Understanding the Kalman Filter," *American Statistician* **37**, 123-127 (1983).
35. E. J. Wegman, "Kalman Filtering," in *Encyclopedia of Statistical Sciences*, N. Johnson and S. Kotz, Eds. (John Wiley and Sons, Inc., New York, 1982).
36. D. B. Duncan and S. D. Horn, "Linear Recursive Dynamic Estimation from the Viewpoint of Regression Analysis," *J. Am. Stat. Assoc.* **67**, 815-821 (1972).
37. D. J. Downing, D. H. Pike, and G. W. Morrison, "Application of the Kalman Filter to Inventory Control," *Technometrics* **22**, 17-22 (1978).
38. G. E. P. Box and G. M. Jenkins, *Time Series Analysis, Forecasting and Control* (Holden-Day, San Francisco, 1970).

39. R. C. Littell and D. J. Downing, discussion of "Statistical Methods for Nuclear Materials Safeguards: An Overview," *Technometrics* 24, 277-279 (1982).
40. W. G. Cochran, *Sampling Techniques* (John Wiley and Sons, Inc., New York, 1977).
41. L. Kish, *Survey Sampling* (John Wiley and Sons, Inc., New York, 1965).
42. "Clinical Uses of Radionuclides: Critical Comparison with Other Techniques," F. A. Goswitz, G. A. Andrews, and M. Viamonte, Jr., Eds., AEC Symposium Series 27, U.S. Atomic Energy Commission, Washington, DC (1972).
43. R. P. Ekins, "Tracer Methods in Organic and Biochemical Analysis," in *Radiochemical Methods of Analysis*, D. I. Coomber, Ed. (Plenum Press, New York, 1975), Chap. 9, pp. 349-406.
44. P. A. Russo, R. B. Strittmatter, E. L. Sandford, I. W. Jeter, E. McCollough, and G. L. Bowers, "Operation of Automated NDA Instruments for In-Line HEU Accounting at Y-12," paper to be presented at the ANS Topical Conference on Safeguards Technology: The Process Safeguards Interface, Hilton Head Island, South Carolina, November 1983; Los Alamos National Laboratory document LA-UR-83-1576.

## APPENDIX A

### USE OF TRACERS IN MATERIALS HOLDUP STUDY

K. K. S. Pillay

#### I. INTRODUCTION

Holdup measurements are generally based on the concept of dividing processing facilities into contiguous collection zones and performing NDAs to estimate residual inventories of SNM. Often nondestructive measurements for holdup are attempted using passive gamma or neutron assay techniques. This approach generally encounters difficulties caused by facility- and process-related problems, which in turn compound the inherent limitations of passive gamma assay techniques for the measurement of SNM. Some of the important limitations of passive assay techniques for the measurement of enriched uranium and plutonium are

1. the low specific activity of the isotopes  $^{235}\text{U}$  and  $^{239}\text{Pu}$  and the accompanying difficulties in the measurement of small amounts of uranium or plutonium in the midst of large background radiations from other parts of an operating plant,
2. the insensitivity of passive neutron assay techniques for the detection and measurement of residual amounts of uranium or plutonium,
3. the dominance of self-attenuation in the matrix of the SNM and the attenuation by construction materials of the low-energy gamma radiations from  $^{235}\text{U}$  and  $^{239}\text{Pu}$ , and
4. the potential variability in the distribution of uranium holdup within the process equipment and the consequent marginal value of conventional calibration techniques.

The limitations of NDA techniques are recognized, and Regulatory Guide 5.13,<sup>A-1</sup> in describing physical inventory procedures that are acceptable to regulatory staff, discusses the acceptability of other methods such as "tracer or step function inventory" for dynamic inventory development. One of the unique methods of overcoming the limitations of passive NDA techniques is the use of a tracer to account for the residual SNM. Safeguards techniques and process inventory determinations using minor isotope techniques have been previously reported.<sup>A-2,A-3</sup> Other suggestions on the potential use of radioactive tracers in materials holdup measurements<sup>A-4</sup> and for the study of materials flow in a large fuels materials preparation plant<sup>A-5</sup> have been made in the past. However, there are no known reports on the use of tracers for the measurement of holdup of SNM for materials accountability purposes. Among the various types of tracers that are in common use, a radioactive tracer that is compatible with the system is the most desirable for passive NDAs.

Tracers are powerful tools in the study of process kinetics, and they have been used extensively in the investigation of biological, geological, environmental, and chemical systems. In several experimental studies of this program to measure the holdup of uranium, radioactive tracers were used in equipment and facilities used in the preparation of nuclear fuel materials. The use of radioactive tracers in these experiments offered considerable advantages to measuring uranium holdup and its variations as a function of throughput and some chosen process parameters. Such tracer applications can be of value to measuring holdup of both uranium and plutonium in production facilities of nuclear materials.

#### II. EXPERIMENTAL STUDIES USING TRACERS

One of the important aspects of the research study reported here was an attempt to develop estimation models for materials holdup at HEU-processing facilities. An integral part of this program was to conduct specially designed experimental studies on several unit processes common to industrial operations

involving the preparation of HEU nuclear fuels. These experiments were conducted to collect data for developing holdup estimators that are equipment and process specific. Three of the experiments in which radioactive tracers were used to measure the amount of uranium holdup are

1. a dust-generating operation at a HEU-processing facility,
2. an ADU precipitation and calcination process, and
3. a solution loop system circulating uranyl solutions.

The first experiment involved the study of uranium holdup during a dust-generating operation in which two types of uranium oxide powder and one type of incinerator ash containing uranium were used. The experimental facility consisted of a glove box, some ductwork, and an exhaust air filter system. The total throughput of uranium through this experimental facility was  $\sim 1$  kg/cycle for a total of 70 kg for seven experiments. Details of this experimental study were reported in Sec. III.

The second experiment, detailed in Sec. V, consisted of the precipitation of uranium as ADU from a uranyl nitrate solution, filtering out the ADU, and calcining it into  $U_3O_8$ . The precipitation processes were carried out in a large, cylindrical, stainless steel vessel. The filtered ADU was calcined in Inconel-600 trays in a Lindberg furnace. The throughput of uranium through this system was  $\sim 1$  kg/batch with a cumulative throughput of  $\sim 50$  kg.

The third experiment (see Sec. VI) consisted of circulating two types of uranyl solutions in two separate loops, one built of stainless steel and the other fabricated from CPVC. The loops were built to incorporate large storage tanks, circulation pump(s), pipes of various dimensions, elbows, tees, unions, flow meters, valves, and terminal valves. One of the solutions pumped through the stainless steel side of the loop was a uranyl nitrate solution containing excess  $HNO_3$  (4 moles of acid per mole of uranium); the other solution, circulated through the CPVC side of the loop, was a uranyl fluoride solution containing excess hydrofluoric acid. The total throughput through the system was equivalent to  $\sim 110$  tonnes of uranium at a circulation rate of  $\sim 50$ -100 kg/h of uranium.

The objectives of these experiments included periodic measurements of the residual uranium in the system and attempts to correlate throughput with holdup. In the early stages of designing these experiments, it was realized that it would be impractical to make the necessary measurements for these experiments by attempting NDA of  $^{235}U$  using scintillation gamma assay techniques. The quantities of materials to be measured during the experiments ranged from few tenths of a gram to a few grams of uranium in large process vessels and equipment. The changes in the quantities of holdup of uranium between measurements were even smaller, and the difficulties of measuring such small amounts of material in experimental facilities located in processing areas were not trivial.

#### A. Qualities of a Tracer

Some of the desirable qualities of a tracer for process holdup measurements are the following.

1. A tracer should have unique characteristics that would make it easily identifiable in a very large matrix. In the case of radioactive tracers, this quality is generally achieved by the uniqueness of the radiations emitted and ease of detection and measurement using simple measurement techniques.
2. The tracer must be physically and chemically compatible with the system and the process under investigation. This is generally accomplished by choosing a distinguishable isotope or a chemical analogue of the element that will follow the major component of the system throughout the process.
3. The tracer must be in extremely small concentrations so that it will not influence the process chemistry or the product of the process under investigation. Tracers in concentrations of parts per million or less would satisfy this requirement.
4. When a radioactive tracer is used, it would be desirable to choose a radioactive isotope of relatively short half-life so that the radioactivity originating from the tracer would soon disappear from the matrix after the useful duration of the experimental study.

These above-mentioned qualities were chosen as criteria for the selection of tracers in our experimental studies.

## B. Tracers Used in HEU Holdup Measurements

In experiment 1, neutron-irradiated samples of (a) powdered uranium oxide and (b) an incinerator ash containing ~10 wt% of uranium oxide were used as tracers. These samples were irradiated in a research reactor until ~ $10^{15}$  fissions were introduced in the tracer sample. The samples were allowed to cool for ~2 weeks to reduce the level of short-lived fission products and to maximize the level of  $^{95}\text{Zr-Nb}$ . In experiments 2 and 3, a chemical analogue of uranium, with a unique neutron activation product, was used as a tracer. This isotope,  $^{46}\text{Sc}$ , was produced by neutron activation of natural scandium as  $\text{Sc}_2\text{O}_3$ . The properties of these radionuclides relevant to these tracer applications are summarized in Table A-I.

The gamma emissions per unit time per unit weight of the radionuclides in Table A-I show that the specific activity of the tracer nuclides is ~11 orders of magnitude higher than that of 100%-enriched  $^{235}\text{U}$ . If the tracer nuclide level in uranium is 1 ppb, there is a specific-activity advantage for the tracers 100 times better than for  $^{235}\text{U}$ . In addition, the higher energy gamma emissions from the tracers in the range of 0.5-1.2 MeV minimizes the interferences from beta and low-energy gammas. Thus, the overall advantage of using these tracers at the part-per-billion level for uranium holdup measurement can be at least two or three orders of magnitude better than the direct NDA of  $^{235}\text{U}$ . Further improvements can be accomplished by using higher levels of tracer and tracers with higher specific activities.

Physical and chemical compatibility of the tracer with the uranium system is essential to the successful function of the additive as a true tracer for uranium. Through careful experimentation, the chemical and physical forms of the tracers for three experiments described here were chosen. Table A-II lists chemically and physically compatible forms of the tracers that were prepared and incorporated into the experimental systems. The tracer levels were monitored at various stages of the processes to assure homogeneity and performance as a true tracer for uranium. Carefully designed bench-scale experiments were performed to confirm that the tracer chosen followed uranium quantitatively throughout the process. The analyses of uranium was performed using destructive chemical assay techniques described in Sec. V.E. Scandium-46 tracer in the system was measured using a well-shielded 7.5- × 7.5-cm NaI(Tl) detector and a single-channel analyzer system.

TABLE A-I. Specific Activities of  $^{235}\text{U}$  and Tracer Isotopes

Nuclide	Half-Life	Prominent $\gamma$ 's (keV)	$\gamma$ -Emissions ( $\text{s}^{-1} \text{g}^{-1}$ )
$^{235}\text{U}$	$7.04 \times 10^8 \text{ yr}$	185.7	$4.32 \times 10^4$
$^{46}\text{Sc}$	83.85 days	889.3 1120.5	$2.5 \times 10^{15}$
$^{95}\text{Zr-Nb}$	64.4 days (31.15 days)	724.2 756.7 765.8	$1.56 \times 10^{15}$

TABLE A-II. Tracers and Their Compatible Forms

Experiment	Tracer	Physical Form	Chemical Form
U <sub>3</sub> O <sub>8</sub> dust generation	Fission products: <sup>95</sup> Zr-Nb & <sup>140</sup> Ba-La	Solid (particle size same as U <sub>3</sub> O <sub>8</sub> )	<i>In situ</i> -generated fission products in U <sub>3</sub> O <sub>8</sub>
ADU precipitation & calcination	<sup>46</sup> Sc	Solution to solids (changed with uranium)	Sc <sup>3+</sup> , Sc(OH) <sub>3</sub> , and Sc <sub>2</sub> O <sub>3</sub>
Uranyl nitrate solution loop	<sup>46</sup> Sc	Solution	Sc <sup>3+</sup>
Uranyl fluoride solution loop	<sup>46</sup> Sc	Solution	[ScF <sub>6</sub> ] <sup>3-</sup>

### C. Limitations of Experimental Facilities

The holdup experiments were conducted at two facilities with large inventories of uranium and/or thorium. Figures A-1 and A-2 illustrate the nature of the interferences by the background radiations at the two facilities. Figure A-1 shows the gamma spectrum of <sup>232</sup>Th and its daughters, which were the dominant background at the facility where the dust-generation experiment was conducted. In this illustration the gamma spectrum of <sup>235</sup>U was inserted to show the relative location of the most abundant primary gamma peak from enriched uranium. Also included in this illustration is the gamma spectrum of a <sup>95</sup>Zr-Nb equilibrium mixture, which was the dominant activity of the tracer used. The gamma radiations from the tracer are clearly distinguishable and measurable in the midst of large background radiations from thorium and its decay products. Similarly, Fig. A-2 shows the background radiations at the uranium-processing facility where experiments 2 and 3 were conducted using <sup>46</sup>Sc as the radioactive tracer. Here again, the advantage of using <sup>46</sup>Sc as a tracer for the NDA of uranium is obvious.

### D. Tracer Levels and Measurement Methods

The amount of radioactivity of the tracers used in these experiments ranged from 1 to 3 × 10<sup>9</sup> Bq/kg of uranium. For <sup>46</sup>Sc, this amounted to an atom ratio of ~1 tracer atom to 10<sup>9</sup> atoms of uranium.

The instrumentation used in these measurements consisted of a shielded NaI(Tl) scintillation detector and a single-channel analyzer and a scaler. With these instruments, it was possible to quantify accurately the tracer levels in the residual uranium holdup without undesirable interferences by the background radiations.

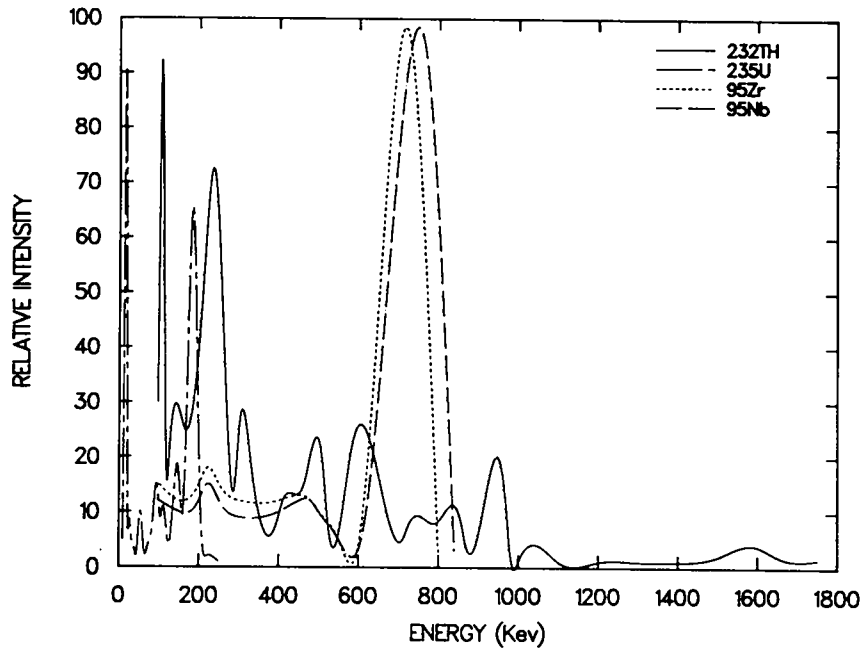


Fig. A-1. A combination of the gamma-spectra of  $^{232}\text{Th}$  and its daughters,  $^{235}\text{U}$ , and the tracer nuclide  $^{95}\text{Zr-Nb}$ .

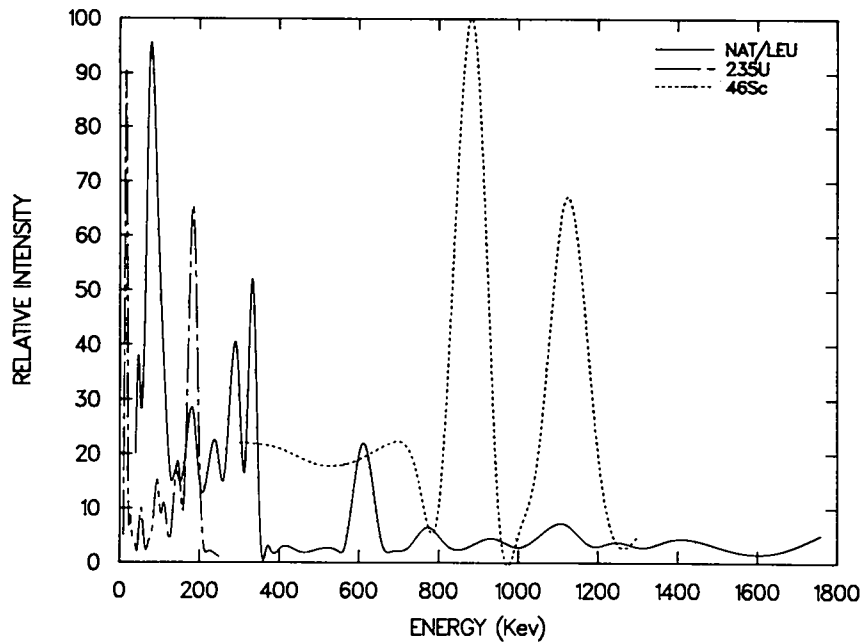


Fig. A-2. A combination of the gamma-spectra of natural and/or low-enriched uranium,  $^{235}\text{U}$ , and tracer nuclide  $^{46}\text{Sc}$ .



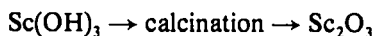
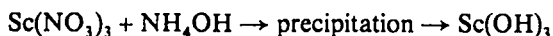
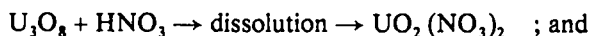
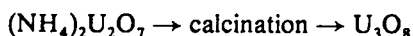
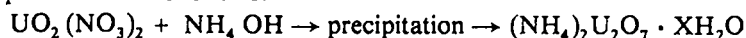
### III. RESULTS AND DISCUSSION

#### A. Homogenization of Tracers in Uranium Matrices

The incorporation of a tracer in a homogeneous solution of uranium is generally easier than the introduction of the tracer in a solid matrix as with the  $U_3O_8$  dust-generation experiment. In this latter case, ~200 mg of  $U_3O_8$  (or ash containing  $U_3O_8$ ) were irradiated in a neutron flux to generate the fission products within the matrix of  $U_3O_8$ . The active  $U_3O_8$  (or ash) was then blended with the bulk material. The mixture was sampled and counted to assure homogeneity of the tracer within the  $U_3O_8$  matrix. The blended material was considered homogeneous if the relative standard deviation of the specific activity of the samples was ~5%.

The uranyl nitrate and the uranyl fluoride solutions used different ionic forms of scandium because of the chemical characteristics of the media. Homogeneous mixtures of the uranyl solutions and corresponding tracer forms were prepared and preserved for up to 2 months in containers made of the the same materials used in the experiment. These mixtures were periodically analyzed to determine the potential segregation of tracer from the uranium matrix. It was determined that the uranyl nitrate solution with  $Sc^{3+}$  ion was compatible with the polyethylene and stainless steel loop and the  $[ScF_6]^{3-}$  ion in uranyl fluoride was compatible with the polyethylene and the CPVC loop with a hastelloy pump.

In the case of the ADU precipitation and calcination, the uranium went from a homogeneous solution to a precipitate and then to a calcined solid. The tracer scandium also followed the physical changes with concomitant chemical changes. The basic chemical reactions of uranium and scandium during this experiment are as follows:



Careful measurements made of the movement of  $^{46}Sc$  tracer with uranium showed no partitioning between uranium and scandium during dissolution, precipitation, and calcination processes nor during recycling of the products in the same processes. Some of the typical results of the quantitative measurements of the movements of  $^{46}Sc$  tracer during various stages of ADU precipitation and calcination are shown in Table A-III. These measurements indicate that scandium, a chemical analogue of uranium, is an excellent trace for uranium during the transformations involved in this unit process.

#### B. NDAs and Cleanout Measurements for Holdup Determination

A number of cleanout measurements were performed during this investigation to compare the results of NDAs using the radioactive tracers. The cleanout measurements were performed by a variety of methods for the various experiments reported here. Among the analytical techniques used were isotope dilution mass spectrometry, titrimetry, spectrophotometric analysis using Arsenazo-III, and gamma-ray spectrometric measurements of the tracer activity in the cleanout material using a well-shielded, high-efficiency

TABLE A-III. Per Cent Tracer Found at Various Stages of ADU Precipitation and Calcination

State of Uranium in the Matrix	State of <sup>46</sup> Sc Tracer	Per Cent of Initial Spike
UO <sub>2</sub> (NO <sub>3</sub> ) solution	Sc <sup>3+</sup>	100
ADU	Sc(OH) <sub>3</sub>	97.9
U <sub>3</sub> O <sub>8</sub>	Sc <sub>2</sub> O <sub>3</sub>	98.1
U <sub>3</sub> O <sub>8</sub> recycled to UO <sub>2</sub> (NO <sub>3</sub> ) <sub>2</sub>	Sc <sup>3+</sup>	98.7
Reprecipitation as ADU	Sc(OH) <sub>3</sub>	96.8
Recalcination to U <sub>3</sub> O <sub>8</sub>	Sc <sub>2</sub> O <sub>3</sub>	97.1

NaI(Tl) detector coupled to a multichannel analyzer. In Table A-IV, the results of some of these cleanout measurements are compared with the corresponding values of NDA measurement of tracers in the residual holdup.

TABLE A-IV. Comparison of NDA Measurements of Holdup with Cleanout Measurements (in Grams of Uranium)

Experiment No.	Equipment/Parts	Tracer NDA Measurement	Cleanout Measurement
1	Ductwork (fine U <sub>3</sub> O <sub>8</sub> )	3.56	3.59
		6.22	5.10
1	Ductwork (ash with U <sub>3</sub> O <sub>8</sub> )	1.66	1.06
		2.50	2.51
1	Ductwork (coarse U <sub>3</sub> O <sub>8</sub> )	1.60	1.89
2	ADU precipitation vessel	12.6	14.6
		9.3	10.2
2	Calcining furnace	1.7	1.5
2	Calcining trays	1.4	1.3
3	Pipes (per meter)	0.37	0.40
		0.16	0.15
3	Elbows	0.02	0.03
		0.03	0.03
3	Valves	0.40	0.37
3	Tees	0.08	0.07
		0.08	0.08
3	Pumps	13.7	11.9
		9.4	7.0

The results of these experimental studies clearly demonstrate that the sensitivity of holdup measurements can be significantly improved by the judicious incorporation of trace levels of radionuclides with a high specific activity and desirable gamma-emission characteristics. This approach is particularly valuable in generating data for the development of holdup estimators and in determining significant holdup patterns of large processing facilities of SNM. The cleanout measurements of materials holdup necessarily involve major disruptions in the operations of the facilities and considerable investment of manpower and resources. The NDA measurements described here using tracers can be performed in a few minutes

without any significant disruptions to facility operations. Further, the data presented in Table A-I and Figs. A-1 and A-2 clearly demonstrate that the passive assay of the gamma radiations from the  $^{235}\text{U}$  for the study of holdup in these experiments would have been futile because of the extremely low specific activity of  $^{235}\text{U}$  and the overwhelming interferences by the background radiations resulting from the large inventories of uranium and/or thorium.

## REFERENCES

- A-1. Regulatory Guide 5.13, "Conduct of Nuclear Material Physical Inventories," US Atomic Energy Commission (November 1973).
- A-2. "Evaluation of Minor Isotope Safeguards Techniques (MIST) in Reactor Fuel Reprocessing," US Atomic Energy Commission report WASH-1154 (February 1970).
- A-3. D. E. Christensen, R. A. Ewing, D. P. Gaines, Jr., R. Kramer, R. A. Schneider, L. A. Stieff, and H. Winter, "A Summary of Results Obtained from First MIST Experiment at Nuclear Fuel Services, West Valley, New York," in *Safeguards Techniques*, Proc. Symp., Karlsruhe, July 6-10, 1970 (International Atomic Energy Agency, Vienna, 1970), Vol. I.
- A-4. T. Gozani, "Review of Evaluation of Holdup Measurements," *Nucl. Mater. Manage.* VI(3), 424-433 (1977).
- A-5. R. S. T. Shaw, "The Investigation of Industrial Plant Process Using Radioactive Tracer," *J. Radioanal. Chem.* 64, 337-349 (1981).

## APPENDIX B

### PRINCIPLES OF REGRESSION AND KALMAN FILTERING

R. R. Picard

#### I. REGRESSION

A brief development of estimates based on regression methodology is presented in the following paragraphs. Such estimates are used in the analyses of the dust-generation experiments and of the liquid-liquid extraction pulse-column data. A more detailed treatment of the results given below can be found in many texts<sup>B-1, B-2</sup> on regression and linear models theory, including several cited in the reference list of this report.

The standard linear model relates a "dependent variable"  $y$  to  $p$  "explanatory variables"  $\{x_i\}$  by

$$y = \beta_1 x_1 + \beta_2 x_2 + \dots + \beta_p x_p + e, \quad (\text{B-1})$$

where the  $\{\beta_i\}$  are unknown parameters and  $e$  denotes the error in measurement. Once parameter estimates  $\{\hat{\beta}_i\}$  have been obtained, predicted values  $\hat{y}$  of the dependent variable take the form

$$\hat{y} = \hat{\beta}_1 x_1 + \hat{\beta}_2 x_2 + \dots + \hat{\beta}_p x_p. \quad (\text{B-2})$$

Several examples of Eq. (B-2) are given in previous sections of this report. Data from the air filters used in the dust-generation experiments conformed to the model (written in the notation of Sec. III)

$$\hat{h}_f(t) = \hat{\alpha}t + \hat{\beta}t^2,$$

where the dependent variable  $h_f(t)$  is the amount of holdup on the filter at throughput  $t$  and depends on the explanatory variables  $t$  and  $t^2$ . A second example, also taken from Sec. III, concerns the modeling of the glove box floor, where the estimated density  $\hat{d}(t,x,y)$  of material at location  $(x,y)$  on the floor when process throughput is  $t$  is

$$\hat{d}(t,x,y) = \hat{\alpha}t + \hat{\beta}tx + \hat{\gamma}ty.$$

As is apparent from inspection of Eq. (B-1), far more complex relationships may also be examined using linear models theory.

The procedure for using observed data on the dependent variable and explanatory variables for purposes of estimating the parameters  $\{\beta_i\}$  in Eq. (B-1) is straightforward. The basic idea is to obtain  $\{\hat{\beta}_i\}$  such that the fitted Eq. (B-2) agrees "best" with the observed data. Often "best" is in a least squares sense as the resulting estimates have desirable properties for the common situation when errors are approximately normally distributed. Standard statistical computer programs contain least squares routines for this reason. For completeness, however, it should be noted that other notions of "best" could be considered, leading to either weighted least squares or to robust estimation.

Derivation of the least squares parameter estimates  $\{\hat{\beta}_i\}$  is most easily accomplished in compact matrix notation. Let  $\underline{y}$  be the vector of observed values of the dependent variable, each value conforming to Eq. (B-1) for its associated  $\{x_i\}$ . For  $\underline{\beta}$  the vector of unknown parameters  $\{\beta_i\}$ ;  $\underline{e}$ , the vector of measurement errors; and  $\underline{X}$ , the "design matrix" of constants of the linear relationship; the model is

$$\underline{y} = \underline{X}\underline{\beta} + \underline{e}.$$

The least squares estimate of  $\underline{\beta}$  is

$$\underline{\hat{\beta}} = (X'X)^{-1} X'y ,$$

and predicted values are obtained as indicated in Eq. (B-2).

## II. KALMAN FILTER

The development of filtered estimates is described in the following paragraphs. To facilitate application of this methodology to problems beyond the steady-state model discussed in analysis of the ADU and solution loop experiments, the Kalman filter is presented in its general form. For additional information, some elementary references <sup>B-3, B-4</sup> are provided. Also, the early development of filtering, largely pursued in the engineering literature, may be consulted.

The objective is to estimate the continually changing "state" of a system based on noisy data. In the text, the state is simply the unknown quantity of holdup in a piece of equipment, and the relevant measurement history comprises the data. The model is represented by the measurement and state equations. In general, the measurement equation is written

$$x(t) = m(t)h(t) + e(t) , \tag{B-3}$$

where the measurement(s)  $x(t)$  and state(s) of the system  $h(t)$  at time  $t$  may be vector valued. The error vector  $e(t)$  is assumed to be distributed with mean zero and covariance matrix  $r(t)$ , and the "measurement matrices"  $\{m(t); t = 1, 2, \dots\}$  are presumed known. Equation (15) of the text's steady-state model is a special case of Eq. (B-3) above with  $x(t)$  and  $h(t)$  scalar valued and  $m(t) \equiv 1$ ,  $r(t) \equiv \sigma_n^2$ .

The state equation, in general form, is

$$h(t) = s(t-1)h(t-1) + c(t-1) + \epsilon(t-1) \tag{B-4}$$

and relates the state of the system  $h(t)$  at time  $t$  to the state  $h(t-1)$  at time  $t-1$ . The "state transition matrices"  $\{s(t)\}$  and "control vectors"  $\{c(t)\}$  are presumed known, and  $\epsilon(t)$  is distributed with mean zero and covariance matrix  $q(t)$ . Further,  $\epsilon(t)$  and  $e(t)$  are uncorrelated. Equation (16) of the text corresponds to Eq. (B-4) with  $s(t) \equiv 1$ ,  $c(t) \equiv 0$ , and  $q(t) \equiv \sigma_p^2$ .

The recursive procedure known as the Kalman filter formally proceeds as follows.

1. Let  $\hat{h}(1)$  be an estimate of the initial system state  $h(1)$  and have covariance matrix  $v(1)$ . Set  $t = 1$ .
2. The state estimate at time  $t + 1$  based on all information through time  $t$  is

$$\hat{h}(t+1) = s(t)\hat{h}(t) + c(t) ,$$

and the error of prediction has covariance matrix

$$p(t+1) = s(t)v(t)s(t)' + q(t) .$$

3. The gain matrix is defined by

$$g(t+1) = p(t+1)m(t+1)'[m(t+1)p(t+1)m(t+1)' + r(t)]^{-1} .$$

4. The state estimate updated for the measurement at time  $t + 1$  is

$$\hat{h}(t+1) = \hat{h}(t+1) + g(t+1)[x(t+1) - m(t+1)\hat{h}(t+1)]$$

and has covariance matrix

$$v(t + 1) = [I - g(t + 1) m(t + 1)] p(t + 1) .$$

5. The recursion continues by repeating steps 2-4. Properties of the filtered estimates  $\{\hat{h}(t); t = 1, 2, \dots\}$  can be found in standard references.<sup>B-3 to B-6</sup>

In a final note, it is also possible to obtain "smoothed" estimates. In contrast to filtering, in which the current state of the system is estimated based on present and past information, smoothing uses all available data to estimate all system states. Thus, a previous filtered estimate can be updated based on the collection of subsequent data. Because smoothed estimates are not overly useful for near-real-time accounting, the subject is not discussed here.

## REFERENCES

- B-1. N. R. Draper and H. Smith, *Applied Regression Analysis*, 2nd Edition (John Wiley and Sons, Inc., New York, 1981).
- B-2. S. Weisberg, *Applied Linear Regression* (John Wiley and Sons, Inc., New York, 1980).
- B-3. R. J. Meinhold and N. D. Singpurwalla, "Understanding the Kalman Filter," *American Statistician* 37, 123-127 (1983).
- B-4. E. J. Wegman, "Kalman Filtering," in *Encyclopedia of Statistical Sciences*, N. Johnson and S. Kotz, Eds. (John Wiley and Sons, Inc., New York, 1982).
- B-5. D. B. Duncan and S. D. Horn, "Linear Recursive Dynamic Estimation from the Viewpoint of Regression Analysis," *J. Am. Stat. Assoc.* 67, 815-821 (1972).
- B-6. D. J. Downing, D. H. Pike, and G. W. Morrison, "Application of the Kalman Filter to Inventory Control," *Technometrics* 22, 17-22 (1978).

## APPENDIX C

### DETAILED DATA FROM CONTROLLED EXPERIMENTAL STUDIES

Note: The number of significant figures in the data tabulated in this appendix is not representative of the accuracy of modeling estimates. The relative errors of estimations may be evaluated from estimated values and system losses computed from measurements.

### DATA FROM EXPERIMENTAL STUDY OF URANIUM HOLDUP IN A DUST-GENERATING FACILITY (Tables C-I through C-XV)

TABLE C-I. Summary of Modeling Results for Medium-Airflow Experiment with  $U_3O_8$

Component	Measurement Points <sup>a</sup>	Model <sup>b</sup>	Estimated Holdup <sup>c</sup> (g)
Glove box sides	1-2	$\hat{h}_s(t) = 0$	0
Glove box floor	3-5	$\hat{h}_f(t) = 0.1617t$	1.617
Vertical segment	6-7	$\hat{h}_v(t) = 0.0173t$	0.173
First elbow	8	$\hat{h}_1(t) = 0.0067t$	0.067
Segment between elbows	9	$\hat{h}_b(t) = 0.0126t$	0.126
Second elbow	10	$\hat{h}_2(t) = 0.0059t$	0.059
Horizontal segment	11-13	$\hat{h}_h(t) = 0.0361t$	0.361
Filter	14	$\hat{h}_f(t) = 0.0545t$ $+ 0.0016t^2$	0.704
System total	1-14	$\hat{h}(t) = 0.2948t$ $+ 0.0016t^2$	3.107
System weight loss			3.198

<sup>a</sup>See Fig. 6 for details.

<sup>b</sup>The function  $\hat{h}_{...}(t)$  represents the estimated holdup within the individual component when the throughput was  $t$  kilograms.

<sup>c</sup>Throughput = 10 kg.

TABLE C-II. Summary of Modeling Results for High-Airflow Experiment with  $U_3O_8$

Component	Measurement Points <sup>a</sup>	Model <sup>b</sup>	Estimated Holdup <sup>c</sup> (g)
Glove box sides	1-2	$\hat{h}_s(t) = 0$	0
Glove box floor	3-5	$\hat{h}_f(t) = 1.582$ $+ 0.1102t$	2.684
Vertical segment	6-7	$\hat{h}_v(t) = 0.9276t$	0.287
First elbow	8	$\hat{h}_1(t) = 0.0106t$	0.106
Segment between elbows	9	$\hat{h}_b(t) = 0.0203t$	0.203
Second elbow	10	$\hat{h}_2(t) = 0.0109t$	0.109
Horizontal segment	11-13	$\hat{h}_h(t) = 0.0528t$	0.528
Filter	14	$\hat{h}_f(t) = 0.1544t$ $+ 0.0076t^2$	2.301
System total	1-14	$\hat{h}(t) = 1.582 + 0.3879t$ $+ 0.0076t^2$	6.218
System weight loss			6.204

<sup>a</sup>See Fig. 6 for details.

<sup>b</sup>The function  $\hat{h}_{...}(t)$  represents the estimated holdup within the individual component when the throughput was  $t$  kilograms.

<sup>c</sup>Throughput = 10 kg.



TABLE C-III. Constants of Integration<sup>a,b</sup>

Area: Glove Box Floor  
Measurement Points 3-5

Measurement Point	Coordinates (x,y) on floor (cm)	Constants		
		1	2	3
3	(13.97, 42.55)	0.1946	1.670	2.536
4	(54.61, 31.75)	0.3692	7.938	4.670
5	(97.79, 34.29)	0.3692	14.210	4.929

<sup>a</sup>See p. 26.

<sup>b</sup>Detectors were reproducibly placed in these locations for all seven experiments so that the above constants were used in all cases.

TABLE C-IV. Table of Measured Holdup Per Unit Area<sup>a</sup>

Experiment: U<sub>2</sub>O<sub>8</sub>  
Glove Box Floor

Airflow	Measurement Point	Throughput <sup>b</sup> (kg)					
		2	4	6	8	10	
LOW	3	0.0264	0.0902	0.0910	0.1263	0.2020	0.2641
	4	0.0395	0.0970	0.1513	0.2559	0.3094	0.3066
	5	0.0902	0.1180	0.1646	0.1958	0.3046	0.2682
MEDIUM	3	0.0211	0.0000	0.1941 <sup>c</sup>	0.0609	0.1747	0.1499
	4	0.0166	0.0524	0.1955 <sup>c</sup>	0.1211	0.1869	0.1536
	5	0.0000	0.0744	0.1221	0.1183	0.0570 <sup>c</sup>	0.1879
HIGH	3	0.1486	---	0.2285	0.1845	0.1655	0.2768
	4	0.2375	0.2108	0.2472	0.2739	0.2444	0.3280
	5	0.1920	0.1714	0.2122	0.1135 <sup>c</sup>	0.2995	0.1304 <sup>c</sup>

<sup>a</sup>The values given are scaled to milligrams per square centimeter. When regressed on the constants of integration (Table C-III) and multiplied by  $c_1 = 0.3692$  times the corresponding throughput (Sec. III), estimates of the parameters ( $\alpha, \beta, \gamma$ ) in the density function are obtained. Integration of the estimated density yields the estimate of holdup.

<sup>b</sup>Zero values indicate the observed negative count rates, which may result from measurement error when the amount of material measured is small relative to background; blanks indicate that no value is available.

<sup>c</sup>An outlier not used in the model fitting.

TABLE C-V. Table of Measured Holdup Per Unit Area<sup>a</sup>

Experiment: U<sub>2</sub>O<sub>8</sub>  
Vertical Segment

Airflow	Measurement Point	Throughput <sup>b</sup> (kg)					
		2	4	6	8	10	
LOW	6	0.0015	0.0039	0.0056	0.0367 <sup>c</sup>	0.0177	0.0282
	7	0.0082	0.0133	0.0011 <sup>c</sup>	0.0284	0.0220	0.0374
MEDUM	6	0.0417	0.0000	0.0000	0.0000	0.0470	0.0000
	7	0.0000	0.0000	0.0141	0.0158	0.0538	0.0414
HIGH	6	0.0147	0.0420	0.0000	0.0028	0.0310	0.0000
	7	0.0412	0.0837	0.0882	0.0868	0.0646	0.0149

<sup>a</sup>The values given are scaled to milligrams per square centimeter. When regressed on the constants of integration (Sec. III), parameter estimates in the density function are obtained. Integration of the density function yields the holdup estimators  $\hat{h}(t)$  as given in Tables C-I and C-II.

<sup>b</sup>Zero values indicate the observed negative count rates, which may result from measurement error when the amount of material measured is small relative to background; blanks indicate that no value is available.

<sup>c</sup>An outlier not used in the model fitting.

TABLE C-VI. Table of Measured Values

Experiment: U<sub>3</sub>O<sub>8</sub>  
 Measurement Points: 8-10, 14

Airflow	Measurement Point	Throughput <sup>a</sup> (kg)					
		2	4	6	8	10	
LOW	8	0.007	0.003	0.013	0.025	0.034	0.023
MEDIUM		0.000	0.000	0.007	0.069	0.096	0.058
HIGH		0.000	0.044	0.023	0.155	0.061	0.122
LOW	9	0.025	0.031	0.052	—	0.090	0.082
MEDIUM		0.032	0.029	0.087	0.153	0.071	0.139
HIGH		0.069	0.118	0.301	0.261	0.159	0.041
LOW	10	0.017	0.014	0.010	0.021	0.040	0.041
MEDIUM		0.000	0.035	0.040	0.053	0.059	0.049
HIGH		0.023	0.056	0.103	0.138	0.077	0.071
LOW	14	0.048	0.117	0.202	0.258	0.373	0.376
MEDIUM		0.120	0.247	0.406	0.495	0.687	0.739
HIGH		0.430	0.787	1.090	—	2.316	2.313

<sup>a</sup>Zero values indicate observed negative count rates, which may result from measurement error when the amount of material measured is small relative to background; blanks indicate that no value is available.

TABLE C-VII. Table of Measured Holdup Per Unit Length of Ductwork<sup>a</sup>

Experiment: U<sub>3</sub>O<sub>8</sub>  
 Horizontal Segment

Airflow	Measurement Point	Throughput <sup>b</sup> (kg)					
		2	4	6	8	10	
LOW	11	0.0058	0.0074	0.0130	0.0275	0.0275	0.0444
	12	0.0000	0.0000	0.0218	0.0142	0.0418	0.0408
	13	0.0144	0.0041	0.0174	0.0311	0.0306	0.0471
MEDIUM	11	0.0000	0.0304	0.0234	0.0543	0.0539	0.0448
	12	0.0161	0.0323	0.0455	0.0645	0.0778	0.0522
	13	0.0391	0.0377	0.0555	—	0.0656	0.0541
HIGH	11	0.0493	0.0621	0.0798	0.1221 <sup>c</sup>	0.0703	0.0354 <sup>c</sup>
	12	0.0000	0.0180	0.0740	0.1110	0.0693	0.1129
	13	0.0334	0.0073	0.0567	0.0617	0.0288 <sup>c</sup>	0.0799

<sup>a</sup>The values given are scaled to milligrams per square centimeter.

<sup>b</sup>Zero values indicate observed negative count rates, which may result from measurement error when the amount of material measured is small relative to background; blanks indicate that no value is available.

<sup>c</sup>An outlier not used in the model fitting.

TABLE C-VIII. Table of Holdup Measurements<sup>a</sup>

Experiment: Coarse U<sub>3</sub>O<sub>8</sub>, high airflow

Measurement Point	Throughput <sup>b</sup> (kg)					
	2	4	6	8	10	
1	0.0000	0.0000	0.0000	0.0000	0.0000	0.0000
2	0.0000	0.0000	0.0000	0.0000	0.0000	0.0000
3	0.0000	0.0000	0.0000	0.0000	0.0285	0.0059
4	0.1031	0.1404	0.1155	0.1225	0.1550	0.1942
5	0.0277	0.0529	0.0642	0.0251	0.0374	0.0778
6	0.0000	0.0056	0.0000	0.0246	0.0290	0.0000
7	0.0006	0.0099	0.0127	0.0325	0.0308	0.0281
8	0.0000	0.0120	0.0180	0.0180	0.0180	0.0030 <sup>c</sup>
9	0.0000	0.0000	0.0000	0.0000	0.0000	0.0000
10	0.0000	0.0000	0.0000	0.0000	0.0000	0.0000
11	0.0000	0.0000	0.0000	0.0000	0.0000	0.0000
12	0.0000	0.0000	0.0199	0.0209	0.0066	0.0000
13	0.0000	0.0041	0.0114	0.0000	0.0000	0.0000
14	0.1630	0.1860	0.2740	0.3520	0.4480	0.4270

<sup>a</sup>At each measurement point, tabulate values are scaled as in the experiments with U<sub>3</sub>O<sub>8</sub> (see Tables C-IV through C-VII); that is, for locations 1-7 and 11-13 units are milligrams per square centimeter, and for locations 8-10 and 14 units are grams.

<sup>b</sup>Zero values indicate observed negative count rates, which may result from measurement error when the amount of material measured is small relative to background; blanks indicate that no value is available.

<sup>c</sup>An outlier not used in the model fitting.

Table C-IX. Summary of Modeling Results for Experiment with Coarse U<sub>3</sub>O<sub>8</sub>

Component	Measurement Points <sup>a</sup>	Model	Estimated Holdup <sup>b</sup> (g)
Glove box sides	1-2	$\hat{h}_s(t) = 0$	0
Glove box floor	3-5	$\hat{h}_f(t) = 0.0934t$	0.934
Vertical segment	6-7	$\hat{h}_v(t) = 0.0199t$	0.199
First elbow	8	$\hat{h}_1(t) = 0.0022t$	0.022
Segment between elbows	9	$\hat{h}_b(t) = 0$	0
Second elbow	10	$\hat{h}_2(t) = 0$	0
Horizontal segment	11-13	$\hat{h}_h(t) = 0$	0
Filter	14	$\hat{h}_f(t) = 0.1241 + 0.0118t + 0.0020t^2$	0.440
System total	1-14	$\hat{h}(t) = 0.1241 + 0.1273t + 0.0020t^2$	1.595
System weight loss			2.266

<sup>a</sup>See Fig. 6 for details.

<sup>b</sup>The function  $\hat{h}_i(t)$  represents the estimated holdup within the individual component when the throughput was  $t$  kilograms.

<sup>c</sup>Throughput = 10 kg.

TABLE C-X. Table of Holdup Measurements<sup>a</sup>

Experiment: Ash, low airflow

Measurement Point	Throughput <sup>b</sup> (kg)						
	1	2	3	4	5	7	10
1	0.0000	0.0000	---	0.0000	0.0000	0.0000	0.0000
2	0.0000	0.0000	---	0.0000	0.0000	0.0000	0.0000
3	0.0262	0.0352	0.0494	0.0611	0.0625	0.1133	0.1389
4	---	---	---	---	---	---	---
5	0.0109	0.0180	0.0310	0.0312	---	0.0535	0.0874
6	0.0101	0.0079	---	---	---	---	0.0149
7	0.0076	0.0062	---	---	---	---	0.0096
8	0.0040	0.0010	0.0070	0.0020	0.0080	0.0080	---
9	0.0040	0.0000	---	---	---	---	0.0160
10	0.0000	0.0000	0.0000	0.0030	0.0050	0.00250	0.0060
11	0.0000	0.0000	---	---	---	---	0.0000
12	0.0000	0.0000	0.0000	0.0000	0.0000	0.0000	0.0000
13	0.0000	0.0000	---	---	---	---	0.0000
14	0.0330	0.0360	0.0360	0.0470	0.0600	0.0560	0.1030

<sup>a</sup>At each measurement point, tabulated values are scaled as in the experiments with U<sub>3</sub>O<sub>8</sub> (see Tables C-IV through C-VII); that is, for locations 1-7 and 11-13 units are milligrams per square centimeter, and for locations 8-10 and 14 units are grams.

<sup>b</sup>Zero values indicate the observed negative count rates, which may result from measurement error when the amount of material measured is small relative to background; blanks indicate that no value is available.

Table C-XI. Summary of Modeling Results for Low-Airflow Experiment with Ash

Component	Measurement Points <sup>a</sup>	Model <sup>b</sup>	Estimated Holdup <sup>c</sup> (g)
Glove box sides	1-2	$\hat{h}_1(t) = 0$	0
Glove box floor	3-5	$\hat{h}_f(t) = 0.1436t$	1.436
Vertical segment	6-7	$\hat{h}_v(t) = 0.0094t$	0.094
First elbow	8	$\hat{h}_1(t) = 0.0013t$	0.013
Segment between elbows	9	$\hat{h}_b(t) = 0.0016t$	0.016
Second elbow	10	$\hat{h}_2(t) = 0.00056t$	0.0056
Horizontal segment	11-13	$\hat{h}_h(t) = 0$	0
Filter	14	$\hat{h}_f(t) = 0.0329$ $+ 0.0003t$ $+ 0.0006t^2$	0.100
System total	1-14	$\hat{h}(t) = 0.0329$ $+ 0.1568t$ $+ 0.0006t^2$	1.664
System weight loss			1.31

<sup>a</sup>See Fig. 6 for details.

<sup>b</sup>The function  $\hat{h}_{...}(t)$  represents the estimated holdup within the individual component when the throughput was  $t$  kilograms.

<sup>c</sup>Throughput = 10 kg.

TABLE C-XII. Table of Holdup Measurements<sup>a</sup>

Experiment: Ash, medium airflow

Measurement Point	Throughput <sup>b</sup> (kg)											
	1	2	3	4	5	6	7	8	9	10		
1	0.0000	0.0000	0.0000	0.0000	0.0000	0.0000	0.0000	0.0000	0.0000	0.0000	0.0000	0.0000
2	0.0000	0.0000	0.0000	0.0000	0.0000	0.0000	0.0000	0.0000	0.0000	0.0000	0.0000	0.0000
3	0.0081	0.0071	0.0143	0.0138	0.0344	0.0264	---	0.0259	0.0420	0.0640	0.0501	0.0542
4	0.0000	0.0000	0.0175	0.0330	0.0414	0.0592	0.0510	0.0626	0.0671	0.0916	0.0879	---
5	0.0073	0.0000	0.0197	0.0228	0.0440	0.0324	0.0420	0.0541	0.0479	0.0696	0.0671	---
6	0.0047	0.0003	0.0000	0.0000	0.0000	0.0000	0.0000	0.0000	0.0000	0.0000	0.0034	0.0000
7	---	0.0093	0.0181	0.0113	0.0164	0.0161	0.0127	0.0065	0.0088	0.0082	0.0099	0.0150
8	0.0140	0.0010	0.0050	0.0090	0.0000	0.0070	0.0060	0.0340	0.0260	0.0260	0.0280	0.0290
9	0.0280	0.0290	0.0210	0.0330	---	---	0.0420	0.0400	0.0550	0.0430	0.0290	0.0570
10	0.0110	0.0080	0.0090	0.0140	0.0060	0.0110	0.0200	0.0210	---	0.0240	0.0220	0.0260
11	0.0119	0.0074	0.0119	0.0058	0.0127	0.0140	0.0201	0.0119	0.0132	0.0132	0.0160	0.0148
12	0.0019	0.0066	0.0133	0.0085	0.0085	0.0057	0.0171	0.0114	0.0161	0.0190	0.0209	0.0285
13	0.0046	0.0082	0.0059	0.0087	0.0187	0.0050	0.0119	0.0087	0.0069	0.0128	0.0091	0.0164
14	0.0540	0.0750	0.1130	0.1370	0.1570	0.1880	---	0.1440 <sup>c</sup>	0.2770	0.3200	0.2830	0.2730

<sup>a</sup>At each measurement point, tabulated values are scaled as in the experiments with U<sub>2</sub>O<sub>5</sub> (see Tables C-IV through C-VII); that is for locations 1-7 and 11-13 units are milligrams per square centimeter, and for locations 8-10 and 14 units are grams.

<sup>b</sup>Zero values indicate the observed negative count rates, which may result from measurement error when the amount of material measured is small relative to background; blanks indicate that no value is available.

<sup>c</sup>An outlier not used in the model fitting.

Table C-XIII. Summary of Modeling Results for Medium-Airflow Experiment with Ash

Component	Measurement Points <sup>a</sup>	Model <sup>b</sup>	Estimated Holdup <sup>c</sup> (g)
Glove box sides	1-2	$\hat{h}_s(t) = 0$	0
Glove box floor	3-5	$\hat{h}_f(t) = 0.0676t$	0.676
Vertical segment	6-7	$\hat{h}_v(t) = 0.0045t$	0.045
First elbow	8	$\hat{h}_1(t) = 0.0025t$	0.025
Segment between elbows	9	$\hat{h}_b(t) = 0.0227t + 0.0023t$	0.046
Second elbow	10	$\hat{h}_2(t) = 0.0024t$	0.024
Horizontal segment	11-13	$\hat{h}_h(t) = 0.0090t$	0.090
Filter	14	$\hat{h}_r(t) = 0.0273t + 0.0267t$	0.295
System total	1-14	$\hat{h}(t) = 0.0500t + 0.1151t$	1.201
System weight loss			1.53

<sup>a</sup>See Fig. 6 for details.

<sup>b</sup>The function  $\hat{h}_i(t)$  represents the estimated holdup within the individual component when the throughput was  $t$  kilograms.

<sup>c</sup>Throughput = 10 kg.

TABLE C-XIV. Table of Holdup Measurements<sup>a</sup>

Experiment: Ash, high airflow

Measurement Point	Throughput <sup>b</sup> (kg)											
	1	2	3	4	5	6	7	8	9	10		
1	0.0000	0.0000	0.0000	0.0000	0.0000	0.0000	0.0000	0.0000	0.0000	0.0000	0.0000	0.0000
2	0.0000	0.0000	0.0000	0.0000	0.0000	0.0000	0.0000	0.0000	0.0000	0.0000	0.0000	0.0000
3	0.0000	0.0383	0.0290	0.0276	0.0724	0.0530	0.0893	0.0684	0.1118	0.1096	0.1088	0.1074
4	0.0082	0.0434	0.0786	0.0730	0.1127	0.0992	0.1060	0.1074	0.1618	0.1451	0.1443	0.1471
5	0.0265	0.0065	0.0569	0.0775	0.0789	0.1026	0.1110	0.1274	0.1457	0.1764	0.1637	0.1460
6	0.0000	0.0095	0.0095	0.0040	0.0078	—	—	0.0243	0.0214	0.0211	0.0157	—
7	0.0178	0.0189	—	0.0291	0.0319	0.0332	0.0322	0.0281	—	—	0.0456	0.0445
8	0.0160	0.0340	0.0240	0.0320	0.0140	0.0160	0.0330	0.0360	0.0460	0.0350	0.0280	0.0320
9	0.0230	0.0060	0.0000	0.0300	0.0030	0.0000	0.0350	0.0500	0.0230	0.0070	0.0000	0.0290
10	0.0000	0.0040	0.0040	0.0080	0.0030	0.0020	0.0110	0.0110	0.0030	0.0020	—	0.0100
11	0.0066	0.0058	0.0000	0.0164	0.0000	0.0066	0.0000	0.0132	0.0000	0.0000	0.0000	0.0000
12	0.0000	0.0047	0.0028	0.0228	0.0114	0.0038	0.0171	0.0000	0.0000	0.0038	0.0057	0.0161
13	0.0073	0.0123	0.0000	0.0174	0.0132	0.0155	0.0187	0.0279	0.0000	0.0069	0.0160	0.0064
14	0.0750	0.1480	0.1870	0.2630	0.3030	0.4280	0.4750	—	0.6180	0.7230	0.7390	0.6660

<sup>a</sup>At each measurement point, tabulated values are scaled as in the experiments with U<sub>1</sub> O<sub>2</sub> (see Tables C-IV through C-VII); that is for locations 1-7 and 11-13 units are milligrams per square centimeter, and for locations 8-10 and 14 units are grams.

<sup>b</sup>Zero values indicate the observed negative count rates, which may result from measurement error when the amount of material measured is small relative to background; blanks indicate that no value is available.

Table C-XV. Summary of Modeling Results for High-Airflow Experiment with Ash

Component	Measurement Points <sup>a</sup>	Model <sup>b</sup>	Estimated Holdup <sup>c</sup> (g)
Glove box sides	1-2	$\hat{h}_s(t) = 0$	0
Glove box floor	3-5	$\hat{h}_f(t) = 0.1466t$	1.466
Vertical segment	6-7	$\hat{h}_v(t) = 0.0207t$	0.207
First elbow	8	$\hat{h}_1(t) = 0.0197t + 0.0015t^2$	0.035
Segment between elbows	9	$\hat{h}_b(t) = 0.0024t$	0.024
Second elbow	10	$\hat{h}_2(t) = 0.0008t$	0.008
Horizontal segment	11-13	$\hat{h}_h(t) = 0.0056t$	0.056
Filter	14	$\hat{h}_r(t) = 0.0622t + 0.0008t^2$	0.707
System total	1-14	$\hat{h}(t) = 0.0197t + 0.2398t + 0.0008t^2$	2.503
System weight loss			3.06

<sup>a</sup>See Fig. 6 for details.

<sup>b</sup>The function  $\hat{h}_{...}(t)$  represents the estimated holdup within the individual component when the throughput was  $t$  kilograms.

<sup>c</sup>Throughput = 10 kg.

**DATA FROM EXPERIMENTAL STUDY OF  
URANIUM HOLDUP IN A LIQUID-LIQUID  
EXTRACTION PULSE COLUMN  
(Tables C-XVI and C-XVII)**

Table C-XVI. Concentration Profile Data

Experimental Run 2A-3							
Extraction/Scrub Column (1-A)				Stripping Column (1-B)			
Sample <sup>a</sup>	Location <sup>b</sup>	Aqueous Uranium <sup>c</sup>	Organic Uranium <sup>c</sup>	Sample <sup>a</sup>	Location <sup>b</sup>	Aqueous Uranium <sup>c</sup>	Organic Uranium <sup>c</sup>
A-1	0.5	0.106	5.208	B-1	0.5	1.487	0.561
A-2	12.5	0.406	5.705	B-2	18.5	2.568	0.723
A-3	24.5	0.749	6.436	B-3	36.5	3.827	1.014
A-4	36.5	0.950	6.790	B-4	54.5	5.731	1.353
A-5	48.5	0.965	6.888	B-5	72.5	6.732	1.561
A-6	52.5	1.281	6.337	B-6	90.5	8.021	1.854
A-7	64.5	0.736	5.598	B-7	104.5	8.805	2.011
A-8	76.5	0.251	2.767				
A-9	88.5	0.110	0.840				
A-10	105.5	0.066	0.287				
A-11	129.5	0.047	0.045				

<sup>a</sup>See Fig. 20.

<sup>b</sup>The top of the working section corresponds to the value zero, and each stage has unit length.

<sup>c</sup>The values given are in units of grams of uranium/stage.

Table C-XVII. Concentration Profile Data

Experimental Run 2D-2							
Extraction/Scrub Column (1-A)				Stripping Column (1-B)			
Sample <sup>a</sup>	Location <sup>b</sup>	Aqueous Uranium <sup>c</sup>	Organic Uranium <sup>c</sup>	Sample <sup>a</sup>	Location <sup>b</sup>	Aqueous Uranium <sup>c</sup>	Organic Uranium <sup>c</sup>
A-1	0.5	0.213	7.841	B-1	0.5	0.063	0.005
A-2	12.5	1.057	8.525	B-2	18.5	0.084	0.006
A-3	24.5	1.512	9.131	B-3	36.5	0.397	0.016
A-4	36.5	1.743	9.570	B-4	54.5	5.089	0.474
A-5	48.5	1.864	9.825	B-5	72.5	9.551	1.145
A-6	52.5	2.354	9.412	B-6	90.5	13.554	1.709
A-7	64.5	2.323	9.328	B-7	104.5	15.253	1.953
A-8	76.5	2.057	8.849				
A-9	88.5	1.002	6.233				
A-10	105.5	0.059	0.899				
A-11	129.5	0.008	0.059				

<sup>a</sup>See Fig. 20.

<sup>b</sup>The top of the working section corresponds to the value zero, and each stage has unit length.

<sup>c</sup>The values given are in units of grams of uranium/stage.



DATA FROM EXPERIMENTAL STUDY OF URANIUM HOLDUP  
DURING ADU PRECIPITATION AND CALCINATION  
(Tables C-XVIII through C-XXII)

Table C-XVIII. Holdup of Uranium in the Precipitation Column

Throughput (kg of U)	Holdup (g of U)	Error (g of U) <sup>a</sup>	Throughput (kg of U)	Holdup (g of U)	Error (g of U) <sup>a</sup>
1	4.66	0.11	29	72.30	0.50
2	27.13	0.23	30	20.25	0.30
3	7.17	0.15	31	14.60	0.30
4	45.56	0.31	32	12.60	0.30
5	12.90	0.21	[Cleanout #1]	—	—
6	7.93	0.17	33	8.23	0.25
7	7.00	0.16	34	6.82	0.23
8	10.23	0.20	35	8.12	0.26
9	33.29	0.29	36	9.82	0.23
10	17.84	0.27	37	7.63	0.25
11	22.07	0.28	38	7.98	0.26
12	23.28	0.32	39	8.25	0.27
13	28.17	0.35	40	8.82	0.27
14	64.63	0.46	[Cleanout #2]	—	—
15	48.52	0.47	41	55.57	0.57
16	50.23	0.48	42	55.25	0.58
17	78.67	0.51	43	17.48	0.39
18	52.25	0.51	44	5.22	0.21
19	67.78	0.55	45	10.95	0.26
20	52.29	0.50	46	10.45	0.29
21	58.02	0.48	47	6.87	0.25
22	46.28	0.46	48	7.72	0.26
23	42.89	0.46	49	8.02	0.18
24	46.39	0.47	50	9.65	0.20
25	31.90	0.46	51	8.87	0.21
26	33.60	0.34	52	9.27	0.20
27	22.28	0.33	[Cleanout #3]	—	—
28	10.81	0.25			

<sup>a</sup>The errors reported here are counting errors only.

Table C-XIX. Holdup of Uranium in the Filter Funnels

Throughput (kg of U)	Holdup (g of U)	Error (g of U) <sup>a</sup>	Throughput (kg of U)	Holdup (g of U)	Error (g of U) <sup>a</sup>
1	2.32	0.01	27	10.40	0.04
2	4.32	0.02	28	4.36	0.03
3	6.01	0.02	29	9.74	0.04
4	7.13	0.02	30	7.22	0.04
5	13.32	0.04	31	12.15	0.03
6	12.03	0.03	32	5.92	0.05
7	16.11	0.04	33	8.99	0.05
8	13.80	0.04	34	7.13	0.06
9	16.54	0.04	35	8.01	0.05
10	15.02	0.04	36	8.84	0.05
11	11.74	0.04	37	11.18	0.05
12	12.31	0.04	38	6.47	0.04
13	10.06	0.04	39	7.46	0.05
14	9.23	0.03	40	5.26	0.04
15	10.24	0.04	41	9.99	0.06
16	10.21	0.04	42	8.24	0.05
17	10.91	0.04	43	9.54	0.05
18	13.48	0.04	44	5.87	0.05
19	12.40	0.04	45	7.29	0.05
20	11.49	0.04	46	6.45	0.05
21	11.06	0.03	47	9.22	0.06
22	8.92	0.04	48	9.56	0.06
23	9.99	0.04	49	8.36	0.04
24	11.34	0.04	50	6.48	0.04
25	7.22	0.04	51	8.89	0.04
26	10.33	0.04	52	10.11	0.04

<sup>a</sup>The errors reported here are counting errors only.

Table C-XX. Holdup of Uranium in the Calciner

Throughput (kg of U)	Holdup (g of U)	Error (g of U) <sup>a</sup>	Throughput (kg of U)	Holdup (g of U)	Error (g of U) <sup>a</sup>
1	0.07	0.01	27	1.17	0.01
2	0.30	0.01	28	1.11	0.01
3	0.64	0.01	29	1.17	0.02
4	0.67	0.01	30	1.16	0.02
5	0.66	0.01	31	1.20	0.02
6	0.87	0.01	32	1.25	0.02
7	1.00	0.01	33	1.11	0.02
8	1.12	0.01	34	1.14	0.02
9	1.21	0.01	35	1.16	0.02
10	1.19	0.01	36	1.18	0.02
11	1.19	0.01	37	1.18	0.02
12	1.20	0.01	38	1.16	0.02
13	1.15	0.01	39	1.18	0.02
14	1.18	0.01	40	1.15	0.02
15	1.30	0.01	41	1.38	0.02
16	1.24	0.01	42	1.31	0.02
17	1.23	0.01	43	1.26	0.02
18	1.21	0.01	44	1.34	0.02
19	1.20	0.01	45	1.41	0.02
20	1.18	0.01	46	1.76	0.03
21	1.18	0.01	47	1.48	0.02
22	1.20	0.01	48	1.33	0.03
23	1.23	0.01	49	1.56	0.02
24	1.21	0.01	50	1.65	0.02
25	1.20	0.02	51	1.74	0.02
26	1.19	0.02	52	1.74	0.02

<sup>a</sup>The errors reported here are counting errors only.

Table C-XXI. Holdup of Uranium in the Calciner Trays

Throughput (kg of U)	Holdup (g of U)	Error (g of U) <sup>a</sup>	Throughput (kg of U)	Holdup (g of U)	Error (g of U) <sup>a</sup>
1	0.11	0.01	27	0.80	0.01
2	0.17	0.01	28	0.82	0.01
3	0.20	0.01	29	0.96	0.02
4	0.28	0.01	30	0.92	0.02
5	0.30	0.01	31	0.98	0.02
6	0.29	0.01	32	1.01	0.02
7	0.30	0.01	33	0.95	0.02
8	0.32	0.01	34	1.03	0.02
9	0.35	0.01	35	1.00	0.02
10	0.40	0.01	36	1.04	0.02
11	0.41	0.01	37	0.94	0.02
12	0.41	0.01	38	1.01	0.02
13	0.38	0.01	39	1.02	0.02
14	0.43	0.01	40	1.04	0.02
15	0.41	0.01	41	1.17	0.02
16	0.44	0.01	42	1.11	0.02
17	0.45	0.01	43	1.12	0.03
18	0.53	0.01	44	1.25	0.03
19	0.66	0.02	45	1.09	0.03
20	0.57	0.01	46	1.08	0.03
21	0.56	0.01	47	1.14	0.03
22	0.60	0.01	48	1.58	0.03
23	0.56	0.01	49	1.30	0.02
24	0.64	0.01	50	1.46	0.02
25	0.68	0.01	51	1.43	0.02
26	0.77	0.01	52	1.35	0.02

<sup>a</sup>The errors reported here are counting errors only.

Table C-XXII. Holdup of Uranium in the Dissolver Vessel

Throughput (kg of U)	Holdup (g of U)	Error (g of U) <sup>a</sup>	Throughput (kg of U)	Holdup (g of U)	Error (g of U) <sup>a</sup>
1	0.31	0.01	27	0.71	0.01
2	0.66	0.01	28	0.80	0.01
3	1.32	0.01	29	0.96	0.01
4	0.92	0.01	30	0.58	0.01
5	0.81	0.01	31	1.13	0.02
6	0.84	0.01	32	0.80	0.01
7	1.62	0.01	33	0.77	0.02
8	0.88	0.01	34	0.80	0.02
9	0.92	0.01	35	0.65	0.02
10	0.73	0.01	36	0.62	0.02
11	0.96	0.01	37	0.74	0.02
12	0.61	0.01	38	0.75	0.02
13	0.86	0.01	39	0.77	0.02
14	0.85	0.01	40	0.86	0.02
15	0.58	0.01	41	0.70	0.02
16	0.58	0.01	42	0.71	0.02
17	1.54	0.02	43	0.56	0.02
18	0.74	0.01	44	0.70	0.02
19	0.70	0.01	45	0.74	0.02
20	0.71	0.01	46	0.68	0.02
21	0.74	0.01	47	1.03	0.02
22	0.62	0.01	48	0.98	0.02
23	0.60	0.01	49	0.98	0.02
24	0.88	0.01	50	0.90	0.02
25	1.36	0.02	51	0.64	0.02
26	0.84	0.01	52	0.73	0.02

<sup>a</sup>The errors reported here are counting errors only.

**DATA FROM EXPERIMENTAL STUDY OF  
URANIUM HOLDUP IN SOLUTION LOOPS  
(Tables C-XXIII through C-XXVII)**

TABLE C-XXIII. Data from Solution Loop Experiments: CPVC Loop, Low Flow Rate

Throughput (Mg U)	Location <sup>a</sup>								
	101 (g)	102 (g)	103 (g)	104 (g/m)	105 (g)	106 (g/m)	107 (g)	108 (g/m)	109 (g)
0.018	0.98	0.01	0.02	0.05	0.01	0.02	0.01	0.01	0.00
1.295	9.70	0.16	0.69	0.55	0.20	0.15	0.12	0.08	0.14
4.106	15.37	0.18	0.68	0.47	0.16	0.11	0.10	0.06	0.13
9.889	24.19	0.18	0.35	0.46	0.15	0.13	0.10	0.09	0.16
14.262	24.89	0.09	0.30	0.49	0.13	0.09	0.11	0.06	0.17
20.104	26.78	0.25	0.44	0.47	0.13	0.10	0.13	0.15	0.16
24.422	31.89	0.25	0.55	0.55	0.12	0.17	0.12	0.14	0.12
28.920	37.91	0.26	0.31	0.51	0.18	0.13	0.13	0.06	0.11
34.184	38.29	0.23	0.29	0.48	0.11	0.15	0.11	0.15	0.11
40.129	40.18	0.27	0.46	0.50	0.22	0.15	0.15	0.13	0.11
42.490	34.51	0.30	0.31	0.27	0.11	0.08	0.12	0.15	0.12

Throughput (Mg U)	Location <sup>a</sup>							
	110 (g)	111 (g)	112 (g)	113 (g/m)	114 (g)	115 (g)	116 (g)	117 (g)
0.018	0.00	0.01	0.01	0.02	0.00	0.01	0.01	0.00
1.295	0.09	0.25	0.29	0.53	0.22	0.69	0.23	0.66
4.106	0.09	0.24	0.30	0.68	0.21	0.77	0.25	0.65
9.889	0.09	0.19	0.26	0.70	0.19	0.58	0.25	0.80
14.262	0.09	0.16	0.29	0.69	0.19	0.42	0.24	0.78
20.104	0.10	0.16	0.30	0.71	0.19	0.44	0.23	0.78
24.422	0.11	0.15	0.28	0.72	0.19	0.63	0.23	0.67
28.920	0.11	0.13	0.23	0.65	0.20	0.45	0.24	0.84
34.184	0.10	0.37	0.27	0.41	0.18	0.41	0.30	0.70
40.129	0.22	0.15	0.26	0.86	0.20	0.58	0.23	0.62
42.490	0.11	0.16	0.22	0.69	0.17	0.55	0.20	0.78

<sup>a</sup>See Fig. 47.

TABLE C-XXIV. Data from Solution Loop Experiments: CPVC Loop, High Flow Rate

Throughput (Mg U)	Location <sup>a</sup>								
	101 (g)	102 (g)	103 (g)	104 (g/m)	105 (g)	106 (g/m)	107 (g)	108 (g/m)	109 (g)
42.610	8.86	0.10	0.24	0.36	0.12	0.10	0.09	0.04	0.11
47.436	10.54	0.08	0.29	0.34	0.12	0.13	0.06	0.09	0.08
59.568	13.41	0.10	0.48	0.34	0.10	0.07	0.07	0.09	0.08
68.354	17.36	0.11	0.48	0.31	0.10	0.09	0.05	0.09	0.06
79.886	10.50	0.07	0.14	0.38	0.11	0.11	0.08	0.03	0.08
88.567	11.52	0.12	0.67	0.39	0.11	0.13	0.09	0.07	0.09
91.555	10.92	0.06	0.10	0.42	0.12	0.14	0.04	0.06	0.06

Throughput (Mg U)	Location <sup>a</sup>							
	110 (g)	111 (g)	112 (g)	113 (g/m)	114 (g)	115 (g)	116 (g)	117 (g)
42.610	0.08	0.13	0.19	0.64	0.15	0.40	0.21	0.60
47.436	0.05	0.13	0.19	0.28	0.14	0.47	0.07	0.63
59.568	0.06	0.11	0.20	0.48	0.14	0.51	0.20	0.62
68.354	0.04	0.13	0.22	0.63	0.18	0.93	0.18	0.73
79.886	0.06	0.13	0.22	0.54	0.16	0.81	0.18	0.90
88.567	0.08	0.13	0.20	0.83	0.22	0.99	0.20	0.93
91.555	0.05	0.13	0.18	0.52	0.17	0.33	0.17	0.87

<sup>a</sup>See Fig. 47.

TABLE C-XXV. Data from Solution Loop Experiments: Stainless Steel Loop, Low Flow Rate

Throughput (Mg U)	Location <sup>a</sup>								
	1 (g)	2 (g)	3 (g)	4 (g/m)	5 (g)	6 (g/m)	7 (g)	8 (g/m)	9 (g)
0.073	1.63	0.40	0.58	0.16	0.54	2.35	0.08	0.12	0.06
2.321	4.00	0.28	1.19	0.28	0.43	1.51	0.10	0.15	0.06
5.764	7.90	0.28	0.65	0.04	0.45	1.41	0.09	0.11	0.07
9.343	8.52	0.23	0.87	0.60	0.44	1.55	0.06	0.01	0.10
14.651	7.73	0.22	0.58	0.14	0.44	1.56	0.07	0.10	0.12
18.633	10.32	0.26	0.67	0.13	0.44	1.73	0.09	0.31	0.14
24.049	10.20	0.19	0.70	0.23	0.46	1.63	0.11	0.18	0.14
27.646	7.81	0.21	1.34	0.26	0.44	1.58	0.09	0.14	0.12
32.417	7.21	0.16	0.65	0.21	0.46	1.66	0.10	0.20	0.13
36.441	8.10	0.23	0.77	0.03	0.44	1.55	0.10	0.16	0.13
41.187	12.57	0.17	0.67	0.13	0.47	1.72	0.08	0.13	0.11

Throughput (Mg U)	Location <sup>a</sup>							
	10 (g)	11 (g)	12 (g)	13 (g/m)	14 (g)	15 (g)	16 (g)	17 (g)
0.073	0.05	0.04	0.04	0.17	0.03	0.10	0.07	0.25
2.321	0.08	0.14	0.06	0.12	0.02	0.17	0.04	0.15
5.764	0.06	0.07	0.11	0.21	0.03	0.09	0.08	0.27
9.343	0.05	0.06	0.08	0.28	0.05	0.36	0.06	0.20
14.651	0.08	0.07	0.09	0.37	0.06	0.37	0.06	0.21
18.633	0.09	0.07	0.09	0.30	0.05	0.40	0.05	0.20
24.049	0.10	0.08	0.09	0.30	0.04	0.37	0.06	0.25
27.646	0.09	0.05	0.07	0.26	0.04	0.36	0.07	0.27
32.417	0.10	0.07	0.09	0.23	0.04	0.38	0.06	0.24
36.441	0.10	0.06	0.08	0.26	0.04	0.38	0.06	0.30
41.187	0.09	0.05	0.08	0.24	0.04	0.37	0.06	0.31

<sup>a</sup>See Fig. 46.

TABLE C-XXVI. Data from Solution Loop Experiments: Stainless Steel Loop, High Flow Rate

Throughput (Mg U)	Location <sup>a</sup>								
	1 (g)	2 (g)	3 (g)	4 (g/m)	5 (g)	6 (g/m)	7 (g)	8 (g/m)	9 (g)
41.237	7.53	0.27	0.44	0.07	0.43	1.49	0.04	0.12	0.08
46.942	9.53	0.21	0.89	0.16	0.49	1.72	0.10	0.19	0.13
59.881	8.74	0.19	1.01	0.15	0.49	1.67	0.08	0.09	0.11
68.971	7.14	0.23	1.04	0.11	0.47	1.72	0.09	0.12	0.16
81.312	8.27	0.21	0.96	0.18	0.51	2.88	0.09	0.14	0.17
90.029	10.18	0.11	0.72	0.05	0.51	1.83	0.10	0.17	0.18
100.673	9.21	0.16	0.78	0.03	0.53	1.80	0.11	0.16	0.16

Throughput (Mg U)	Location <sup>a</sup>							
	10 (g)	11 (g)	12 (g)	13 (g/m)	14 (g)	15 (g)	16 (g)	17 (g)
41.237	0.07	0.05	0.07	0.26	0.03	0.15	0.06	0.27
46.942	0.10	0.05	0.06	0.20	0.03	0.25	0.07	0.29
59.881	0.08	0.05	0.07	0.27	0.04	0.31	0.07	0.30
68.971	0.09	0.07	0.06	0.22	0.03	0.46	0.11	0.38
81.312	0.10	0.06	0.08	0.30	0.05	0.50	0.12	0.43
90.029	0.11	0.08	0.08	0.23	0.05	0.41	0.15	0.62
100.673	0.09	0.08	0.12	0.50	0.09	0.38	0.14	0.52

<sup>a</sup>See Fig. 46.

Table C-XXVII. Holdup Estimates<sup>a</sup> for Each Measurement Location at the Conclusion of the Experiment

Location <sup>b</sup>	Low Flow Rate			High Flow Rate		
	SS	CPVC	Difference	SS	CPVC	Difference
2/102	0.17	0.30	-0.13	0.16	0.06	0.10
3/103	0.67	0.31	0.36	0.78	0.17	0.61
4/104	0.12	0.32	-0.20	0.04	0.41	-0.37
5/105	0.47	0.12	0.36	0.53	0.12	0.39
6/106	1.69	0.09	1.60	1.81	0.14	1.67
7/107	0.08	0.12	-0.04	0.11	0.04	0.07
8/108	0.14	0.15	-0.01	0.16	0.06	0.10
9/109	0.11	0.12	-0.01	0.16	0.06	0.10
10/110	0.09	0.12	-0.03	0.09	0.05	0.04
11/111	0.05	0.16	-0.11	0.08	0.13	-0.05
12/112	0.08	0.23	-0.15	0.12	0.18	-0.06
13/113	0.24	0.71	-0.47	0.46	0.56	-0.10
14/114	0.04	0.17	-0.13	0.09	0.17	-0.08
15/115	0.37	0.55	-0.18	0.38	0.34	0.04
16/116	0.06	0.20	-0.14	0.14	0.17	-0.03
17/117	0.31	0.77	-0.46	0.52	0.87	-0.35

<sup>a</sup>Units are in grams of uranium except for the pipes, where holdup is expressed in grams of uranium per meter of pipe, as indicated in Figs. 49-60.

<sup>b</sup>See Figs. 46 and 47.



DISTRIBUTION

	<u>Copies</u>
Nuclear Regulatory Commission, RS, Bethesda, Maryland	228
Technical Information Center, Oak Ridge, Tennessee	2
Los Alamos National Laboratory, Los Alamos, New Mexico	50
	<u>350</u>

NRC FORM 336 (6.83)		U.S. NUCLEAR REGULATORY COMMISSION		1 REPORT NUMBER (Assigned by TIDC, add Vol. No., if any) NUREG/CR-3678 LA-10038	
<b>BIBLIOGRAPHIC DATA SHEET</b>				2 Leave blank	
3 TITLE AND SUB-TITLE Estimation Methods for Process Holdup of Special Nuclear Materials				4 RECIPIENT'S ACCESSION NUMBER	
6 AUTHOR(S) K. K. S. Pillay, R. R. Picard, R. S. Marshall				5 DATE REPORT COMPLETED MONTH   YEAR February   1984	
				7 DATE REPORT ISSUED MONTH   YEAR June   1984	
8 PERFORMING ORGANIZATION NAME AND MAILING ADDRESS (Include Zip Code) Los Alamos National Laboratory Los Alamos, NM 87545				9 PROJECT/TASK/WORK UNIT NUMBER	
11 SPONSORING ORGANIZATION NAME AND MAILING ADDRESS (Include Zip Code) Division of Facility Operations Office of Nuclear Research U. S. Nuclear Regulatory Commission Washington, DC 20555				10 FIN NUMBER A7226	
				12a TYPE OF REPORT Formal	
13 SUPPLEMENTARY NOTES				12b PERIOD COVERED (Inclusive dates)	
14 ABSTRACT (200 words or less) <p>Los Alamos National Laboratory studied the use of statistical estimation methods for materials holdup at highly enriched uranium (HEU)-processing facilities. Use of historical holdup data from processing facilities and selected holdup measurements at two operating facilities confirm the need for high-quality data and reasonable control over process parameters in developing these models. Large-scale experiments were conducted to demonstrate the value of the models from good-quality experimental data. Using these data, we developed statistical models to estimate residual inventories of uranium in large process equipment and facilities. Some important findings are the following:</p> <ul style="list-style-type: none"> <li>o Holdup in some equipment at HEU-processing facilities, such as air filters, ductwork, calciners, dissolvers, pumps, pipes, and pipefittings can be readily modeled.</li> <li>o Holdup profiles of process equipment such as glove boxes, precipitators, and rotary drum filters can change with time, necessitating several measurements at the time of inventory.</li> <li>o Reasonable estimation of hidden inventories of holdup to meet regulatory requirements can be accomplished through good measurements and statistical modeling.</li> </ul>					
15a KEY WORDS AND DOCUMENT ANALYSIS			15b DESCRIPTORS		
16 AVAILABILITY STATEMENT Unlimited			17 SECURITY CLASSIFICATION (This report) Unclassified		18 NUMBER OF PAGES
			19 SECURITY CLASSIFICATION (This page) Unclassified		20 PRICE \$

Available from

GPO Sales Program

Division of Technical Information and Document Control

US Nuclear Regulatory Commission

Washington, DC 20555

and

National Technical Information Service

Springfield, VA 22161

Los Alamos